Electronic Supplementary Material (ESI) for Chemical Communications.

High-Throughput Screening of Solid-State Catalysts for Nerve Agent Degradation

Joseph M. Palomba, Cy V. Credille, Mark Kalaj, Jared B. DeCoste, Gregory W. Peterson, Trenton M. Tovar, and Seth M. Cohen*

Department of Chemistry and Biochemistry, University of California, San Diego, La Jolla, California 92093, United States

Edgewood Chemical Biological Center
U.S. Army Research, Development and Engineering Command
5183 Blackhawk Road
Aberdeen Proving Ground, MD 21020, United States

SUPPORTING INFORMATION

Experimental

Materials. All solvents and starting materials were purchased from chemical suppliers and used without further purification (Sigma Aldrich, Alfa Aesar, EMD, and TCI). Some materials for screening were purchased from suppliers and used without further purification.

Synthetic Procedures. MOFs purchased from Suppliers were used without further purification. All MOFs regardless of synthesis conditions were subjected to overnight activation at 80 °C in a vacuum oven under active vacuum. MOFs were characterized via powder X-ray diffraction (Figures S4-7; S13-93).

- *UiO-66-NH_2 [DMF/AcOH]:* Was synthesized according to literature procedure with BDC-NH_2 as ligand.[1] This MOF was treated with an additional washing step to avoid formylation found in literature in synthesis of UiO-66-NH_2.[2] Using a modified procedure, the formyl groups were restored to free amine. 2 g of UiO-66-NH_2 was added to 100 mL MeOH:H_2O 1:1 mixture with 5 mL of conc. HCl and refluxed overnight. Solid was collected by filtration and washed with MeOH. ^{1}H NMR was used to characterize the completeness of removal of formyl group as in the reference.[2]
- *UiO-66-COOH [DMF/AcOH]:* Components were mixed together in the following molar ratio in a glass vial with 0.4 vol% diH_2O as an additive and heated at 150 °C for 24 h. $ZrO(NO_3)_2 \bullet H_2O$/BDC/AcOH/DMF = 1/2/100/90. White solid was collected by centrifugation and washed with DMF and EtOH.
- *ZIF-4*: 1.5 g (5 mmol) of $Zn(NO_3)_2 \bullet 6H_2O$ was added to a 125 mL glass jar with 113 mL of DMF. To this 1.13 g (16.5 mmol) of imidazole was added and mixture was heated to 100 °C for 72 h. White solid was collected by filtration and washed with DMF and EtOH.

Powder X-ray Diffraction (PXRD). PXRD data was collected at room temperature on a Bruker D8 Advance diffractometer running at 40 kV, 40 mA for Cu Kα (λ = 1.5418 Å), with a scan speed of 0.5 sec/step, a step size of 0.01° in 2θ, and a 2θ range of 2-50° at room temperature.

Scanning Electron Microscopy (SEM). MOFs were placed on conductive carbon tape on a sample holder and coated using an Ir-sputter coating for 7 sec. A Zeiss Sigma 500 ESEM microscope was used for acquiring images using a 2-3 kV energy source under vacuum at a working distance of 5 mm.

Preparation of *N*-ethylmorpholine Buffers. To prepare 20 mM *N*-ethylmorpholine buffer, 0.5 mL (4.0 mmol) of *N*-ethylmorpholine was added to 200 mL of diH_2O with stirring and the pH was monitored. The 20 mM *N*-ethylmorpholine solution produced a pH of 10.4. To adjust to the desired pH (8.0 or 10.0), ~1 M HCl was added dropwise while continuously monitoring the pH.

Calibration Curves for *p*-Nitrophenol. In order to determine the relationship between concentration of *p*-nitrophenol and plate reader absorbance, a calibration curve was prepared. Five solutions of *p*-nitrophenol were made at varying concentrations in both pH = 8 and 10 buffers. The absorbance was measured in 8 wells and averaged. Results are shown in Table S3 and Figure S3. Using the slopes from these curves, the rate of hydrolysis (k) can be determined for each sample based on the initial rate calculated from slope (Abs/sec).

HTS Validation. Validation tests assays were carried out in Olympus Plastics clear, flat-bottom 96-well plates. Each well was prepared with 100 μL total volume containing: 95 μL buffer (20 mM *N*-ethylmorpholine adjusted to pH 8 or 10); and MOF (X μg/mL, where X = 600, 450, 300, 150, 100, 75); and 5 μL substrate (25 mM stock solution of methyl paraoxon in methanol; 1.25 mM total concentration; 0.125 μmol). Note, methanol was used as solubilizing agent as DMNP has limited solubility in water. The use of short-chain alcohols or dimethyl sulfoxide as solubilizing agents at concentrations <10% in biological HTS assays is common.[3, 4] MOF suspensions were prepared by weighing 12 mg of MOF powder into a 15 mL centrifuge tube and adding 10 mL of corresponding 20 mM buffer solutions. All suspensions were sonicated in a water-bath for 30 min to disperse the powders. These concentrated suspensions were diluted with buffer solution to achieve final concentrations tested (Table S). Before any transfer, great care was taken to achieve a stable suspension to provide the most accurate dilution following the steps: 1) sonicated suspension for 30 sec; 2) mix with vortex mixer for 15 sec; 3) invert centrifuge tube three times; 4) mix with vortex mixer for an additional 15 sec; 5) transfer immediately to the plate. These suspensions (1 mL total volume) were used to prepare individual wells of the 96-well plate. The same suspension procedure as above was employed before adding 95 μL to each well. In a typical run, six replicates of each condition were prepared by plating 3 wells, repeating the suspension procedure and then plating 3 more wells. In addition each column included two negative controls: 1) buffer and substrate only (used to calculate background hydrolysis) and 2) buffer and MOF without substrate. Upon the addition of substrate with multi-channel pipette hydrolysis was monitored by change in absorbance at over 60 min at 24 °C with 5 sec shaking of plate every 40 sec (λ_{max} = 407 nm). Activity was measured as initial linear rate, measured from 10 to 50 min using Excel software. Reported activity is average slope for six replicates with a background subtraction from the hydrolysis rate in the presence of 20 mM *N*-ethylmorpholine without MOF (Figure S1).

Evaluation of Dispensing of MOFs for HTS. Precision and accuracy for catalytic rates for a particular concentration of MOF was evaluated based on suspected error in dispensing. The concentration of MOF materials were varied and evaluated in the assay. Three MOFs: ZIF-8, UiO-66, and NU-1000 were assessed based on their anticipated activity (low, medium, and high activity, respectively) to test six different MOF concentrations (Figure S1). The results in Figure S1 show that the assay conditions are valid for identifying hits even accounting for variance in quantity of MOF dispersed, and that the observed activity directly tracks with the concentration of MOF added.

Evaluation of Different Buffers. To confirm effect of pH on DMNP hydrolysis, two additional buffers were tested: 1) Tris and 2) HEPES. Both buffers were prepared in the same fashion as for *N*-ethylmorpholine and tests for dispensing validation experiments for these buffers were carried out the same as outlined above. Results confirm that MOF activity is pH dependent (Figure S2).

Evaluation of HTS assay using Z-factor. By running a large number of both sample and control tests, a Z-factor for both UiO-66 and NU-100 at pH= 8.0 and pH= 10.0 were calculated. Using the methods described above (HTS development) at 300 μg/mL, 14 wells were prepared for 6 samples: UiO-66 (pH=8), NU-1000 (pH=8), No MOF (pH=8), UiO-66 (pH=10), NU-1000 (pH=10), No MOF (pH=10). The average slope from t = 10 min to 50 min was calculated. In this case background was not subtracted from average slope of MOF samples. Instead an average and

standard deviation (μ_s and σ_s) was calculated from all 14 wells for each MOF sample. In addition average and standard deviation (μ_c and σ_c) was calculated from all 14 wells for each control. These values were used in Equation S1 to determine the Z-factors for both MOFs with each condition (Table S1). Z-factor was also used for evaluation of top 15 MOFs (Figure 2 and Table S5). These Z-factors indicate that the assay is valid for the top performing MOFs.

HTS of Library Samples. All samples were prepared and analyzed using the screening method described above (HTS Validation) at a concentration of 300 μg/mL with one procedure change. Instead of preparing material suspensions in 10 mL of buffer solution, 6 mg of material was diluted with 10 mL of diH_2O. 500 μL of this suspension was then diluted with 500 μL of 40 mM *N*-ethylmorpholine of corresponding pH. This resulted in the same final concentration of buffer and allowed for the same diH_2O suspension to be used for all pHs tested. Due to the variety in materials included in library, all materials were prepared in equal mass content (not molar).

Equations, Tables, and Figures

Equation S1. Z-factor (screening window coefficient) calculation, where μ = average slope, σ = average standard deviation, s = sample, c = control, the full derivation can be found in the original literature reference.[5]

$$Z = 1 - \frac{(3\sigma_s + 3\sigma_c)}{|\mu_s - \mu_c|}$$

Equation S2. Hydrolysis rate calculation, see Table S3 and Figure S3.

$$\frac{Initial\ Rate\ \left(\frac{Abs}{sec}\right)}{slope\ of\ calibration\ curve\left(\frac{Abs}{mM}\right)} = k\ \left(\frac{mM}{sec}\right)$$

Table S1. Activity of MOFs based on first-order kinetics screened via HTS method as CWA degradation catalysts. Literature values shown for comparison. Note, $t_{1/2}$ calculation ($t_{1/2} = \ln(2)/k$) is estimated for first-order kinetics in all cases.

MOF	Literature		This Work			
	pH = 10.4		pH = 10.0		pH = 8.0	
	MOF conc.	($t_{1/2}$ in min)	MOF conc.	($t_{1/2}$ in min)	MOF conc.	($t_{1/2}$ in min)
UiO-66	2.5 mg/ mL	25-45[6]	0.3 mg/ mL	900	0.3 mg/ mL	112
UiO-66-NH_2	2.5 mg/ mL	1[7]		132		164
UiO-67	2.5 mg/ mL	4.5[8]		340		40
NU-1000	3.0 mg/ mL	1.5-15[9]		108		340
PCN-222	2.4 mg/ mL	8[10]		56		88

Table S2. Statistical parameters for UiO-66 NU-1000 and top 15 MOFs at both pH = 8 and 10; μ = average slope and σ = average standard deviation. Control tests are buffer and substrate without MOF. Z-factors were calculated based on Equation S1. "n" indicates number of replicates used for statistics. R^2 values were calculated based on average over slope range.

	pH = 8						
MOF	**μ- sample**	**σ- sample**	**μ- control**	**σ- control**	**n**	**Z-factor**	**R^2 of slope**
UiO-66 [DMF/HCl]	2.54E-04	4.62E-05	6.25E-07	3.71E-07	14	0.45	0.9995
NU-1000	4.02E-05	6.00E-06	6.25E-07	3.71E-07	14	0.52	0.9970
UiO-66 [DMF/AcOH]	4.98E-04	5.12E-05	7.44E-07	3.53E-07	3	0.69	0.9995
UiO-67	4.95E-04	2.97E-05	8.78E-07	1.57E-07	3	0.82	0.9859
PCN-222	4.09E-04	1.36E-04	8.78E-07	1.57E-07	3	0.00	0.9938
MOF-808	3.34E-04	1.70E-05	5.33E-07	1.48E-07	3	0.85	0.9987
UiO-66-NH_2-HD	3.21E-04	1.12E-05	6.67E-07	1.81E-07	3	0.89	0.9874
UiO-66-NH_2 [DMF/HCl]	2.57E-04	1.37E-05	7.44E-07	3.53E-07	3	0.84	0.9963
UiO-66(Hf)	2.49E-04	3.06E-05	7.18E-07	2.22E-07	3	0.63	0.9988
UiO-66 [Acetone/HCl]	2.21E-04	1.81E-05	8.78E-07	1.57E-07	3	0.75	0.9983
UiO-66-NH_2 [Acetone/HCl]	2.06E-04	1.26E-05	8.78E-07	1.57E-07	3	0.81	0.9970
UiO-66-NH2-MD	2.01E-04	9.25E-06	6.67E-07	1.81E-07	3	0.86	0.9445
UiO-66-$(OH)_2$ [DMF/HCOOH]	3.14E-05	2.23E-06	8.78E-07	1.57E-07	3	0.77	0.9210
UiO-66 [DMF/HCOOH]	1.71E-04	7.97E-06	8.78E-07	1.57E-07	3	0.86	0.9975
UiO-66-OH [DMF/HCOOH]	1.51E-04	5.13E-06	8.78E-07	1.57E-07	3	0.89	0.9978
Strem UiO-66-NH_2	1.23E-04	7.16E-06	7.44E-07	3.53E-07	3	0.82	0.9989
	pH = 10						
MOF	**μ- sample**	**σ- sample**	**μ- control**	**σ- control**	**n**	**Z-factor**	**R^2 of slope**
UiO-66 [DMF/HCl]	1.29E-04	2.15E-05	2.41E-06	1.66E-06	14	0.46	0.9979
NU-1000	2.54E-04	2.99E-05	3.45E-06	1.17E-06	14	0.63	0.9962

UiO-66 [DMF/AcOH]	8.28E-05	1.87E-05	2.41E-06	1.66E-06	3	0.24	0.9941
UiO-67	1.51E-04	1.92E-05	2.14E-06	3.25E-07	3	0.61	0.9979
PCN-222	6.13E-04	4.63E-05	2.14E-06	3.25E-07	3	0.77	0.9945
MOF-808	6.10E-04	1.91E-05	4.39E-06	1.56E-07	3	0.90	0.9917
UiO-66-NH_2-HD	1.62E-04	5.88E-06	2.27E-06	2.15E-07	3	0.89	0.9972
UiO-66-NH_2 [DMF/HCl]	2.50E-04	1.24E-06	2.41E-06	1.66E-06	3	0.96	0.9933
UiO-66(Hf)	1.57E-05	3.51E-07	2.56E-06	5.66E-07	3	0.79	0.9861
UiO-66 [Acetone/HCl]	6.55E-05	4.20E-06	2.14E-06	3.25E-07	3	0.79	0.9915
UiO-66-NH_2 [Acetone/HCl]	2.88E-04	2.52E-06	2.14E-06	3.25E-07	3	0.97	0.9972
UiO-66-NH2-MD	2.38E-04	1.26E-05	2.27E-06	2.15E-07	3	0.84	0.9957
UiO-66-$(OH)_2$ [DMF/HCOOH]	3.44E-05	2.14E-06	2.14E-06	3.25E-07	3	0.77	0.9558
UiO-66 [DMF/HCOOH]	1.72E-05	1.49E-06	2.14E-06	3.25E-07	3	0.64	0.9862
UiO-66-OH [DMF/HCOOH]	3.36E-05	2.64E-06	2.14E-06	3.25E-07	3	0.72	0.9848
Strem UiO-66-NH_2	3.99E-04	5.34E-06	2.41E-06	1.66E-06	3	0.95	0.9950

Table S3. Material Identity, Formula Unit, Metal, Metal Atomic Number (*Z*), and Slope (average of three wells, in mM/sec × 10^{-6}) for DMNP Hydrolysis at pH = 8.0 and pH = 10.0 with standard deviations (σ) for each material tested. Rounded brackets () indicate metal; square brackets [] indicate modulator used in synthesis. Suppliers (where applicable) are listed before name of material.

#	Material	Formula Unit[a]	Metal	Z	Slope; pH=8	σ; pH=8	Slope; pH=10	σ; pH=10	Cit./ Sup.[b]
1	PIM-1	$C_{14}O_2N$	C	6	-4.49	6.55	-0.53	1.79	[11]
2	Coconut Cabon	C	C	6	1.97	4.93	0.17	1.00	GA
3	BPL	C	C	6	8.14	6.08	1.30	1.09	CCC
4	$Mg(OH)_2$	$Mg(OH)_2$	Mg	12	2.99	2.50	11.67	16.52	NAM
5	Al-PMOF	$TCPP(AlOH)_2$	Al	13	-3.18	3.01	-4.78	0.30	[12]
6	CAU-10-NH_2	$Al(OH)(ISO\text{-}NH_2)$	Al	13	10.39	11.85	8.43	18.01	[13]
7	CAU-10-CH_3	$Al(OH)(ISO\text{-}CH_3)$	Al	13	14.84	25.26	8.48	13.95	[13]
8	CAU-10-OH	Al(OH)(ISO-OH)	Al	13	0.88	5.41	0.80	2.27	[13]
9	MIL-96(Al)	$Al_{12}O(OH)_{18}(H_2O)_3(Al_2(OH)_4)(BTC)_6$	Al	13	0.44	1.11	1.94	3.48	[14]
10	MIL-53(Al)	Al(OH)(BDC)	Al	13	-2.72	1.24	-0.64	0.30	[15]
11	MIL-53(Al)-Br	Al(OH)(BDC-Br)	Al	13	-1.31	4.41	-1.09	0.24	[15]
12	MIL-53(Al)-NH_2	$Al(OH)(BDC\text{-}NH_2)$	Al	13	-1.13	0.90	-0.92	0.82	[15]
13	Al_2O_3	Al_2O_3	Al	13	-0.01	0.01	-0.31	0.29	NAM
14	Silicalite	SiO_2	Si	14	3.83	1.16	0.22	0.35	GA
15	SAPO-34	SiO_2	Si	14	-4.29	1.58	-0.42	0.37	GA
16	H-ZSM-5	SiO_2	Si	14	2.29	3.87	0.61	0.19	GA
17	HY	$(Si)_{0.5}(Al)_{0.5}O_2$	Si	14	-0.08	0.43	0.74	0.76	GA
18	Na-ZSM-5	$(Si)_{0.9}(Al)_{0.1}O_2$	Si	14	-2.58	2.84	1.32	1.45	GA
19	Zeolite 4A	SiO_2	Si	14	-0.84	0.64	0.03	1.20	ASGE
20	Aldrich MCM-41	SiO_2	Si	14	-0.11	0.24	0.08	0.06	SA
21	Y-54 DR	SiO_2	Si	14	-0.36	0.98	0.39	0.68	GA
22	MIL-125(Ti)-NH_2	$Ti_8O_8(OH)_4(BDC\text{-}NH_2)_6$	Ti	22	0.92	0.34	0.48	0.65	[16]
23	TiO_2	TiO_2	Ti	22	-1.37	0.76	-0.85	0.76	NAM
24	Aldrich TiO_2	TiO_2	Ti	22	0.65	7.07	-1.73	0.06	SA
25	Aldrich TiO_2 Anatase	TiO_2	Ti	22	0.64	0.97	-0.23	0.29	SA
26	Degussa P_{25} TiO_2	TiO_2	Ti	22	-2.62	3.90	-1.40	0.46	DC
27	PCN-415	$Ti_8Zr_2O_{12}(BDC)_{16}$	Zr/Ti	22	20.85	0.86	26.65	0.75	[17]
28	MIL-101(Cr)	$Cr_3F(H_2O)_2O(BDC)_3$	Cr	24	1.05	4.35	2.80	12.35	[18]

29	MIL-53(Cr)	$Cr(OH)(BDC)$	Cr	24	-1.48	0.32	-1.41	0.67	[19]
30	PCN-250(Mn)	$Mn_3(\mu_3\text{-}O)(H_2O)_3(ABTEC)_6$	Mn	25	0.63	0.65	2.01	4.50	NMT
31	MIL-53(Fe)	$Fe(OH)(BDC)$	Fe	26	-0.03	0.35	-3.57	1.59	[20]
32	MIL-88B(Fe)	$Fe_3O(BDC)_3(H_2O)_2(X)$, X=OH, Cl	Fe	26	3.60	4.35	7.93	12.47	[21]
33	MIL-100(Fe)	$Fe_3OX(BTC)_2$, X=OH, F, Cl	Fe	26	-3.67	4.74	2.25	4.12	[22]
34	Aldrich MIL-100(Fe)	$Fe(OH)(BTC)$	Fe	26	-5.59	34.54	-2.43	1.06	SA
35	Strem PCN-250(Fe)	$Fe_3(\mu_3\text{-}O)(H_2O)_3(ABTEC)_6$	Fe	26	0.17	3.08	-4.43	7.14	SC
36	PCN-250(Fe)	$Fe_3(\mu_3\text{-}O)(H_2O)_3(ABTEC)_6$	Fe	26	1.34	0.95	0.12	0.92	NMT
37	Fe_2O_3	Fe_2O_3	Fe	26	6.11	5.39	3.87	1.10	NAM
38	ZIF-67	$Co(MEIM)_2$	Co	27	3.13	4.69	2.58	6.39	[23]
39	Co-NIC	$Co_2(NIC)_4(\mu\text{-}H_2O)$	Co	27	0.01	0.03	0.16	0.75	[24]
40	Co_3O_4	Co_3O_4	Co	27	-4.25	0.85	-4.81	3.52	NAM
41	Zn/Co BTEC	$ZnCo(BTEC)$	Zn/Co	27	0.72	1.40	-0.22	0.27	[25]
42	ZIF-8/67	$ZnCo(MEIM)_4$	Zn/Co	27	2.29	2.38	0.52	0.61	[23]
43	Ni-NIC	$Ni_2(NIC)_4(lH_2O)$	Ni	28	0.14	0.26	-0.13	0.11	[24]
44	CuBDC	$CuO(BDC)_2$	Cu	29	0.99	2.82	-2.22	6.59	[26]
45	Cu-PCN	$Cu_2(PCN)_2(H_2O)_2$	Cu	29	-1.21	2.16	2.06	5.84	[27]
46	PCN-250(Cu)	$Cu_3(\mu_3\text{-}O)(H_2O)_3(ABTEC)_6$	Cu	29	1.58	2.81	6.48	8.38	NMT
47	MOF-74(Cu)	$Cu_2(DOBDC)$	Cu	29	6.90	7.87	1.60	4.82	NMT
48	Aldrich HKUST-1	$Cu_3(BTC)_2$	Cu	29	11.16	10.31	-3.12	0.62	SA
49	MOF-508	Zn (BDC) (BPY)	Zn	30	-2.43	4.30	0.48	1.08	[28]
50	ZIF-8	$Zn(MEIM)_2$	Zn	30	0.28	5.03	0.76	3.17	[23]
51	ZIF-4	$Zn(IM)_2$	Zn	30	-0.72	2.65	-0.94	1.82	See Above
52	ZIF-62	$Zn(IM)_{1.75}(BIM)_{0.25}$	Zn	30	0.66	1.73	1.72	1.41	[29]
53	ZIF-71	$Zn(IM\text{-}Cl_2)_2$	Zn	30	1.77	3.41	-2.02	1.12	[30]
54	ZnO	ZnO	Zn	30	6.40	16.92	-1.57	1.11	NAM
55	DMOF-1	$Zn_2(BDC)_2DABCO$	Zn	30	5.33	7.38	0.53	1.33	NMT
56	PCN-700	$Zr_6O_8(OH)_8(Me_2\text{-}BPDC)_4$	Zr	40	8.93	4.37	13.83	13.59	[31]
57	MOF-801	$Zr_6O_4(OH)_4(FUM)_6$	Zr	40	4.33	0.63	11.22	6.20	[32]
58	MOF-802	$Zr_6O_4(OH)_4(PZDC_4)_5(HCOO)_2(H_2O)_2$	Zr	40	3.69	1.98	5.27	1.66	[32]
59	UiO-66 [DMF/AcOH]	$Zr_6O_6(BDC)_{12}$	Zr	40	142.68	14.70	20.31	4.68	[1]
60	UiO-66 [DMF/HCl]	$Zr_6O_6(BDC)_{12}$	Zr	40	100.62	6.77	11.21	1.44	[33]
61	UiO-66-NH_2 [DMF/AcOH]	$Zr_6O_6(BDC\text{-}NH_2)_{12}$	Zr	40	24.28	1.02	44.86	2.70	[1*]
62	UiO-66-NH_2 [DMF/HCl]	$Zr_6O_6(BDC\text{-}NH_2)_{12}$	Zr	40	73.34	3.94	62.24	0.31	[33]
63	Strem UiO-66-NH_2	$Zr_6O_6(BDC\text{-}NH_2)_{12}$	Zr	40	35.18	2.06	99.57	1.34	SC

64	UiO-66-SO_3H [DMF/BzOH]	$Zr_6O_6(BDC\text{-}SO_3H)_{12}$	Zr	40	16.63	0.80	9.68	0.36	[34]
65	UiO-66-COOH [DMF/AcOH]	$Zr_6O_6(BDC\text{-}COOH)_{12}$	Zr	40	2.59	0.03	7.46	0.28	See above
66	DUT-67(Zr)	$Zr_6O_6(OH)_2(TDC)_4$	Zr	40	3.46	16.78	5.66	0.52	[35]
67	NU-1000	$Zr_6(OH)_{16}(TBAPY)_2$	Zr	40	34.71	6.49	56.57	2.96	NMT
68	polyUiO-66	$Zr_6O_6(pbdc8\text{-}a\text{-}u)_6$	Zr	40	14.30	1.93	18.25	7.36	[36]
69	UiO-66-NH_2-LD	$Zr_6O_6(BDC\text{-}NH_2)_{12}$	Zr	40	4.02	2.28	44.20	7.68	[37]
70	UiO-66-NH_2-MD	$Zr_6O_6(BDC\text{-}NH_2)_{12}$	Zr	40	57.63	2.66	59.20	3.17	[37]
71	UiO-66-NH_2-HD	$Zr_6O_6(BDC\text{-}NH_2)_{12}$	Zr	40	91.86	3.23	40.58	1.47	[37]
72	$Zr(OH)_4$ Type B	$Zr(OH)_4$	Zr	40	4.94	2.91	2.79	3.97	MEL
73	$Zr(OH)_4$ Type A	$Zr(OH)_4$	Zr	40	-3.44	2.75	2.43	0.91	MEL
74	$Zr(OH)_4$ Type C	$Zr(OH)_4$	Zr	40	4.18	0.48	5.63	12.90	MEL
75	$Zr(OH)_4$ 0880	$Zr(OH)_4$	Zr	40	4.24	0.64	2.30	1.63	MEL
76	$Zr(OH)_4$ Type C $KMnO_4$	$Zr(OH)_4$	Zr	40	4.32	2.53	0.53	3.73	MEL
77	UiO-67	$Zr_6O_6(BPDC)_{12}$	Zr	40	141.79	8.54	37.24	4.81	NMT
78	UiO-66 [Acetone/HCl]	$Zr_6O_6(BDC)_{12}$	Zr	40	63.07	5.21	15.91	1.05	[38]
79	PCN-222	$Zr_6(\mu_3\text{-}OH)_8(OH)_8(TCPP)_2$	Zr	40	117.38	38.93	153.05	11.60	[39]
80	UiO-66-NH_2 [Acetone/HCl]	$Zr_6O_6(BDC\text{-}NH_2)_6$	Zr	40	58.83	3.63	71.50	0.63	[38]
81	UiO-66-NH_2 [DMF/HCOOH]	$Zr_6O_6(BDC\text{-}NH_2)_6$	Zr	40	18.71	2.07	2.44	0.42	[34]
82	UiO-66-$(COOH)_2$ [DMF/HCOOH]	$Zr_6O_6(BDC\text{-}(COOH)_2)_{12}$	Zr	40	8.81	0.64	8.03	0.54	[34]
83	UiO-66-$(OH)_2$ [DMF/HCOOH]	$Zr_6O_6(BDC\text{-}(OH)_2)_{12}$	Zr	40	49.70	1.63	14.29	1.26	[34]
84	UiO-66 [DMF/HCOOH]	$Zr_6O_6(BDC)_{12}$	Zr	40	48.89	2.29	3.83	0.37	[34]
85	UiO-66-OH [DMF/HCOOH]	$Zr_6O_6(BDC\text{-}OH)_{12}$	Zr	40	42.96	1.47	8.20	0.66	[34]
86	UiO-66-NO_2 [DMF/HCOOH]	$Zr_6O_6(BDC\text{-}NO_2)_{12}$	Zr	40	9.50	0.79	3.36	0.72	[34]
87	UiO-66-OCF_3 [DMF/HCOOH]	$Zr_6O_6(BDC\text{-}OCF_3)_{12}$	Zr	40	12.47	0.85	53.49	5.94	[34]
88	MOF-808	$Zr_6O_4(OH)_4(BTC)_2(COOH)_6$	Zr	40	95.90	4.89	151.88	4.80	[32]
89	UiO-66(Ce)	$Ce_6O_6(BDC)_{12}$	Ce	58	4.64	1.71	4.85	5.27	[40]
90	CeO_2	CeO_2	Ce	58	9.26	4.83	18.35	4.78	NAM
91	Eu_2O_3	Eu_2O_3	Eu	63	-0.58	7.58	-2.05	0.25	NAM
92	DUT-67(Hf)	$Hf_6O_6(OH)_2(TDC)_4$	Hf	72	4.21	0.31	1.70	0.87	[35]
93	UiO-66(Hf)	$Hf_6O_6(BDC)_{12}$	Hf	72	71.31	8.78	3.24	0.09	[1]

[a] Ligand Abbreviations: (ISO) = isophthalic acid; (BTC) = benzene-1,3,5-tricarboxylic acid; (BDC) = benzene-1,4-dicarboxylic acid; (ABTEC) = azobenzene tetracarboxylic acid; (MEIM) = 2-methyl-1*H*-imidazole; (NIC) = nicotinic acid; (BTEC) = 1,2,4,5-Benzenetetracarboxylic acid; (PCN) = 4-pyridinecarboxylic acid; (DOBDC) = 2,5-dihydroxyterephthalic acid; (BPY) = 4,4′−bipyridyl; (IM) = 1*H*-imidazole; (BIM) = 1*H*-benzo[*d*]imidazole; (DABCO) = 1,4-diazabicyclo[2.2.2]octane; (Me_2-BPDC) =

2,2'-dimethyl-[1,1'-biphenyl]-4,4'-dicarboxylic acid; (FUM) = fumaric acid; (PZDC) = 1*H*-pyrazole-3,5-dicarboxylic acid; (TDC) = 2,5-Thiophenedicarboxylic acid; (TBAPY) = 1,3,6,8-tetrakis(p-benzoate)pyrene; (BPDC) = [1,1'-biphenyl]-4,4'-dicarboxylic acid; (TCPP) = meso-tetra(4-carboxyl-phenyl)porphyrin;

[b] Supplier Abbrviations: NAM = Nanostructured & Amorphous Materials; GA = Guild Associates; CCC = Calgon Carbon Corporation; SA = Sigma Aldrich; ASGE = Advanced Specialty Gas Equipment; DC = Degussa Corporation; NMT = NuMat Technologies; SC = Strem Chemicals; MEL = Magnesium Electron, Inc.

Table S4. Particle size and DMNP hydrolysis rates (average of three wells, in mM/sec × 10^{-6}) in for four UiO-66 MOFs (Subset 1) in 20 mM N-ethylmorpholine at pH= 8.0 and 10.0.

#	MOF	Particle Size (nm)		pH=8		pH=10	
		average	std. dev.	Slope	σ	Slope	σ
78	UiO-66 [Acetone/HCl]	210.8	182.5	22.0	1.8	6.3	0.4
84	UiO-66 [HCOOH]	190.5	49.9	17.0	0.8	1.5	0.1
59	UiO-66 [DMF/AcOH]	131.4	15.7	49.7	5.1	8.1	1.9
60	UiO-66 [DMF/HCl]	145.0	35.7	38.4	3.5	2.3	0.2

Table S5. DMNP hydrolysis rates (average of three wells, in arbitrary units of rate) of selected MOFs in 20 mM *N*-ethylmorpholine at pH = 8.0, 9.0, and 10.0.

#	MOF	pH=8		pH=9		pH=10	
		Slope	σ	Slope	σ	Slope	σ
69	UiO-66-NH_2-Low Defect	1.40	0.79	2.87	0.77	17.64	3.06
70	UiO-66-NH_2-Mid Defect	20.07	0.92	36.40	5.19	23.62	1.26
71	UiO-66-NH_2-High Defect	31.99	1.12	47.27	4.23	16.19	0.59

Table S6. Calibration Curves for p-nitrophenol in buffer solutions

pH = 10		pH = 8	
[p-nitrophenol]	**Abs**	**[p-nitrophenol]**	**Abs**
0.0000	0.0495	0.0000	0.0494
0.0766	0.3562	0.0766	0.3265
0.1531	0.6747	0.1531	0.5921
0.3063	1.2766	0.3063	1.1318
0.6125	2.4959	0.6125	2.1853
slope (Abs/mM)	3.9904	**slope (Abs/mM)**	3.4825
R^2	1.0000	**R^2**	0.9999

Table S7. Dilution ratios for preparation of MOF suspensions used in development of HTS at different concentrations.

Concentration (µg/mL)	MOF+Buffer (µL)	Buffer (µL)
600	500	500
450	375	625
300	250	750
150	125	875
100	93.8	906.2
75	62.5	937.5

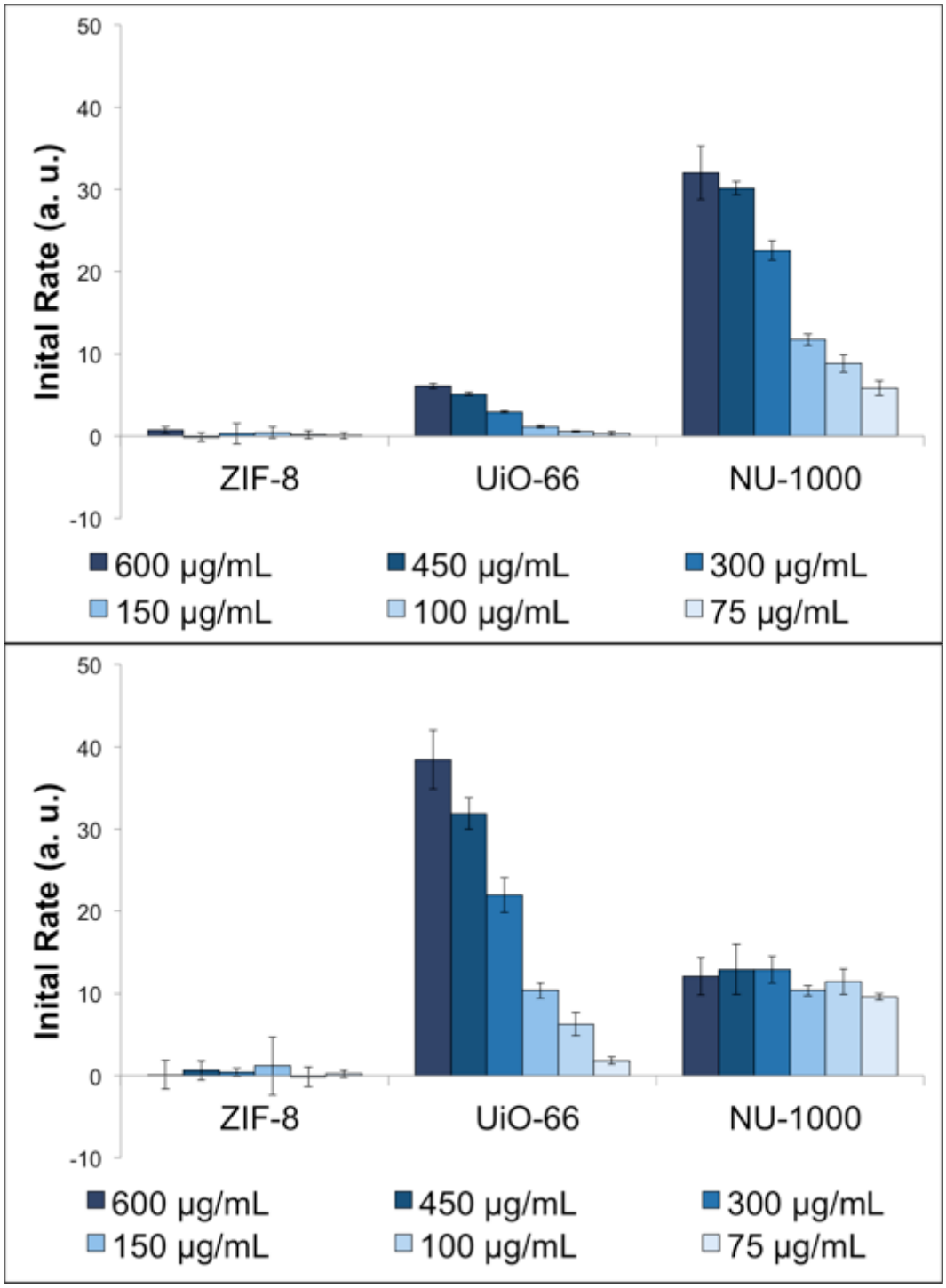

Figure S1. DMNP hydrolysis rates for ZIF-8, UiO-66, and NU-1000 for N-ethylmorpholine at pH = 10.0 (*top*) and pH = 8.0 (*bottom*).

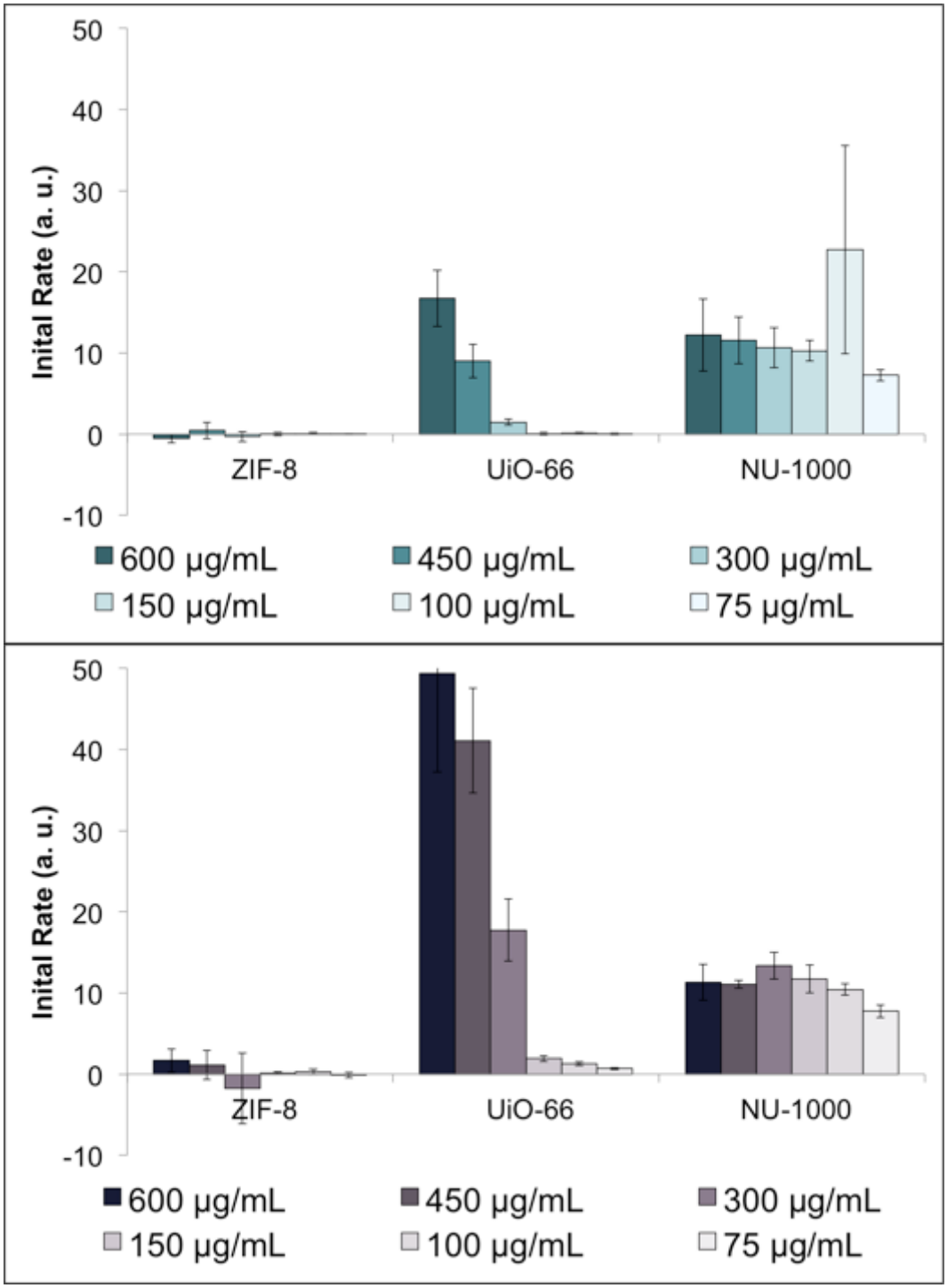

Figure S2. DMNP hydrolysis rates for ZIF-8, UiO-66, and NU-1000 for pH=8.0 in Tris (*top*) and HEPES (*bottom*) buffer.

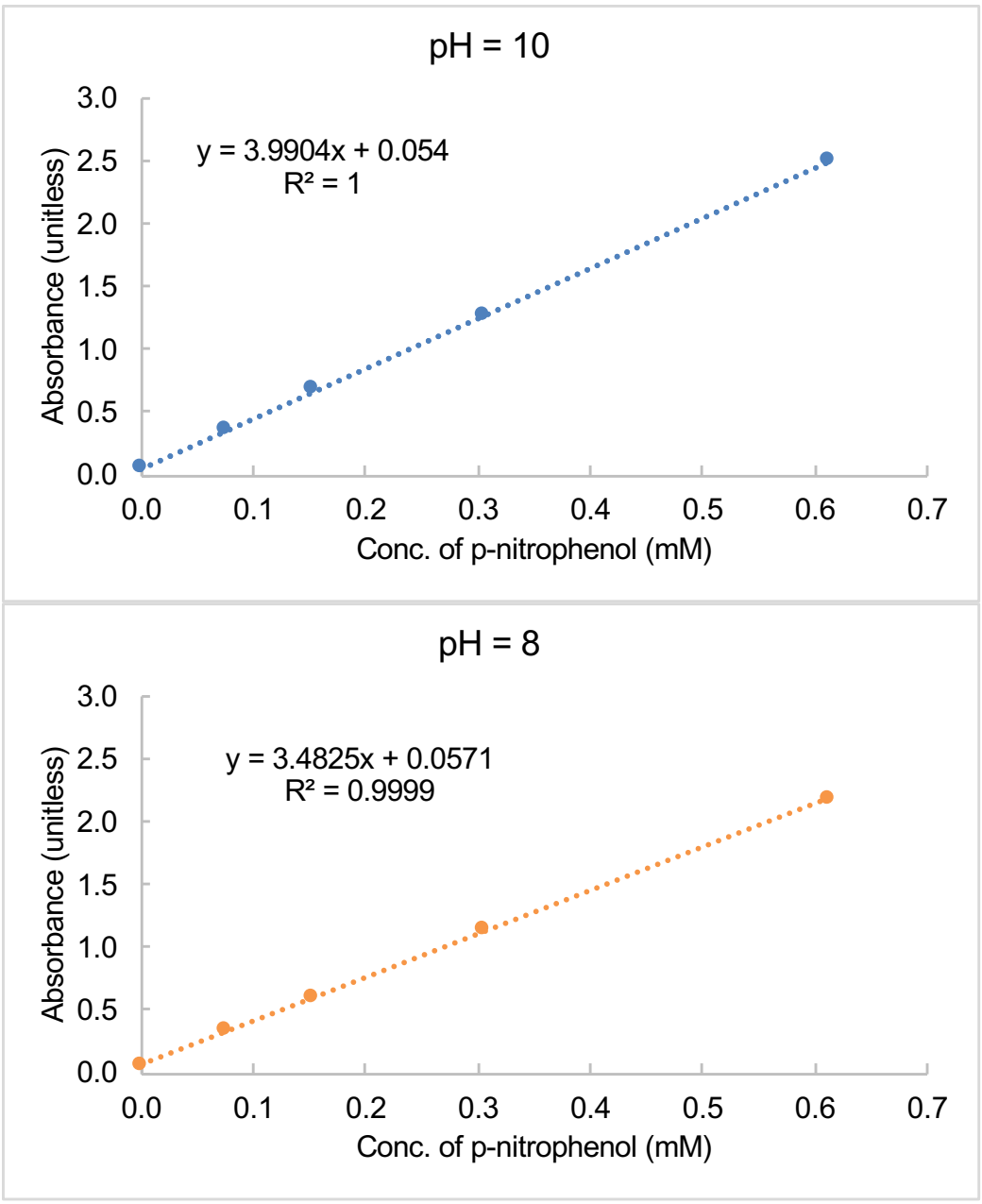

Figure S3. Calibration Curves for *p*-nitrophenol at pH = 10.0 (*top*) and pH = 8.0 (*bottom*).

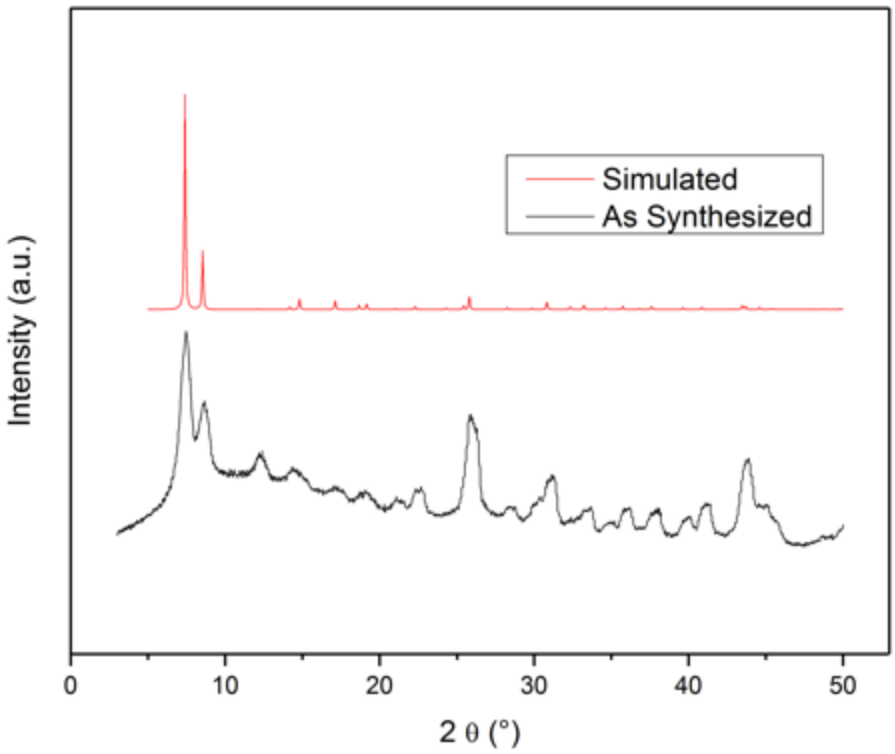

Figure S4. PXRD of as-synthesized UiO-66 [Acetone/HCl].

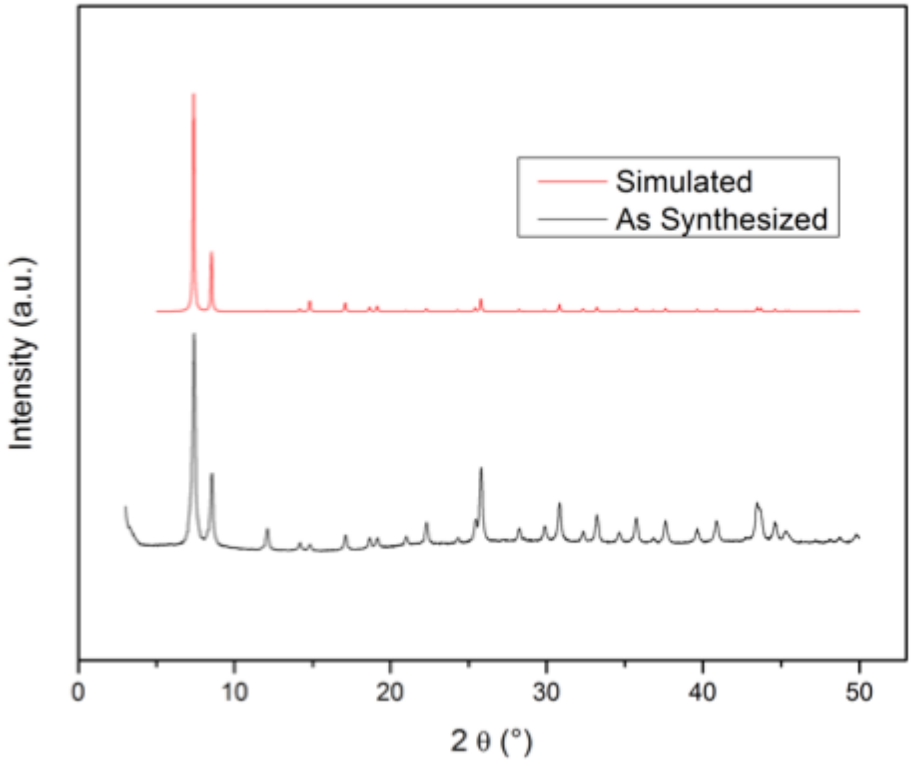

Figure S5. PXRD of as-synthesized UiO-66 [DMF/HCl].

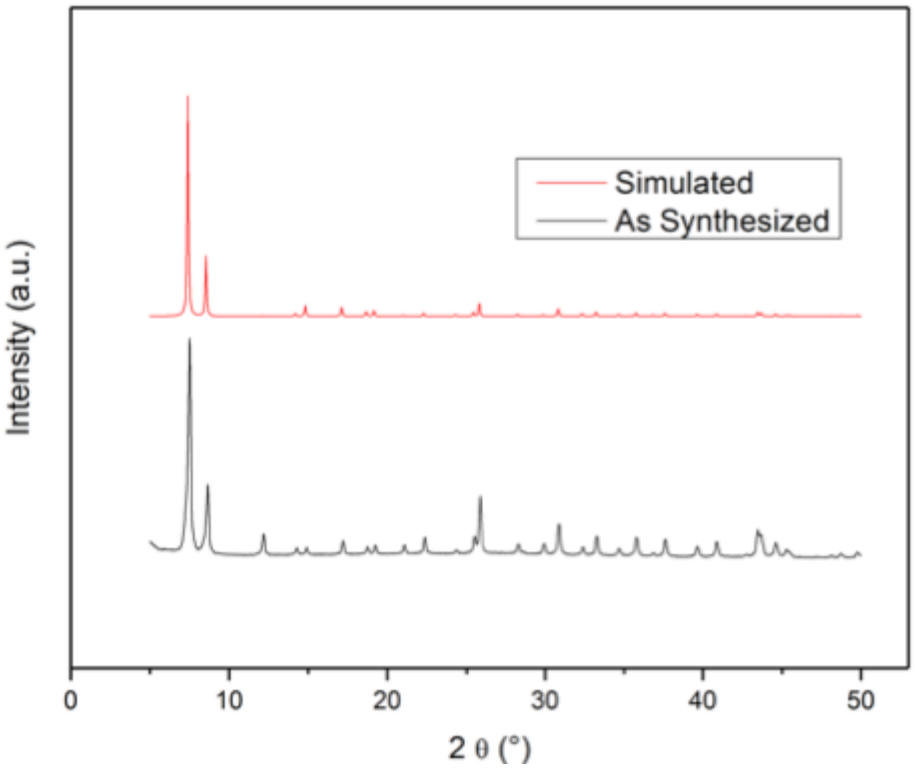

Figure S6. PXRD of as-synthesized UiO-66 [DMF/AcOH].

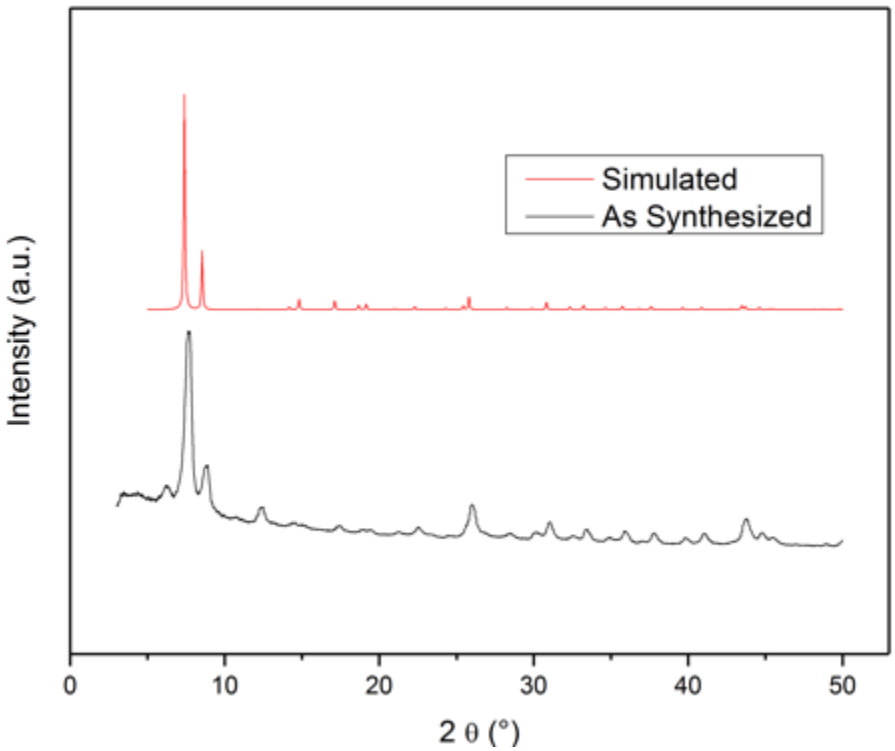

Figure S7. PXRD of as-synthesized UiO-66 [DMF/HCOOH].

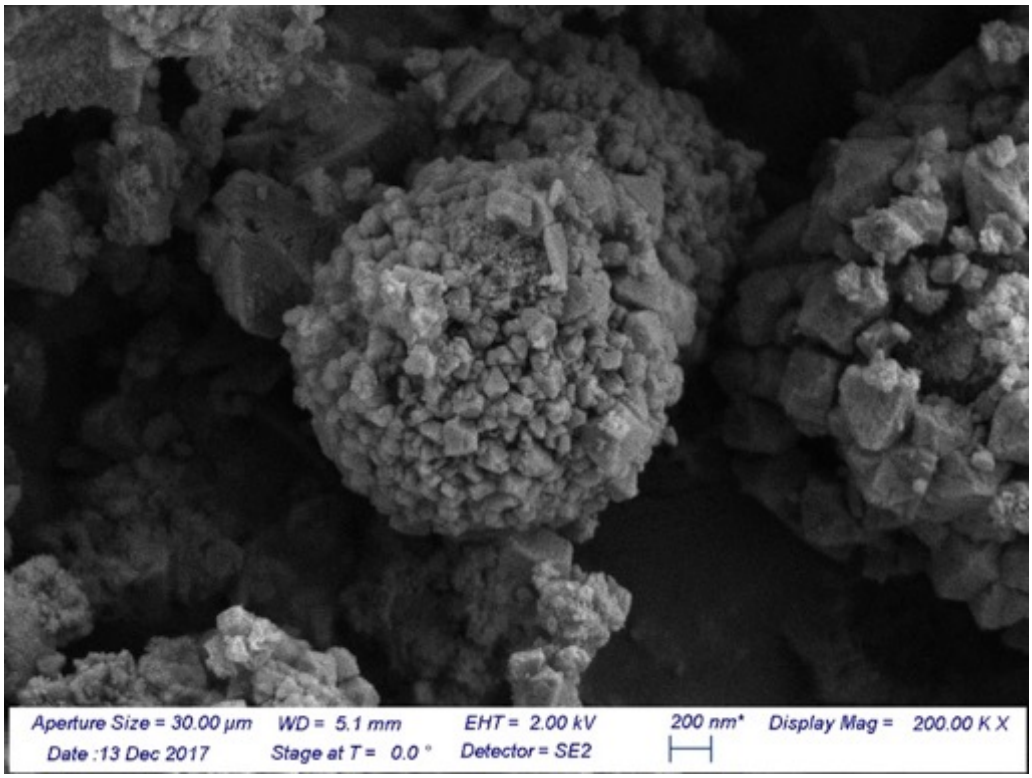

Figure S8. SEM image of UiO-66 [Acetone/HCl].

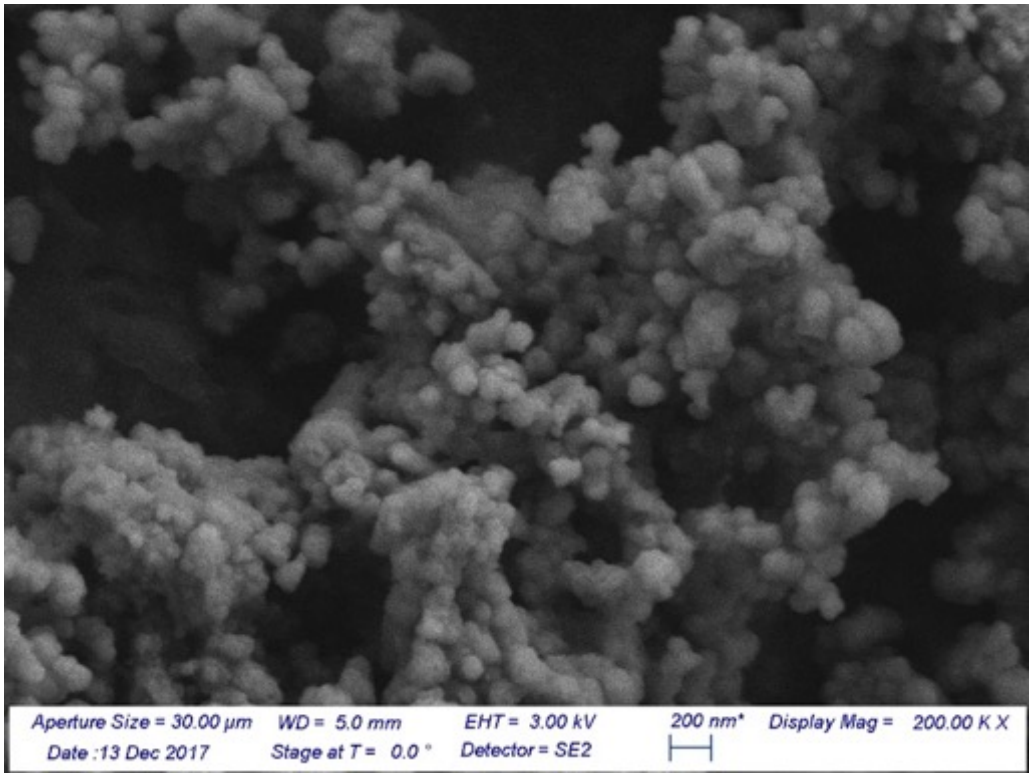

Figure S9. SEM image of UiO-66 [DMF/HCl].

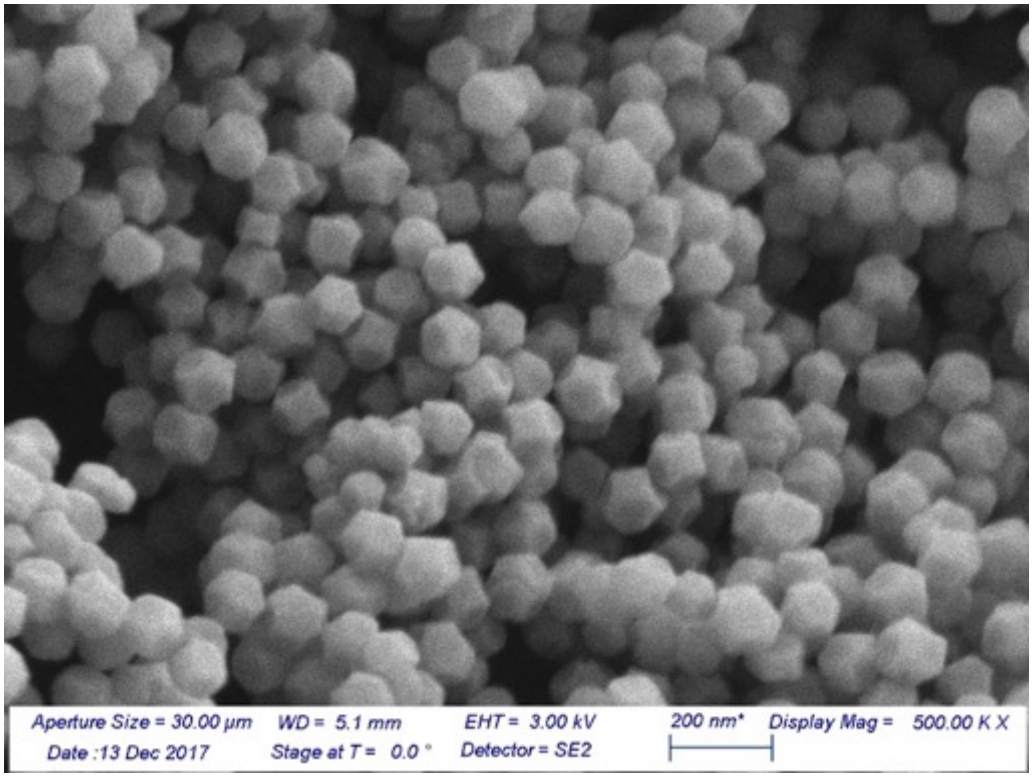

Figure S10. SEM image of UiO-66 [DMF/AcOH].

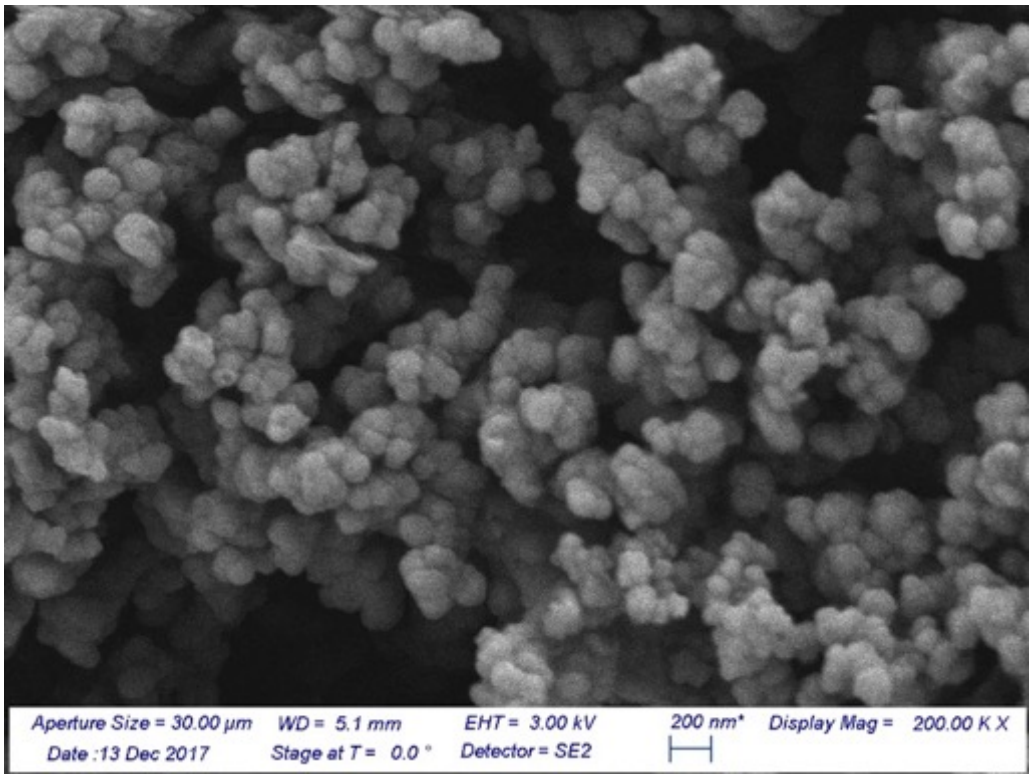

Figure S11. SEM images of UiO-66 [DMF/HCOOH].

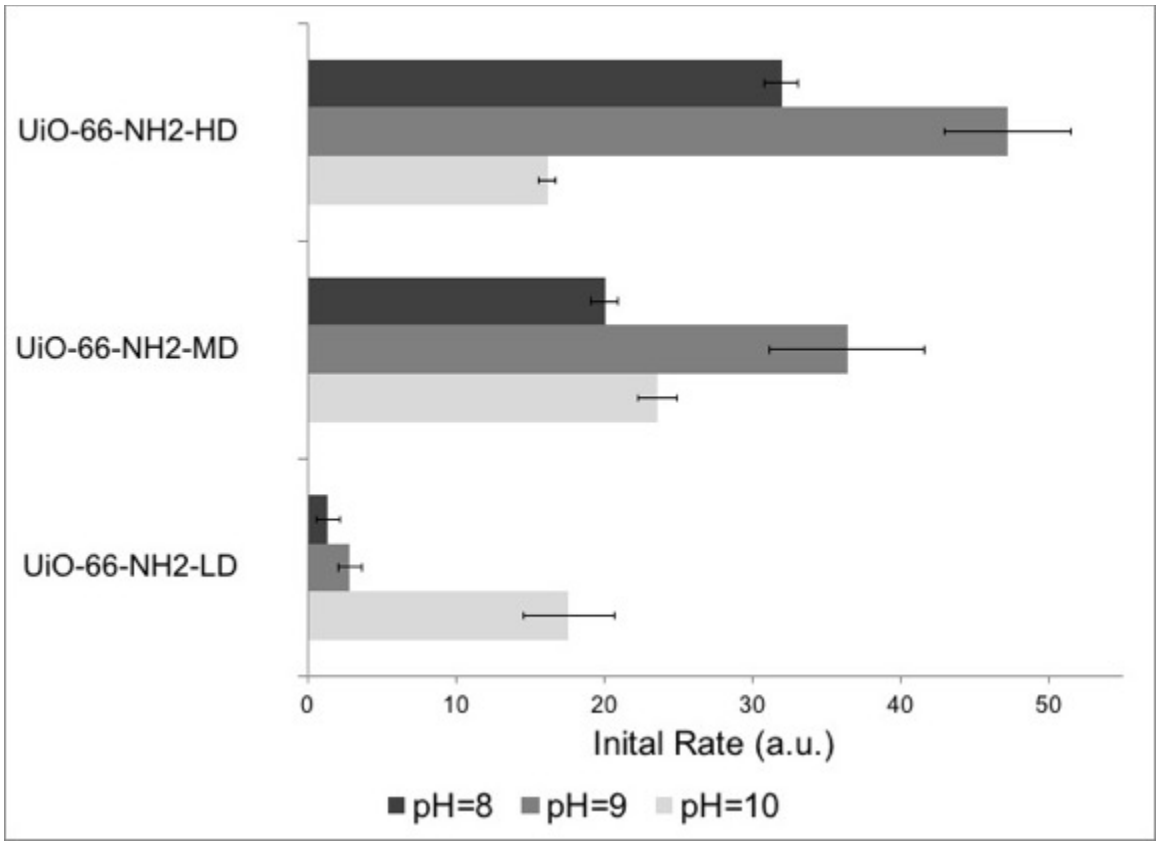

Figure S12. DMNP hydrolysis rates for UiO-66 at three concentrations of defects sites (low, medium, and high) in 20 mM *N*-ehtylmorpholine at pH = 8.0, 9.0, and 10.0.

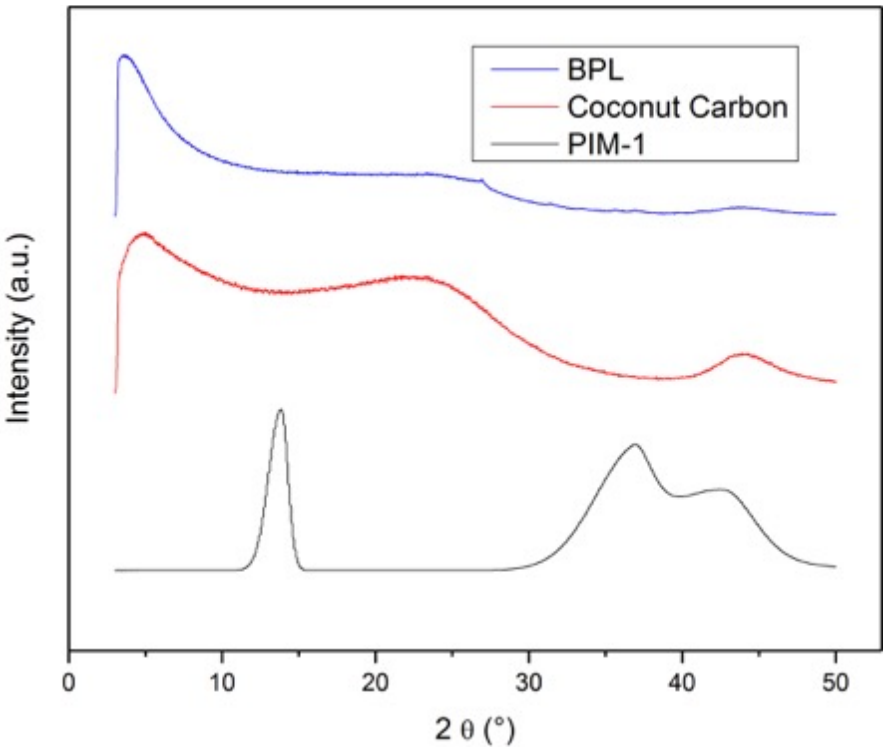

Figure S13. PXRD of as synthesized carbon materials: PIM-1, Coconut Carbon, and BPL.

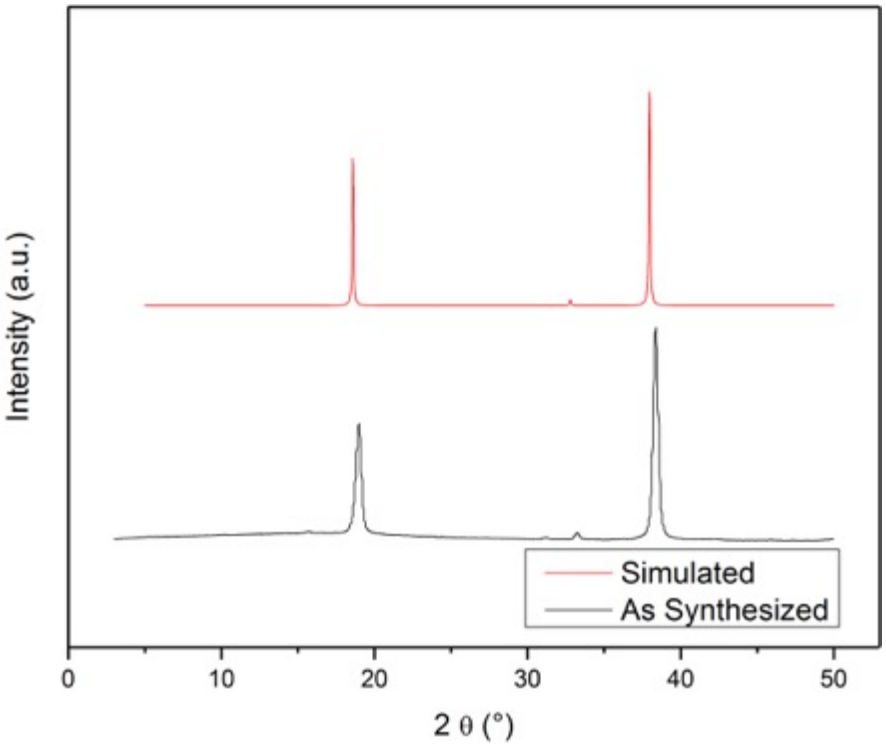

Figure S14. PXRD of as-purchased $Mg(OH)_2$.

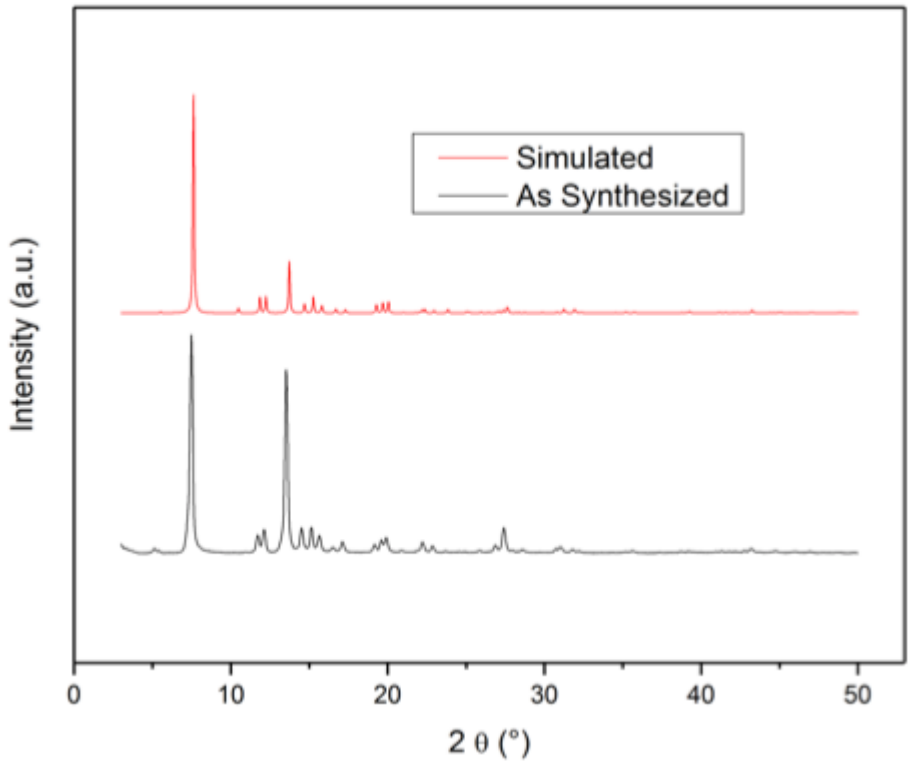

Figure S15. PXRD of as-synthesized Al-PMOF.

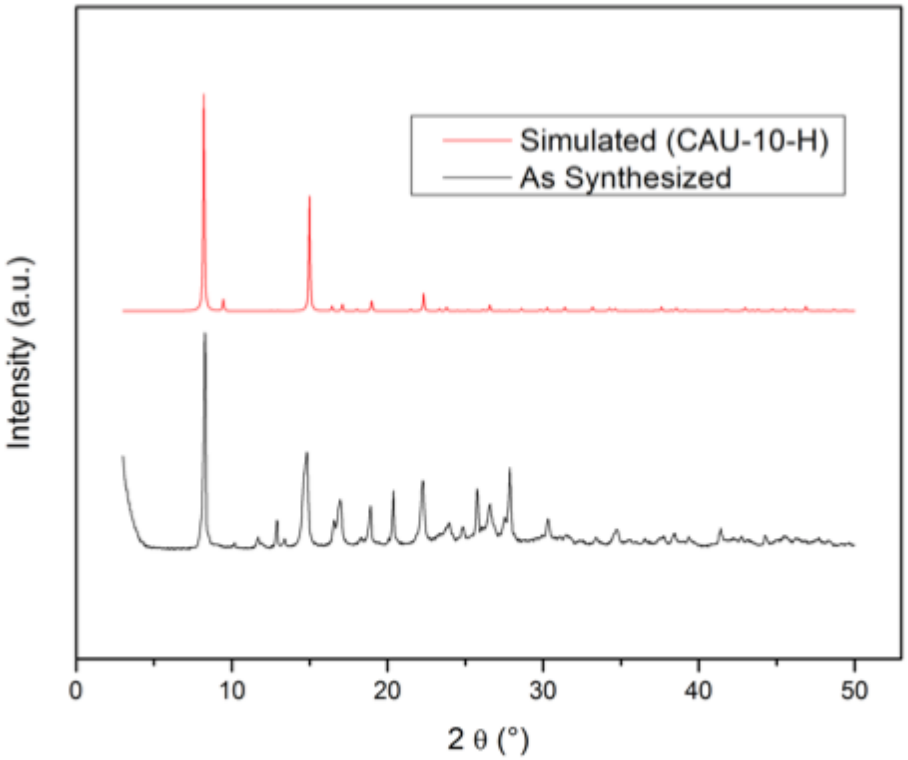

Figure S16. PXRD of as-synthesized CAU-10-NH_2.

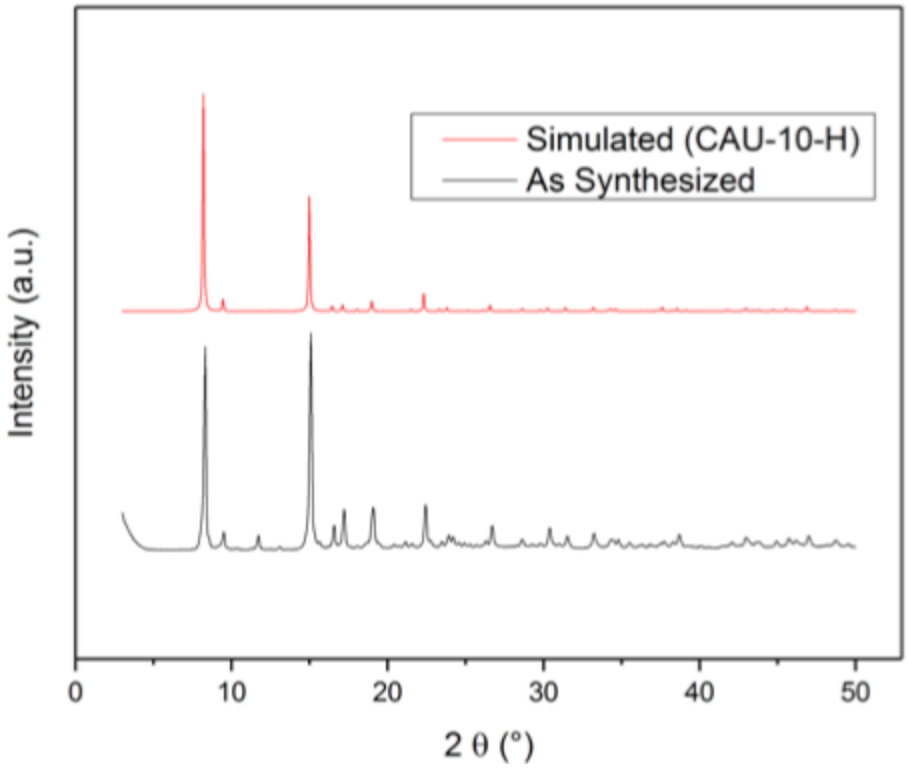

Figure S17. PXRD of as-synthesized CAU-10-CH_3.

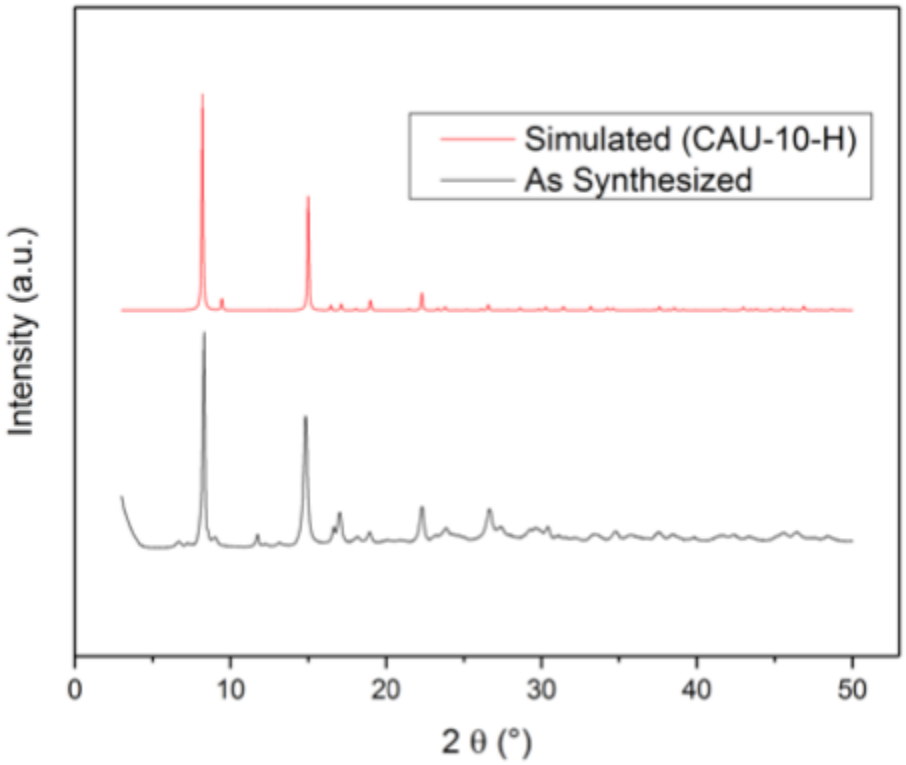

Figure S18. PXRD of as-synthesized CAU-10-OH.

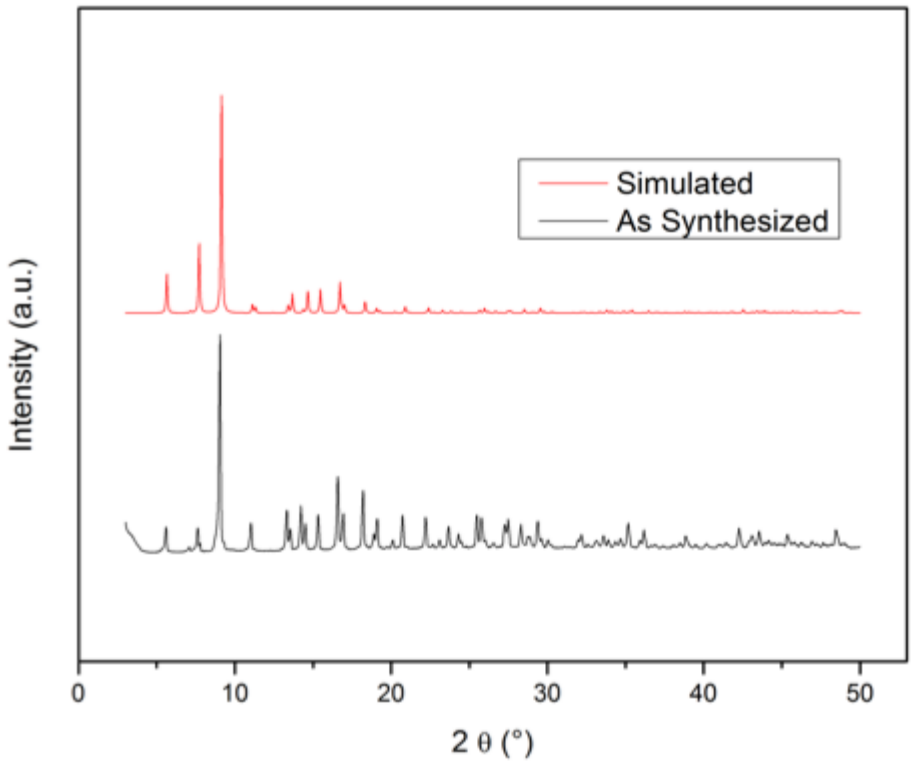

Figure S19. PXRD of as-synthesized MIL-96(Al).

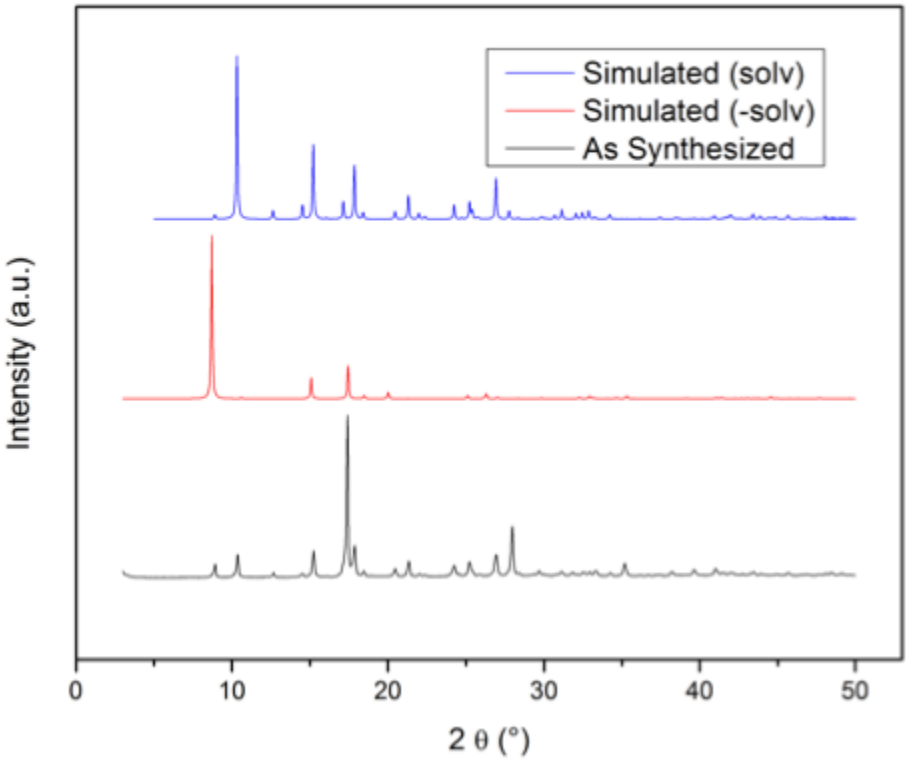

Figure S20. PXRD of as-synthesized MIL-53(Al).

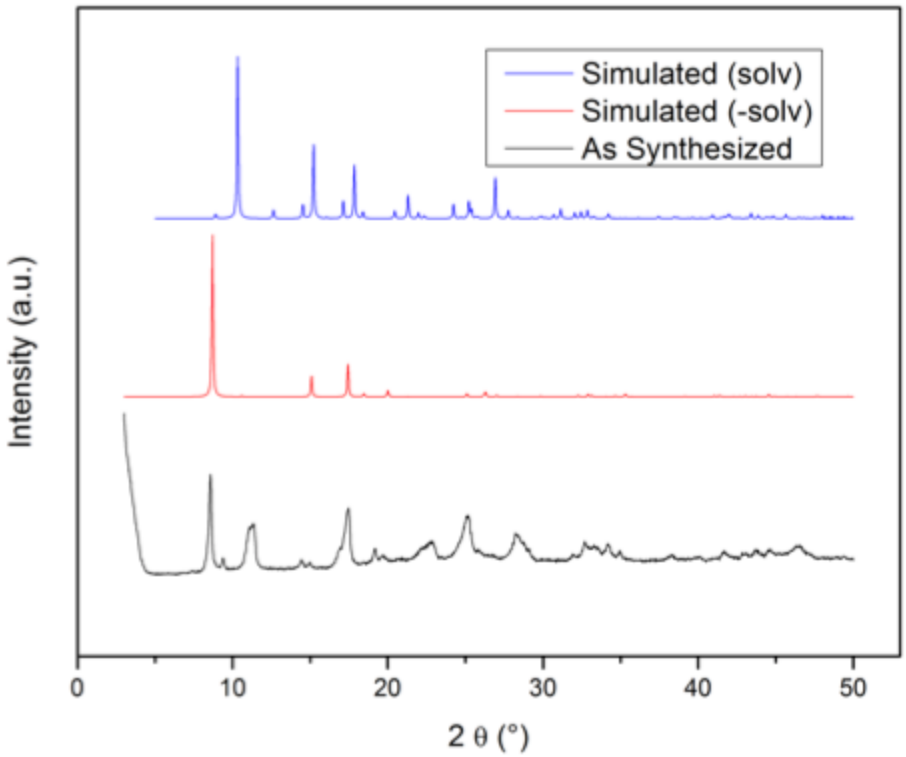

Figure S21. PXRD of as-synthesized MIL-53(Al)-Br.

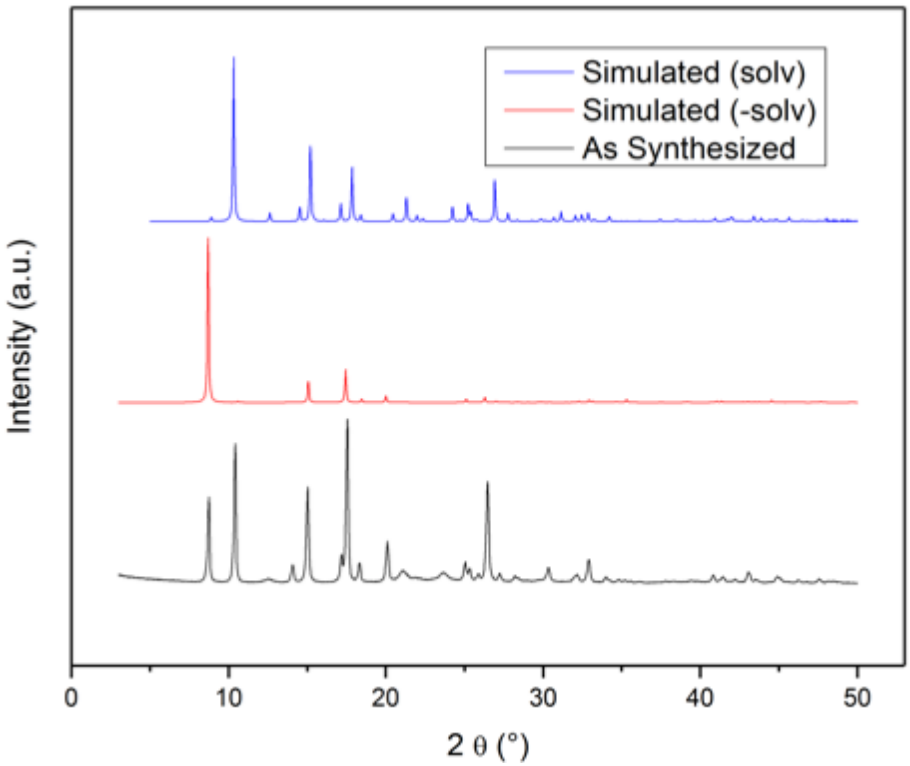

Figure S22. PXRD of as-synthesized MIL-53(Al)-NH_2.

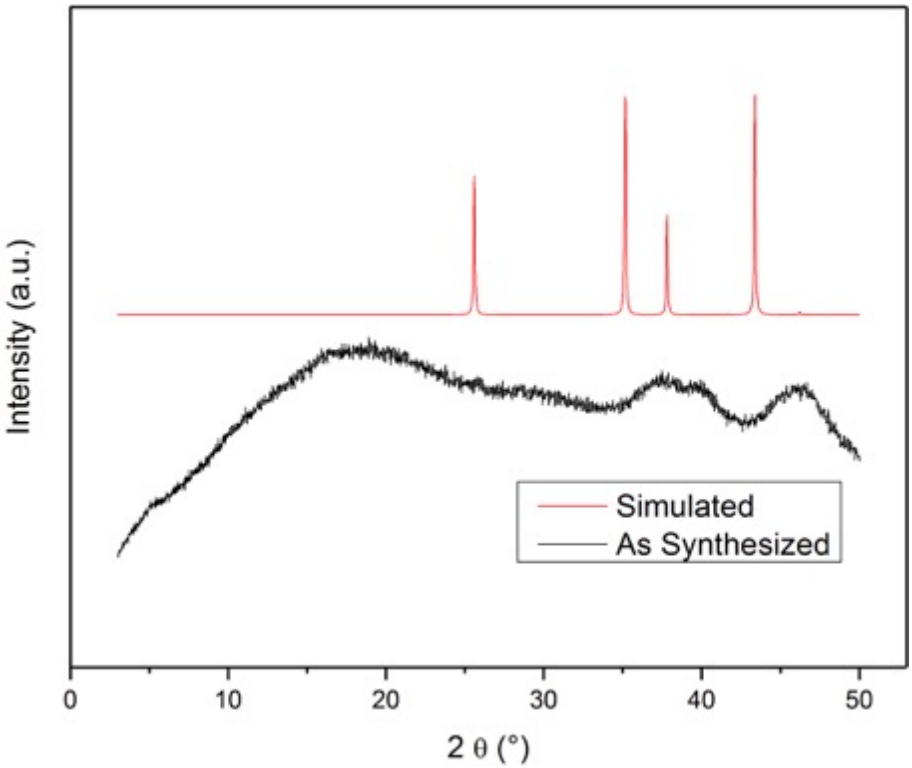

Figure S23. PXRD of as-purchased Al_2O_3.

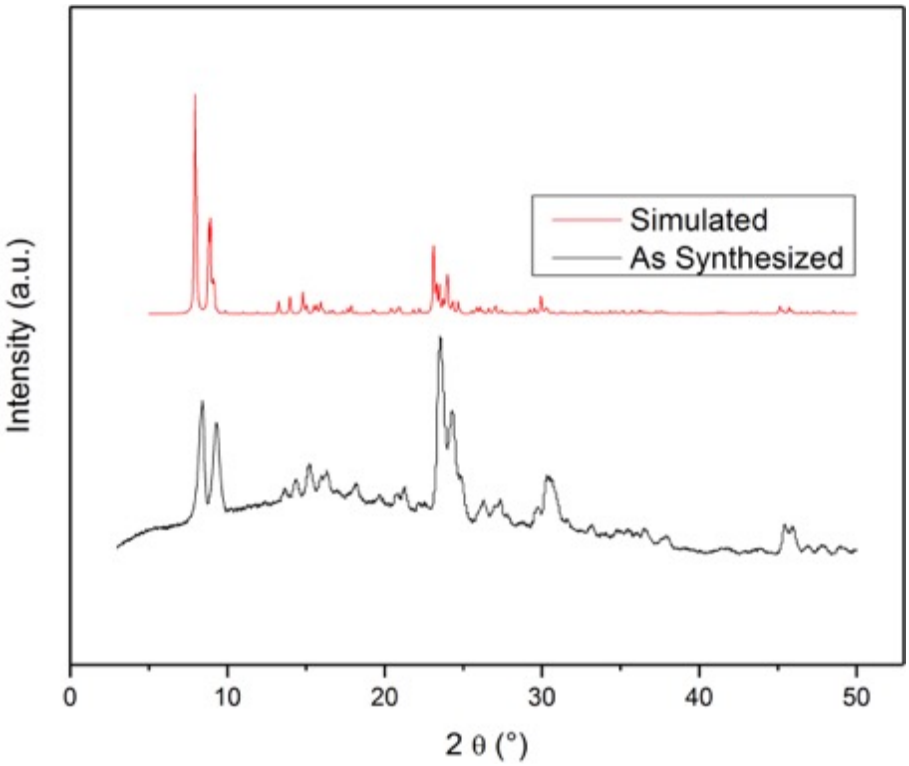

Figure S24. PXRD of as-purchased Silicalite.

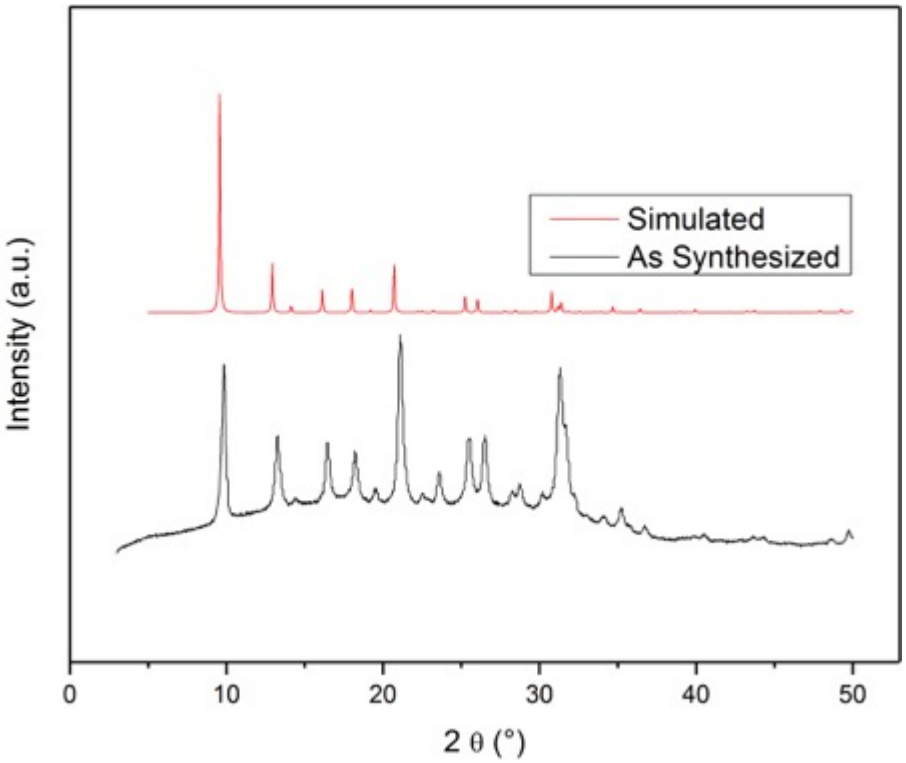

Figure S25. PXRD of as-purchased SAPO-34**.**

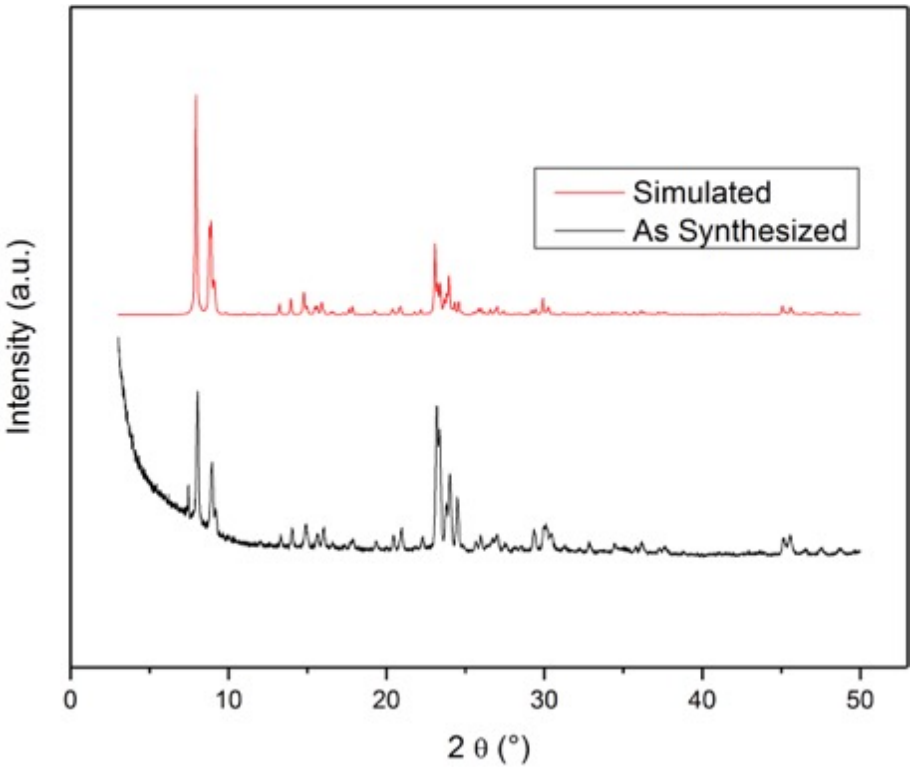

Figure S26. PXRD of as-purchased H-ZSM-5.

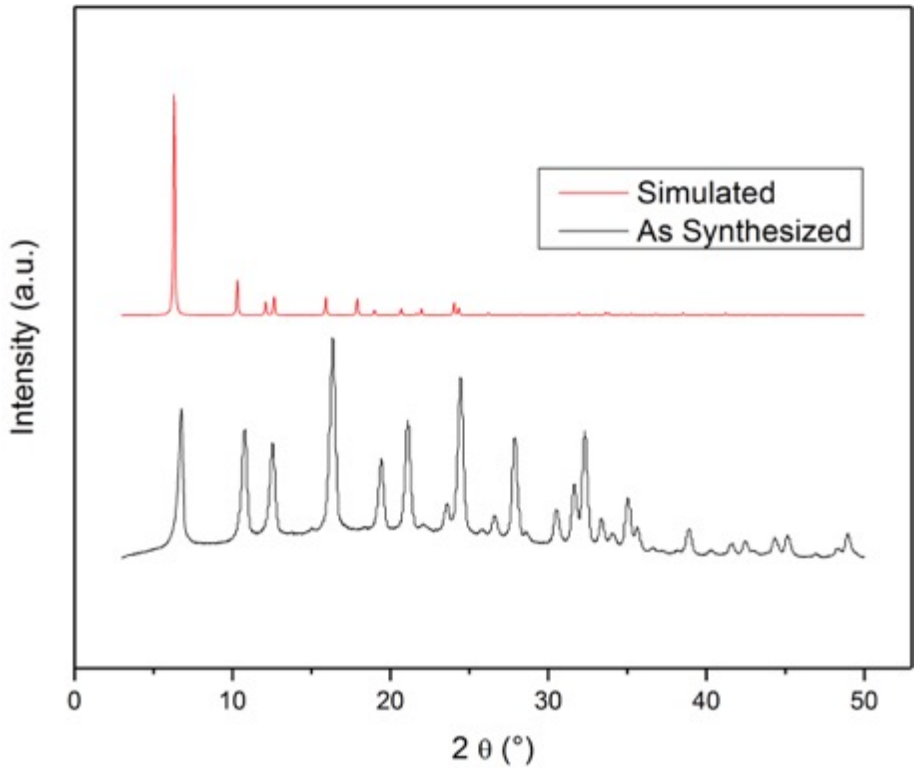

Figure S27. PXRD of as-purchased HY.

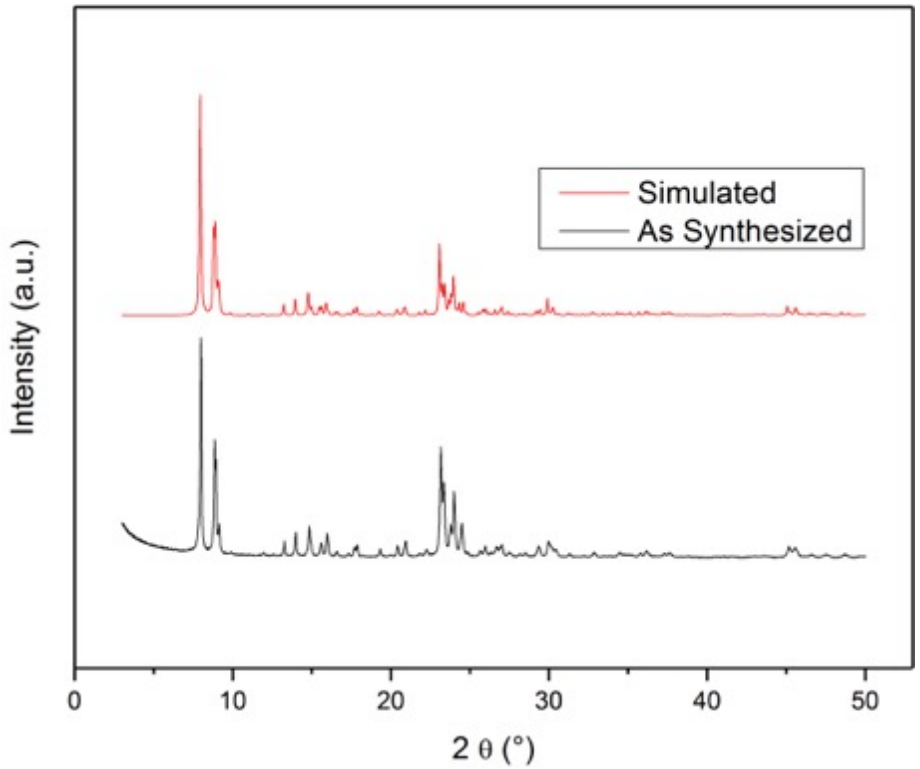

Figure S28. PXRD of as-purchased Na-ZSM-5.

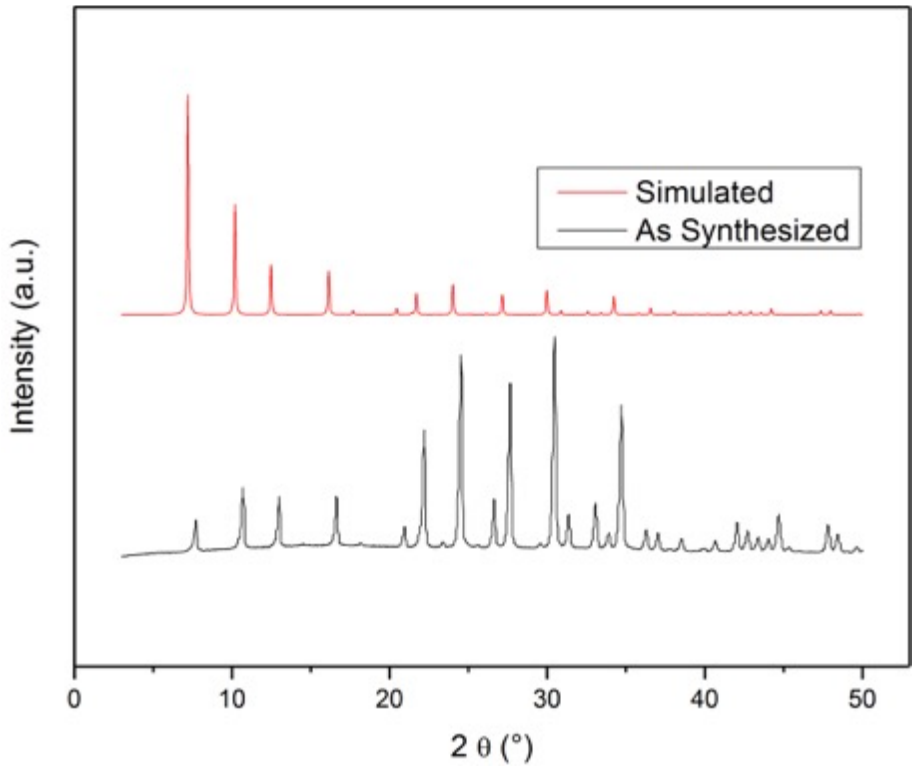

Figure S29. PXRD of as-purchased Zeolite 4A.

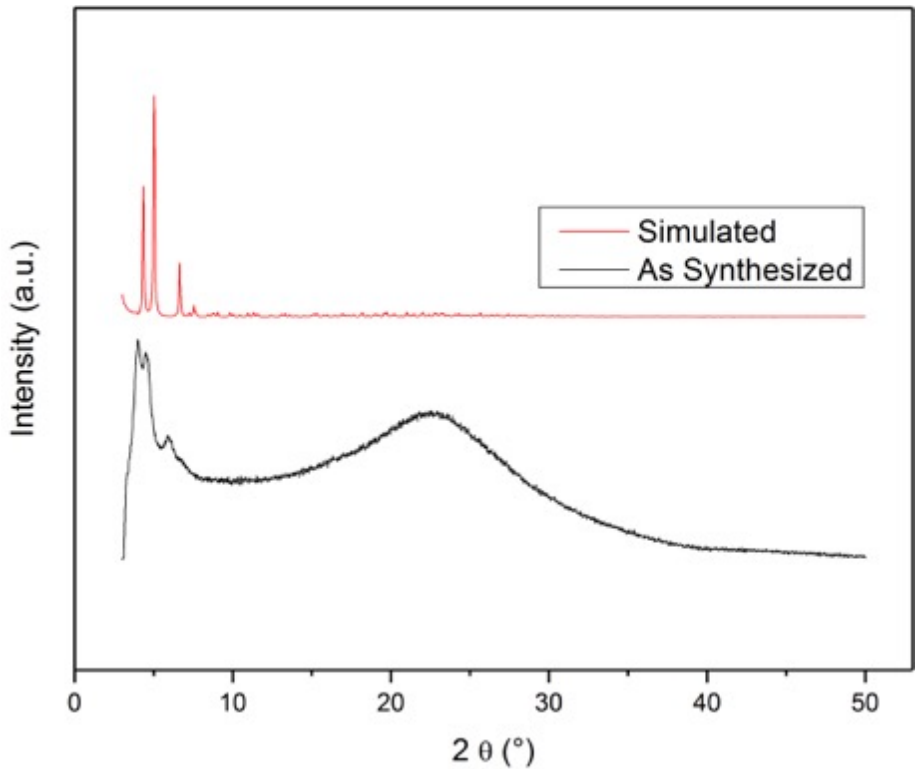

Figure S30. PXRD of as-purchased Aldrich MCM-41**.**

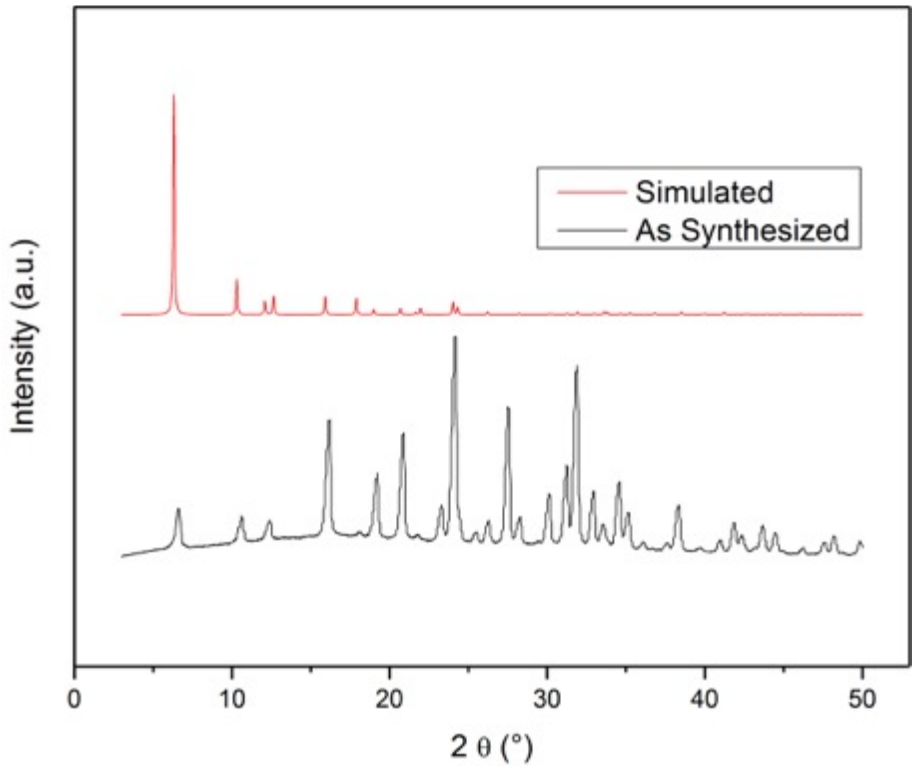

Figure S31. PXRD of as-purchased Y-54 DR.

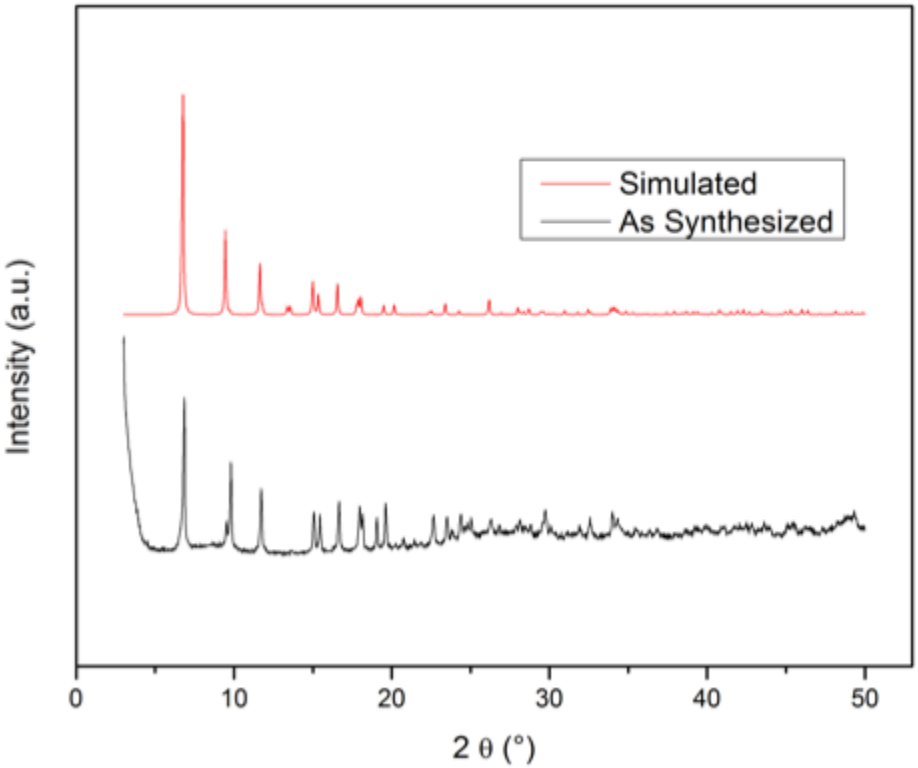

Figure S32. PXRD of as-synthesized MIL-125(Ti)-NH_2.

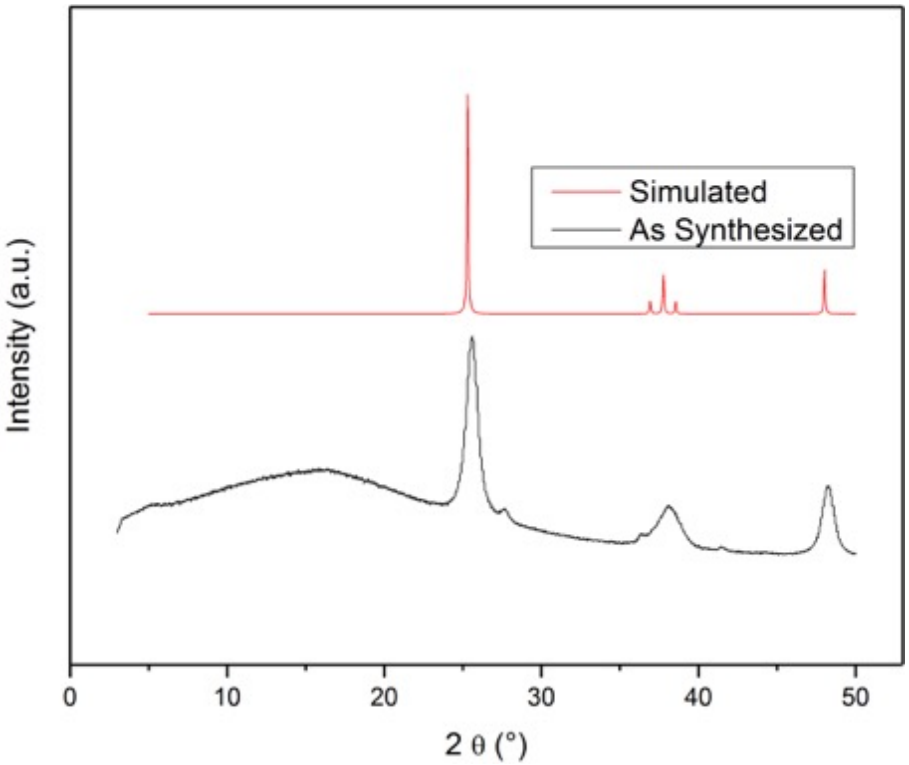

Figure S33. PXRD of as-synthesized TiO_2.

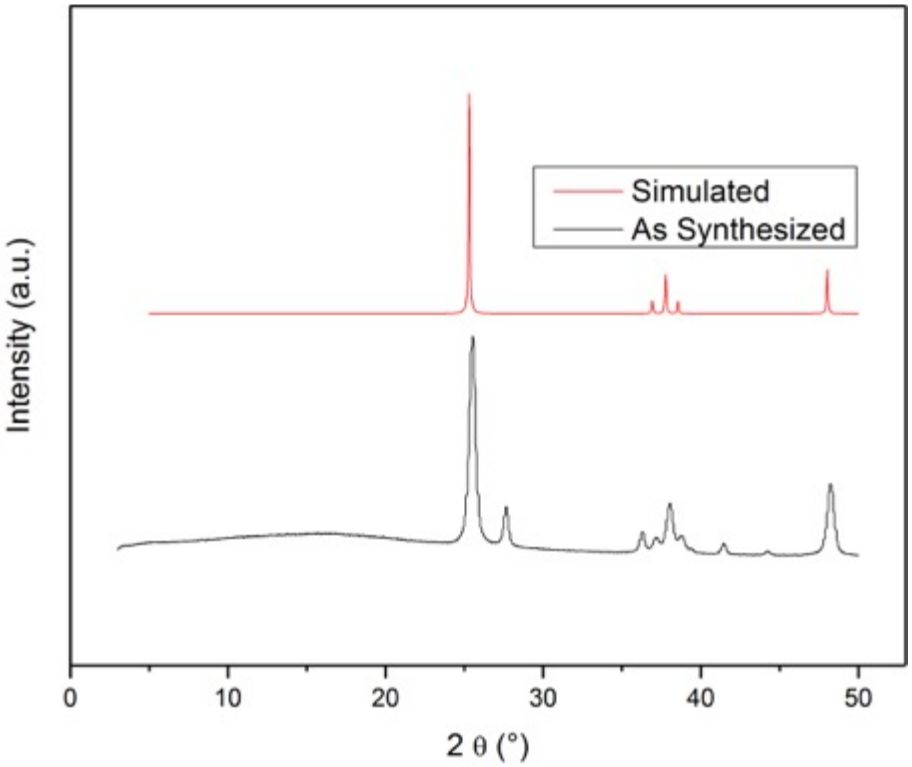

Figure S34. PXRD of as purchased Aldrich TiO_2.

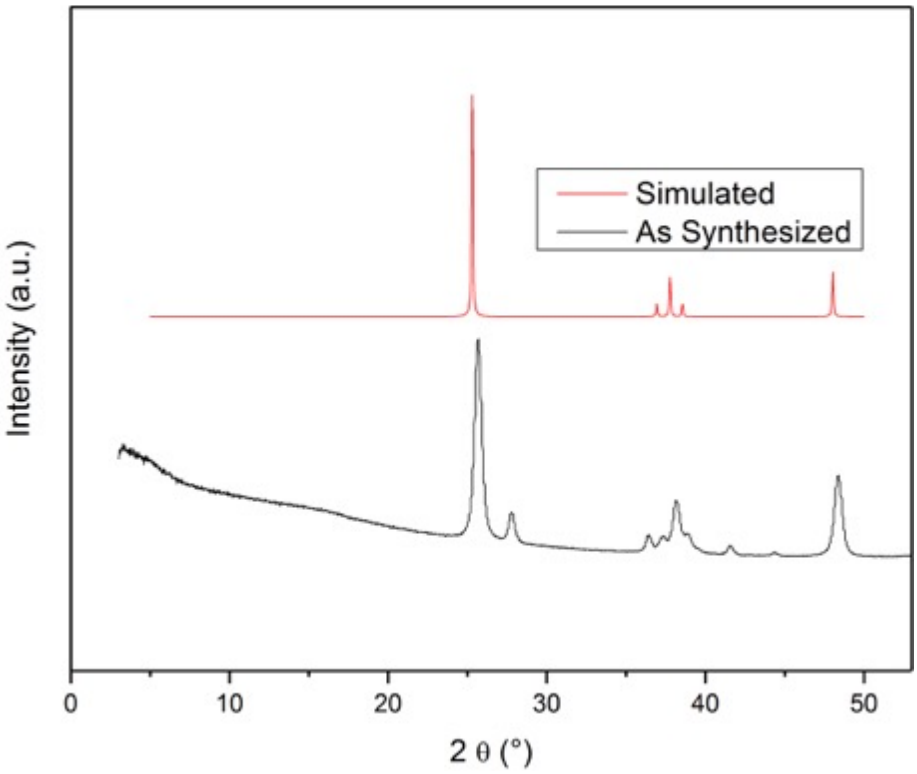

Figure S35. PXRD of as-purchased Aldrich TiO_2 Anatase.

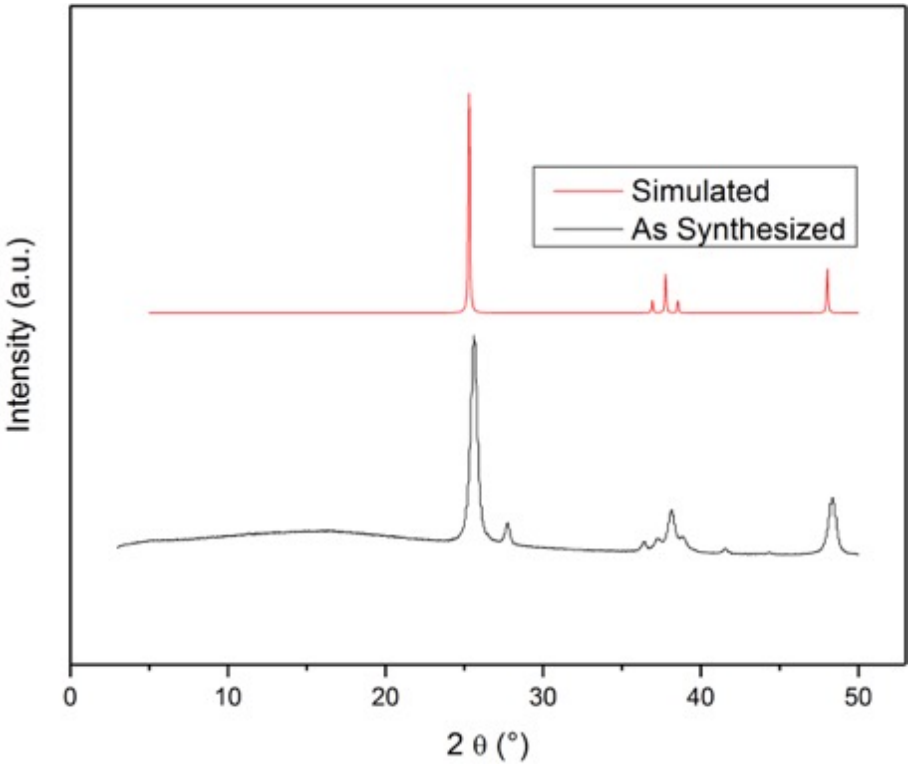

Figure S36. PXRD of as-purchased Degussa P25 TiO_2.

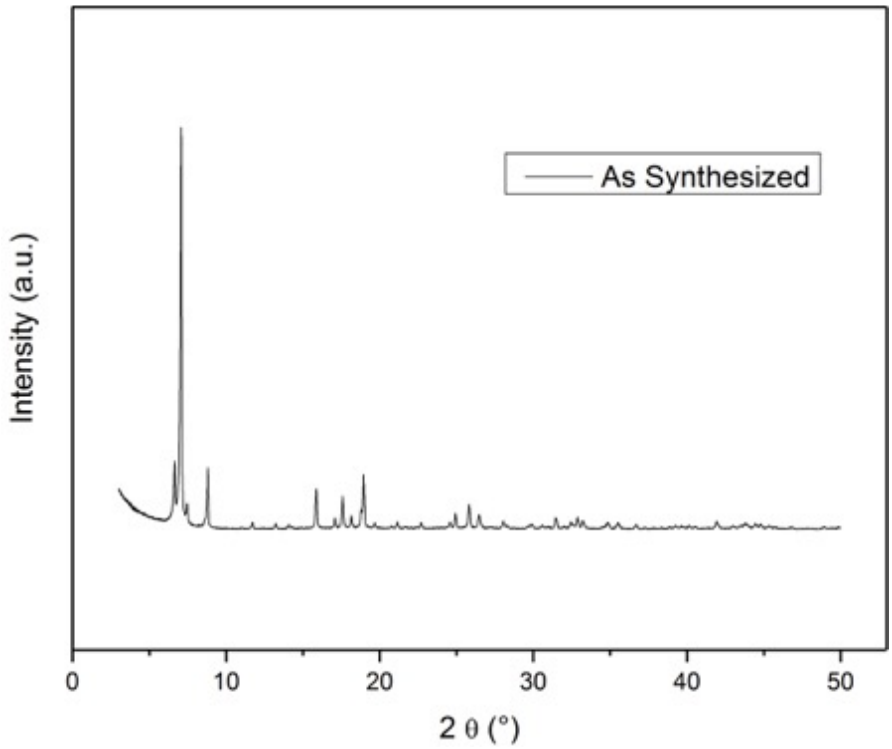

Figure S37. PXRD of as-synthesized PCN-415.

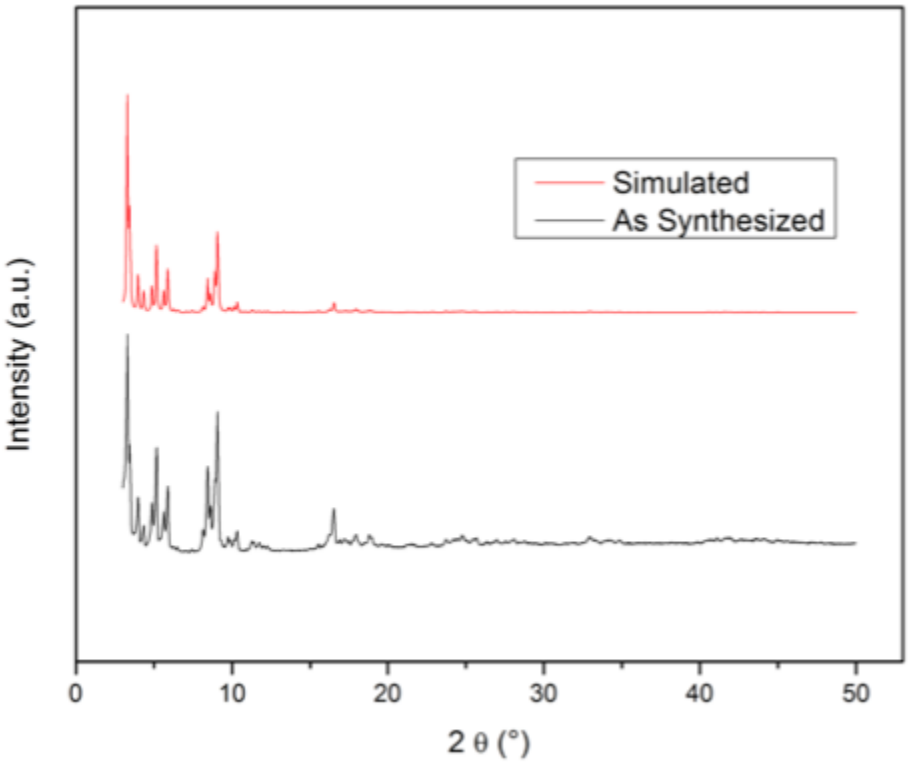

Figure S38. PXRD of as-synthesized MIL-101(Cr).

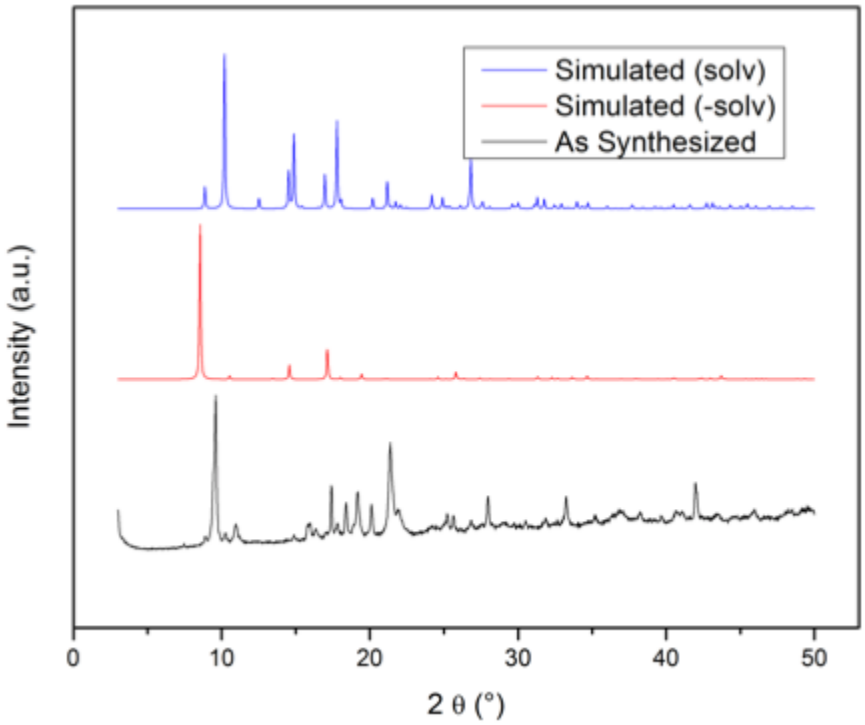

Figure S39. PXRD of as-synthesized MIL-53(Cr). MIL-53(Cr) can adopt multiple crystalline conformations based on solvation, simulated patterns of fully solvated and non-solvated are plotted here.

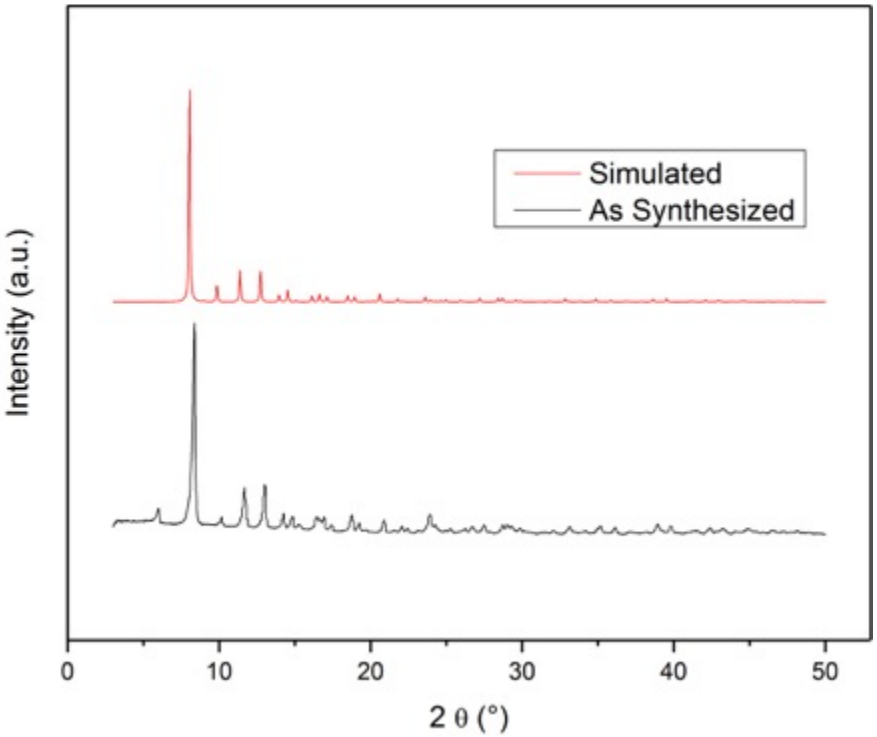

Figure S40. PXRD of as-synthesize PCN-250(Mn).

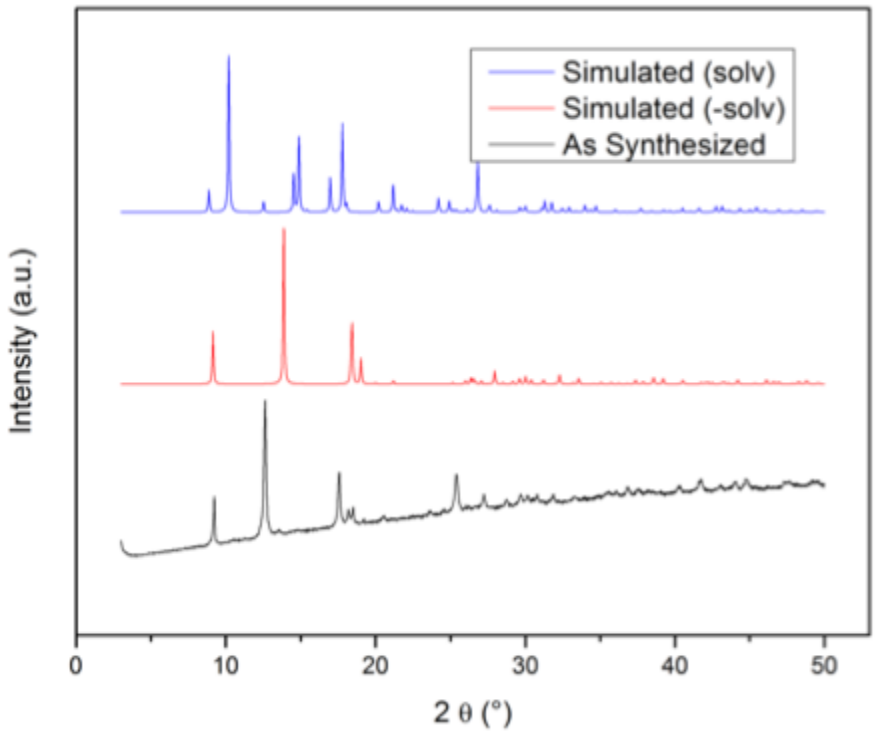

Figure S41. PXRD of as-synthesized MIL-53(Fe). MIL-53(Fe) can adopt multiple crystalline conformations based on solvation, simulated patterns of fully solvated and non-solvated are plotted here.

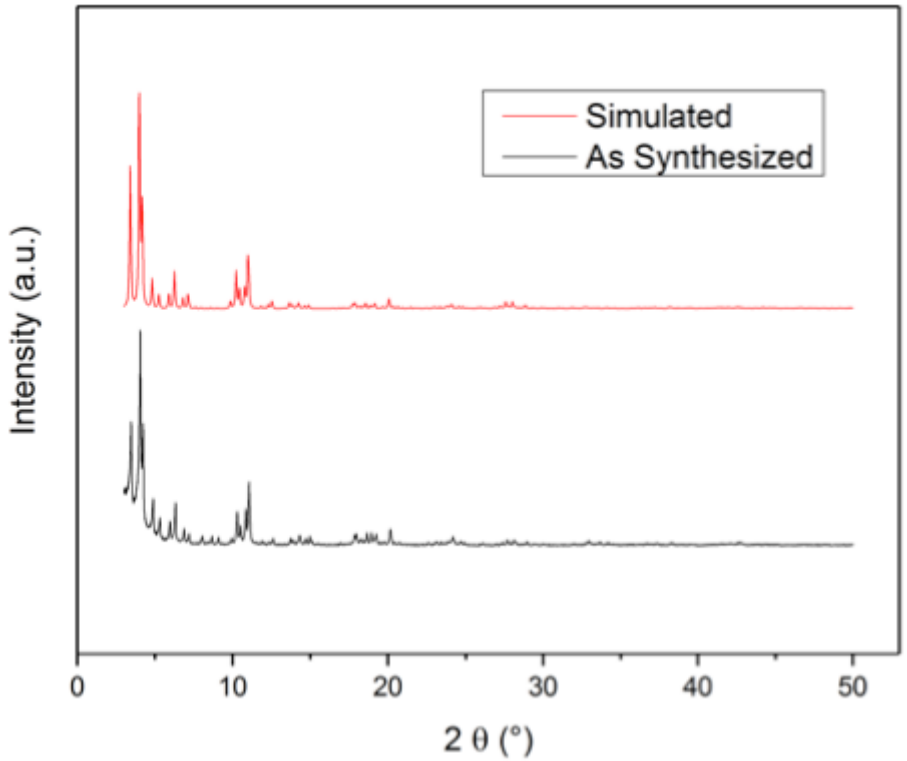

Figure S42. PXRD of as-synthesized MIL-100(Fe).

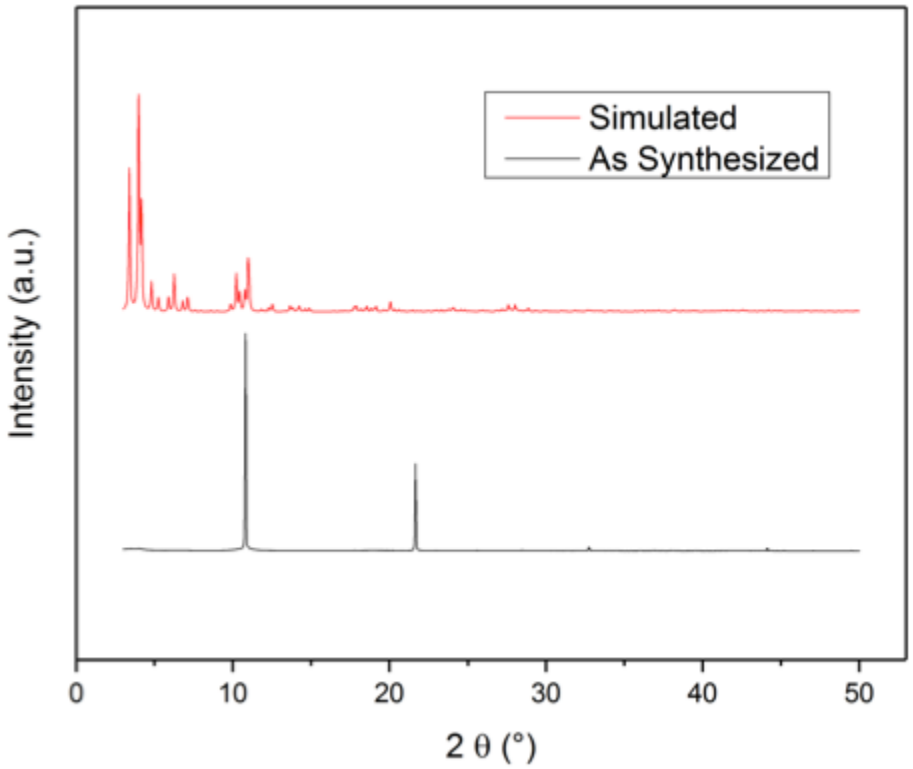

Figure S43. PXRD of as-synthesized Aldrich MIL-100(Fe).

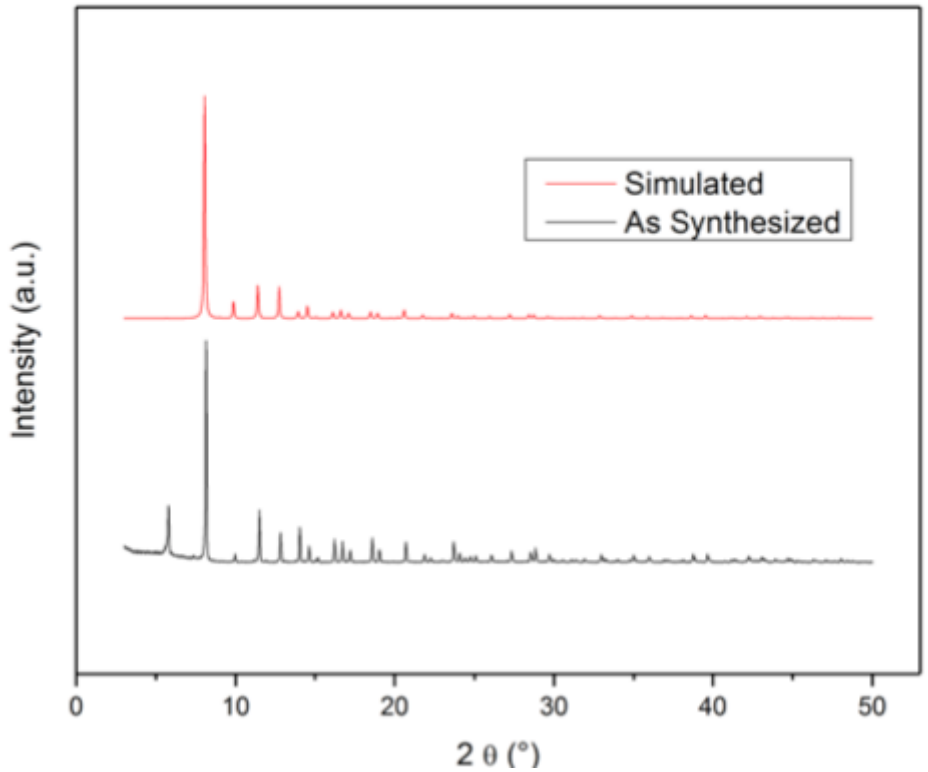

Figure S44. PXRD of as-purchased Strem PCN-250(Fe).

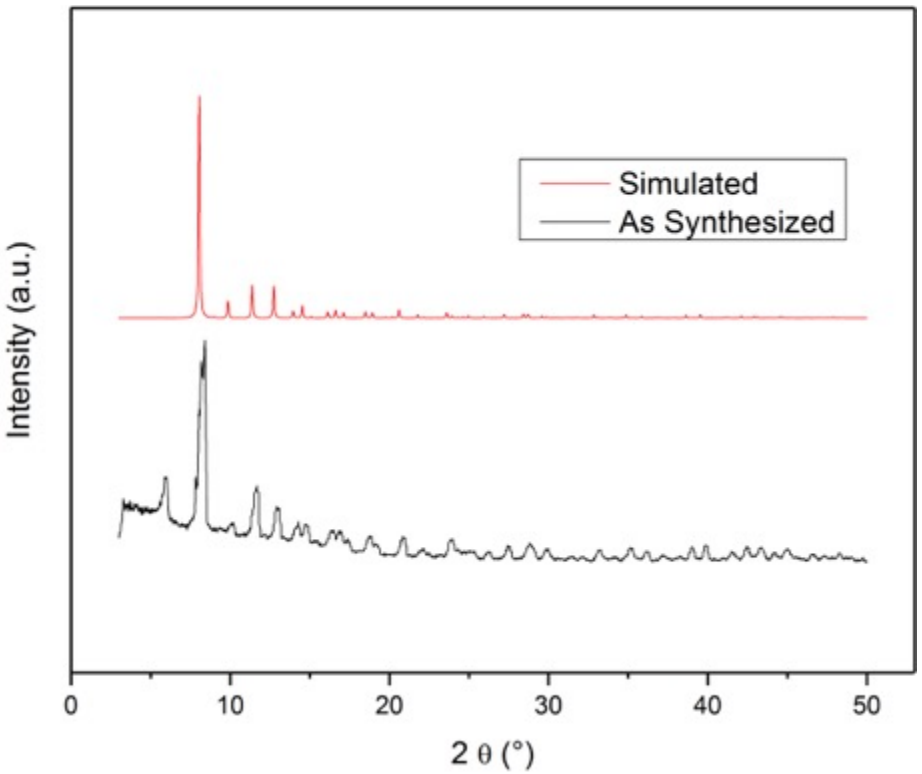

Figure S45. PXRD of as-synthesized PCN-250(Fe).

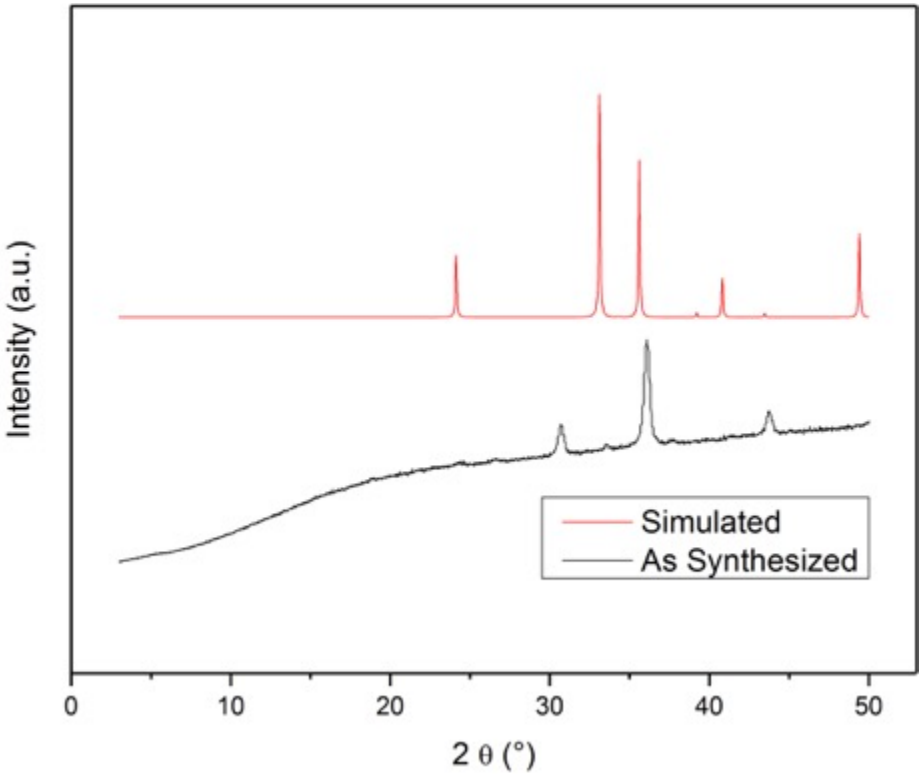

Figure S46. PXRD of as-purchased Fe_2O_3.

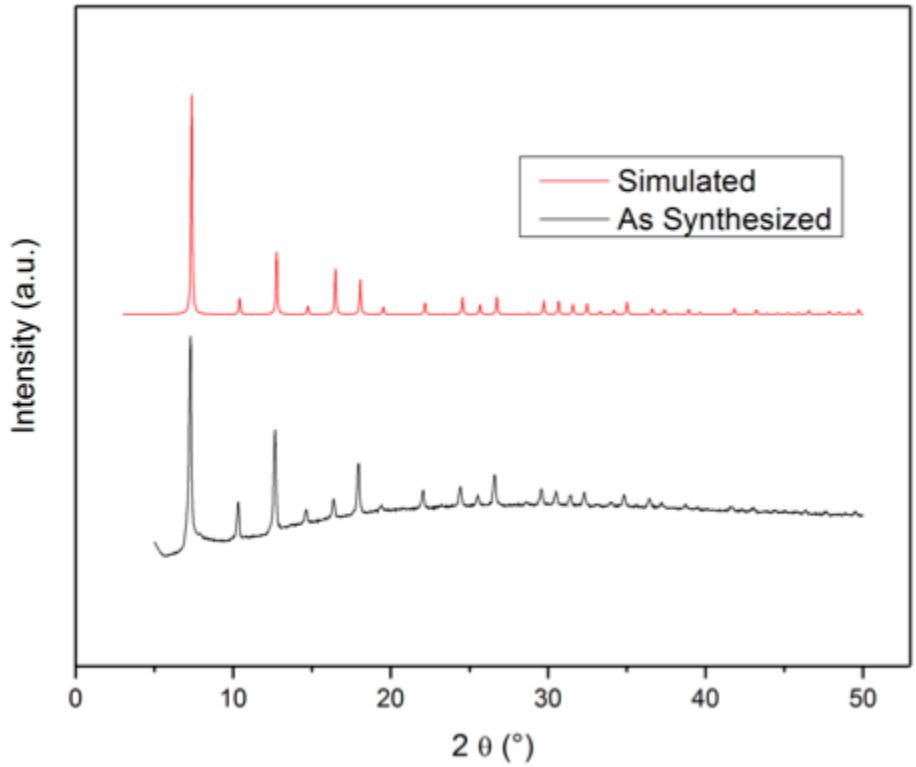

Figure S47. PXRD of as-synthesized ZIF-67.

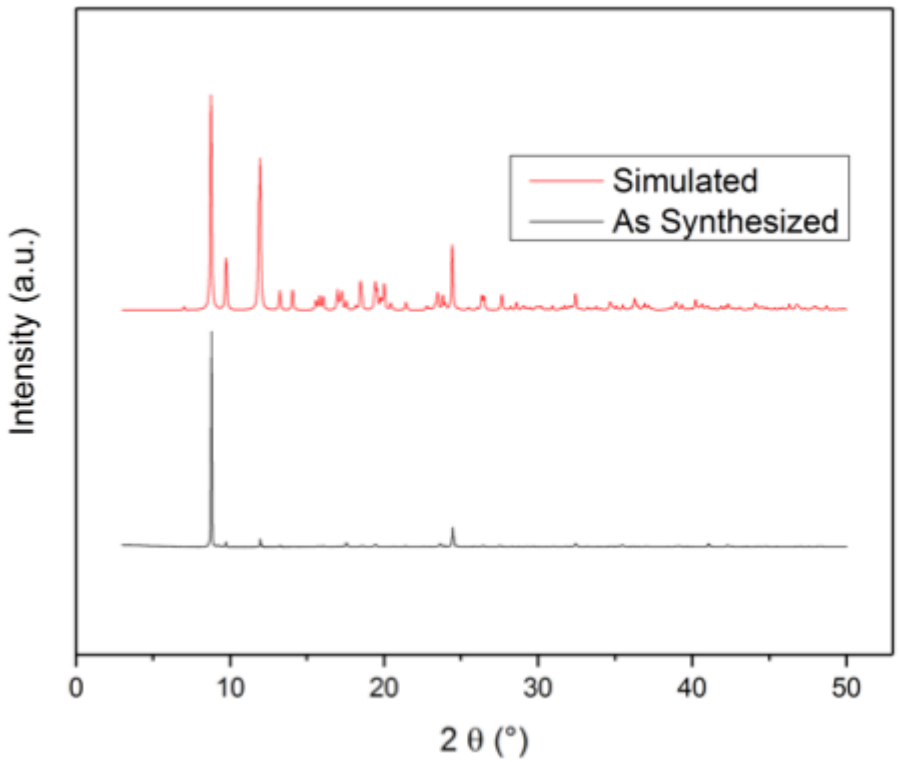

Figure S48. PXRD of as-synthesized Co-NIC.

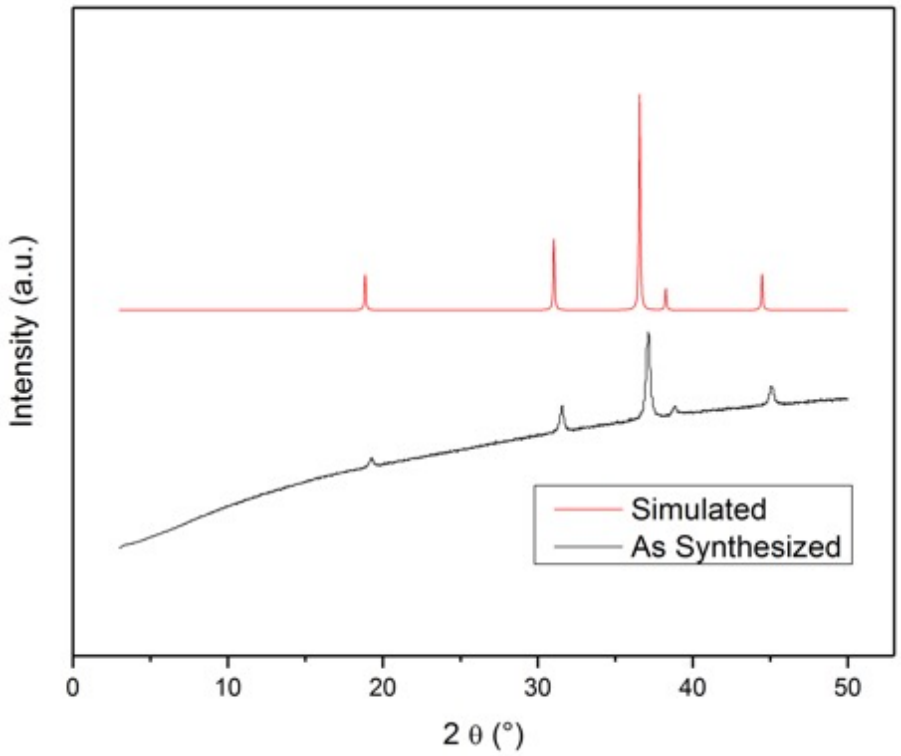

Figure S 49. PXRD of as-purchased Co_3O_4.

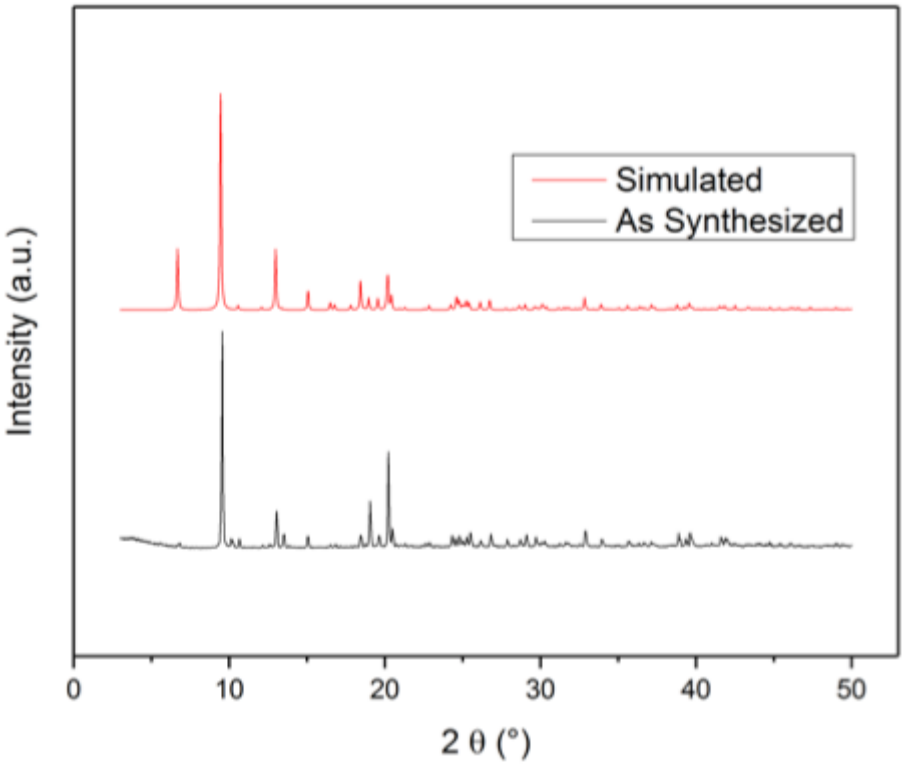

Figure S50. PXRD of as-synthesized Zn/Co BTEC.

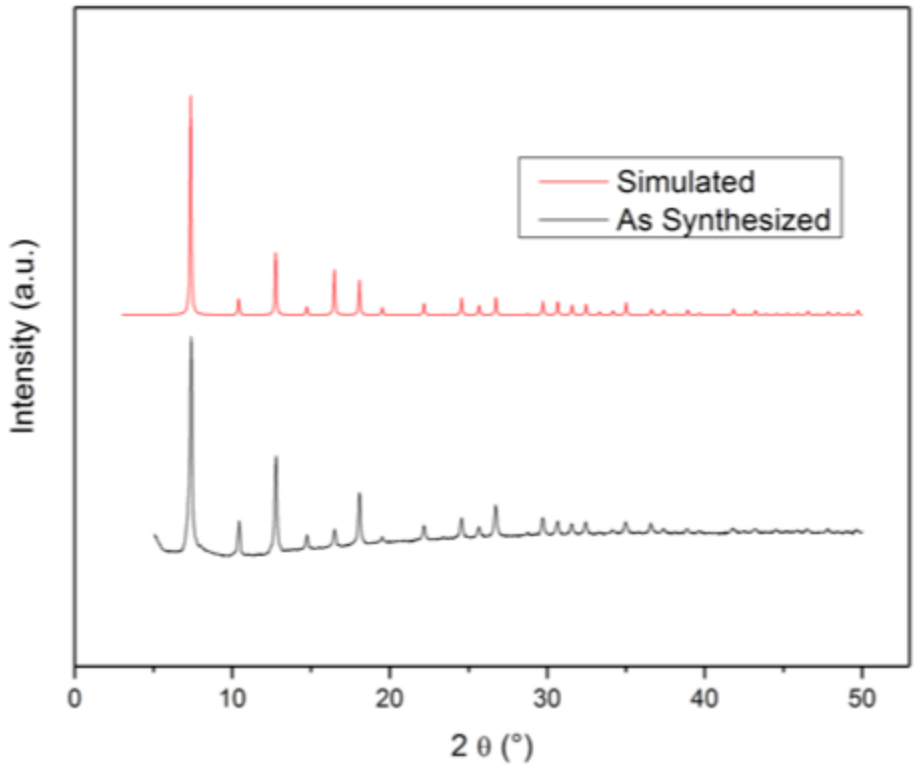

Figure S51. PXRD of as-synthesized ZIF-8/67(Zn/Co).

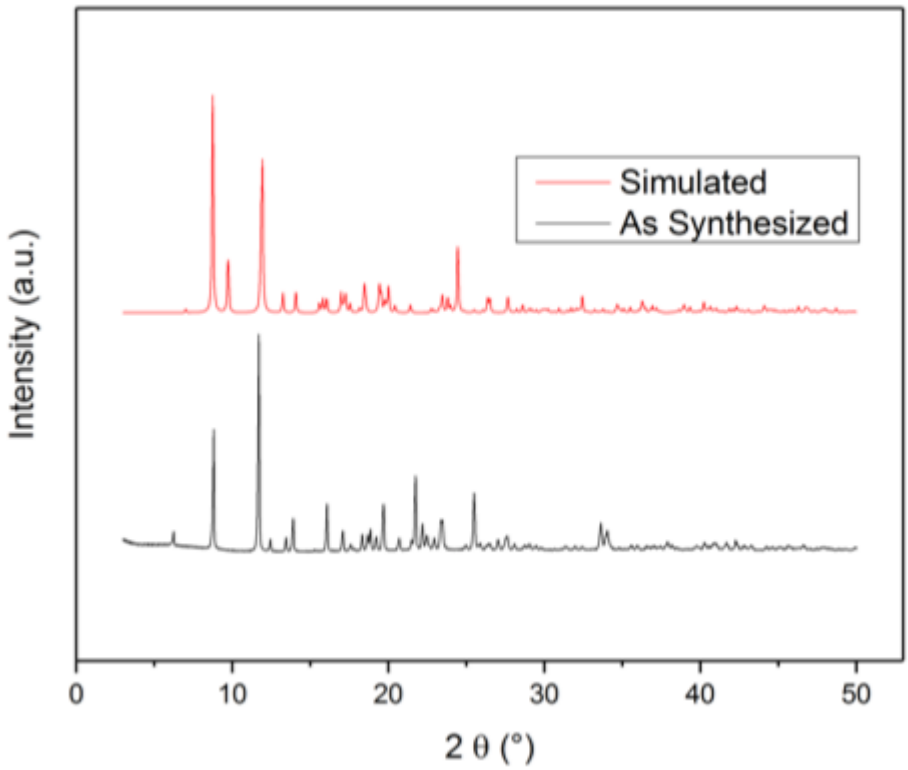

Figure S52. PXRD of as-synthesized Ni-NIC.

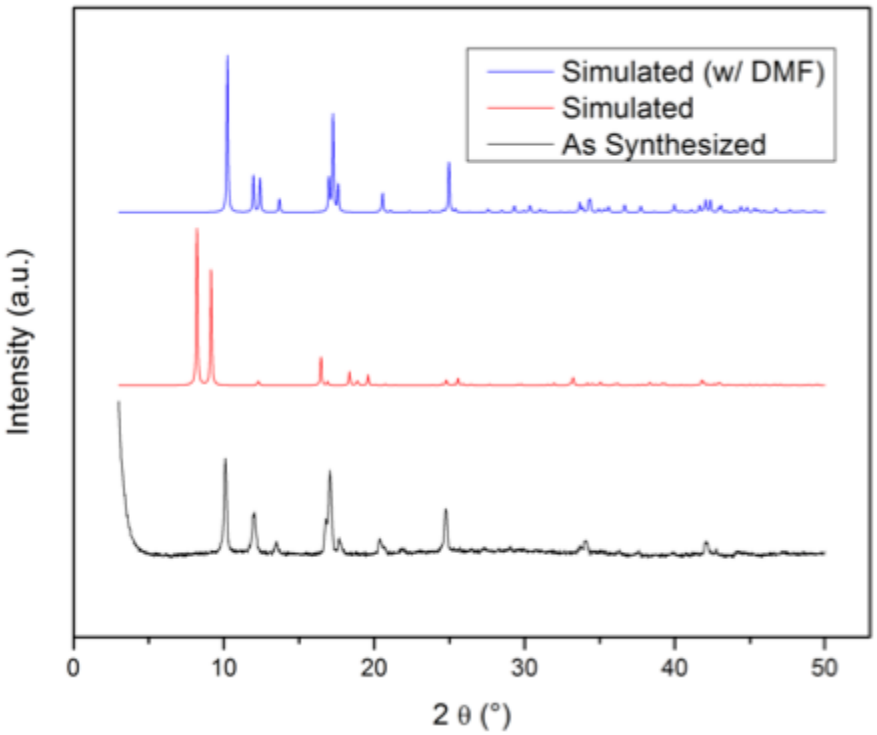

Figure S53. PXRD of as-synthesized CuBDC. CuBDC can adopt two crystalline conformations, both simulated patterns are plotted here.

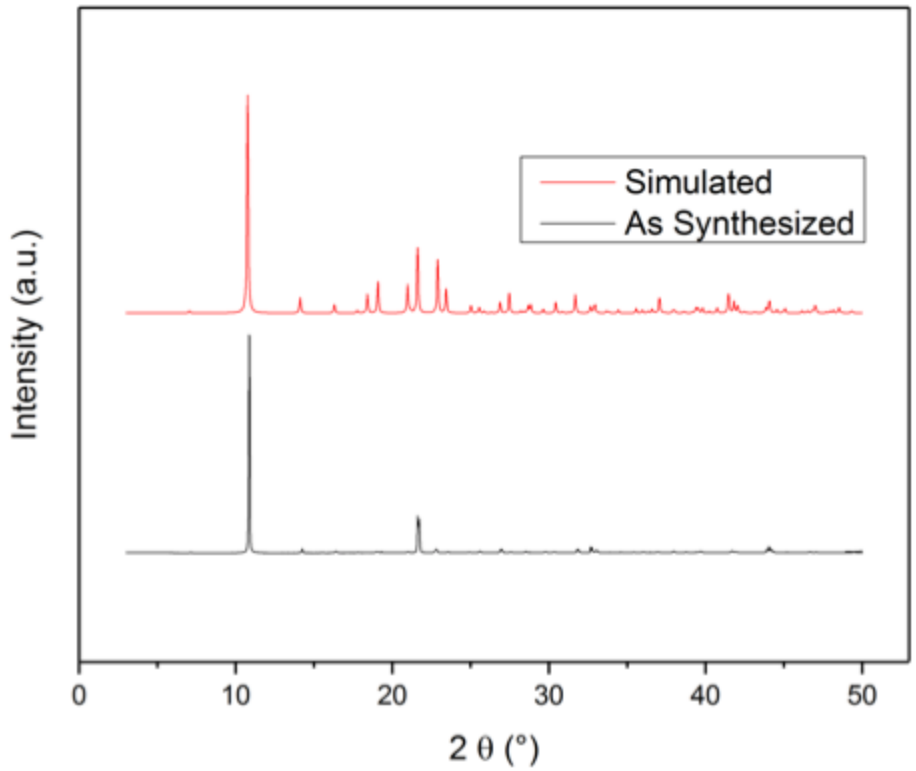

Figure S54. PXRD of as-synthesized Cu-PCN.

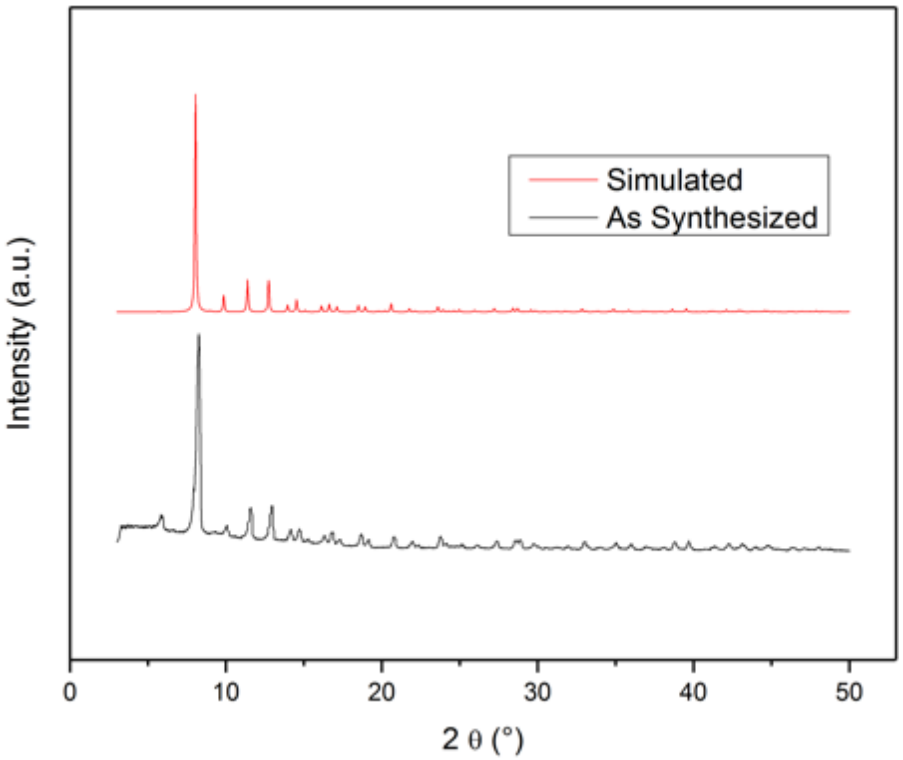

Figure S55. PXRD of as-synthesized PCN-250(Cu).

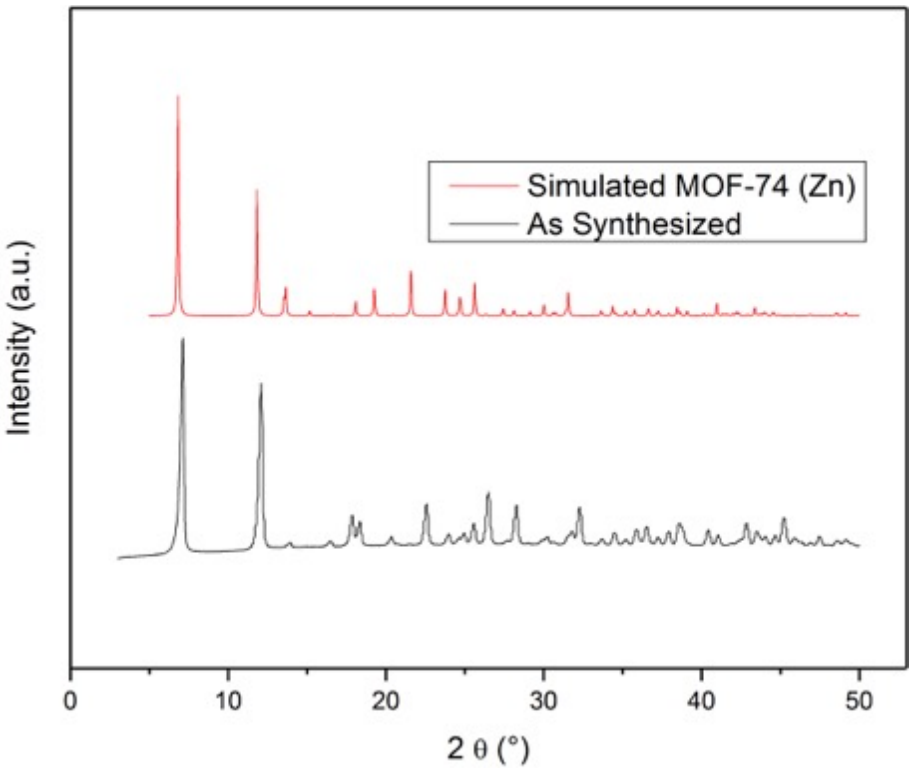

Figure S56. PXRD of as-synthesized MOF-74(Cu).

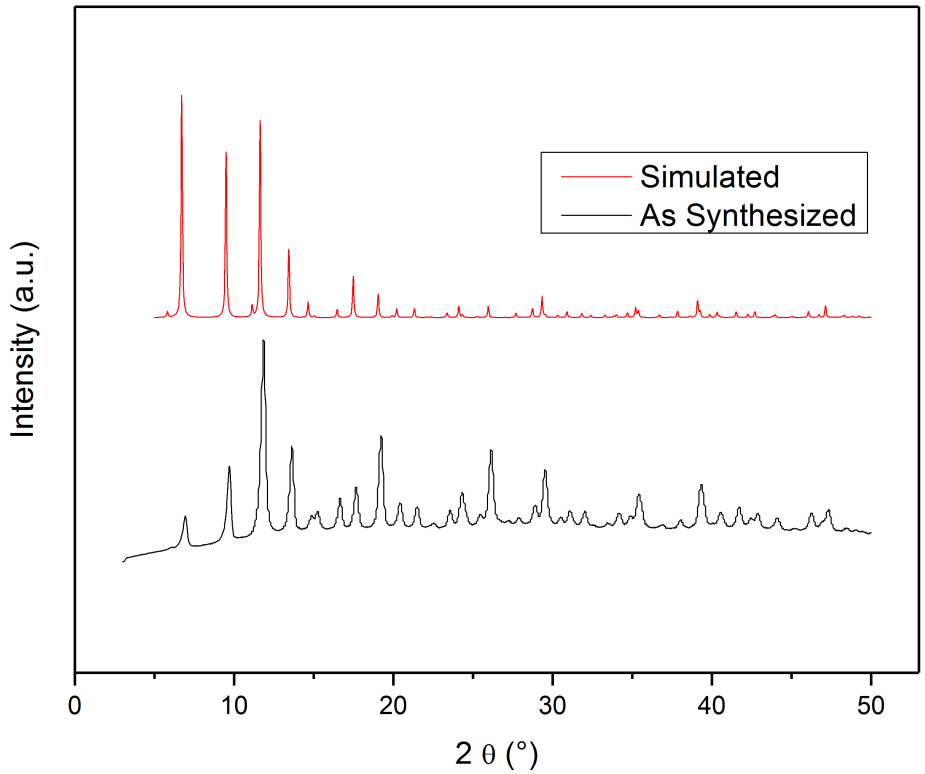

Figure S57. PXRD of as-synthesized Aldrich HKUST-1.

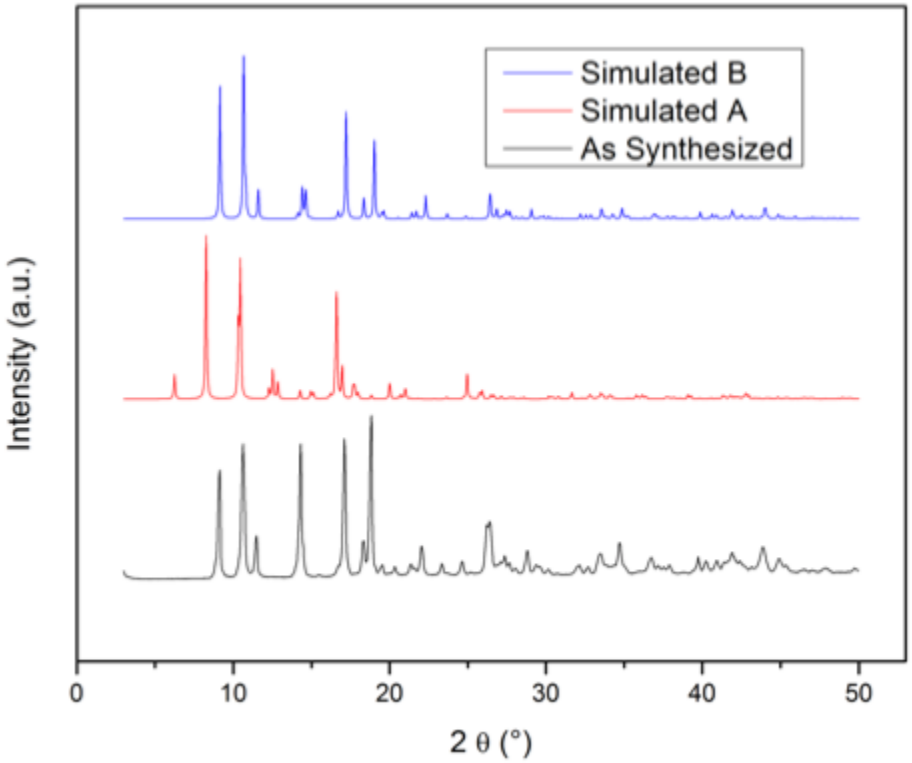

Figure S58. PXRD of as-synthesized MOF-508. MOF-508 can adopt two crystalline conformations, both simulated patterns are plotted here.

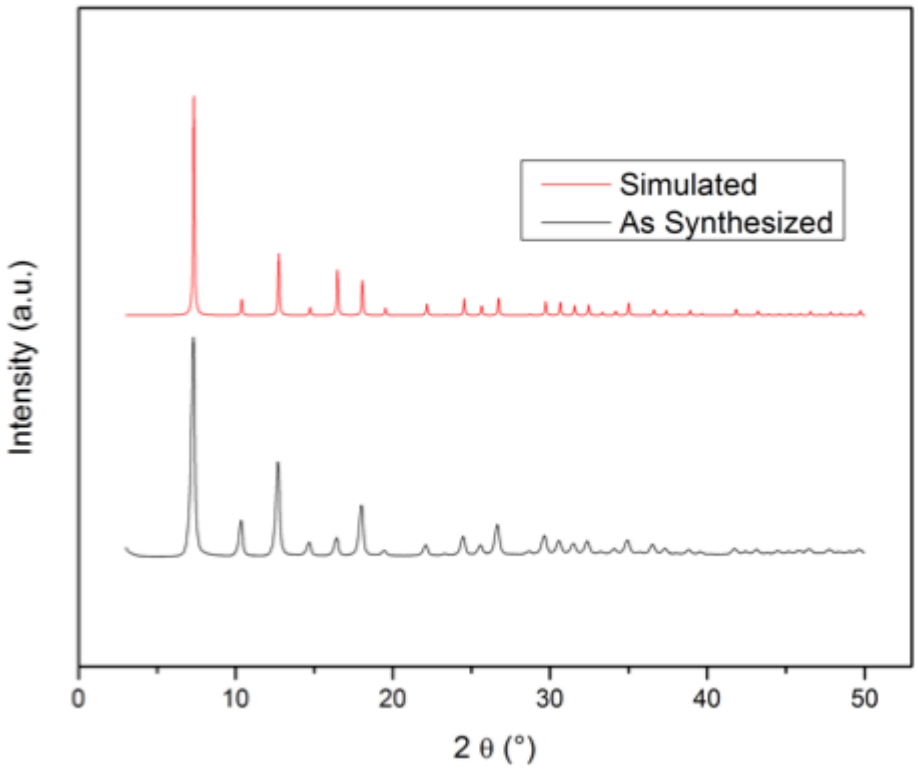

Figure S59. PXRD of as-synthesized ZIF-8.

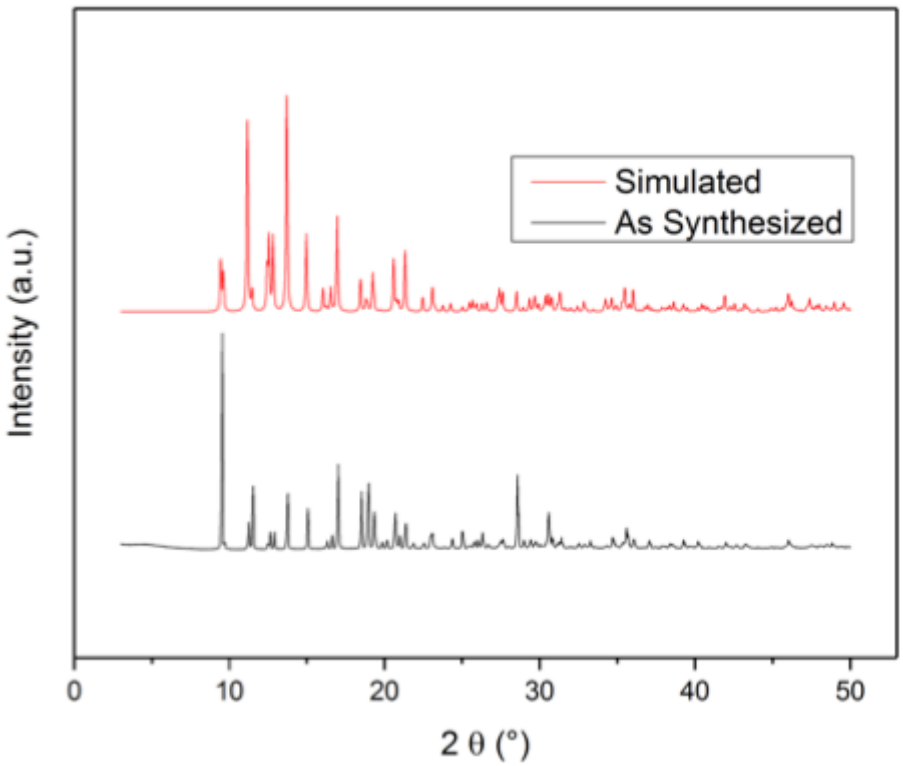

Figure S60. PXRD of as-synthesized ZIF-4.

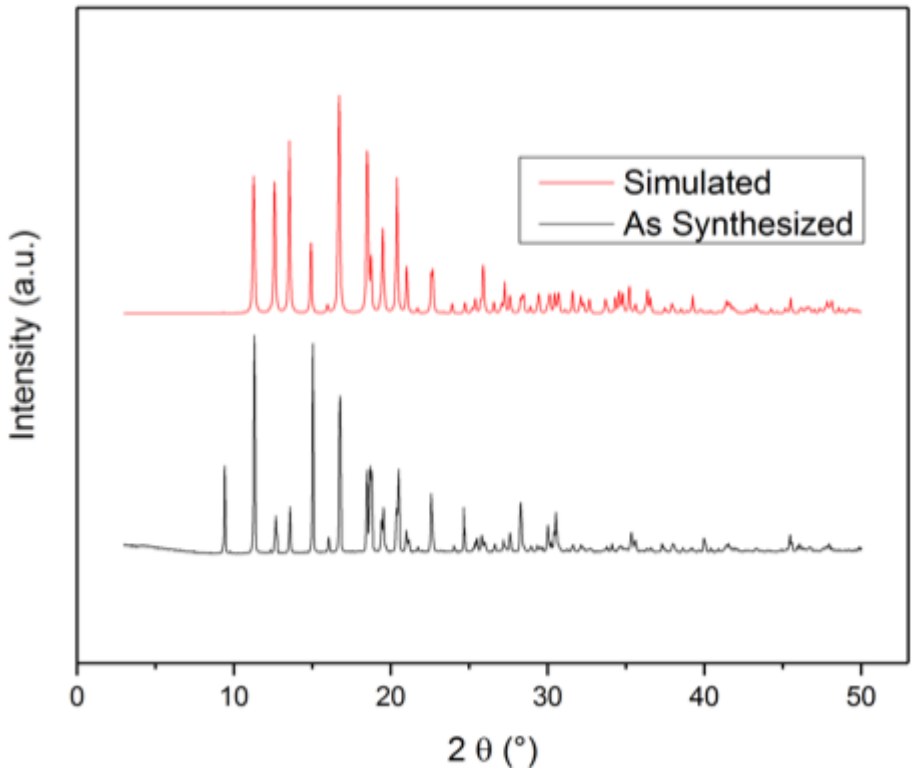

Figure S61. PXRD of as-synthesized ZIF-62.

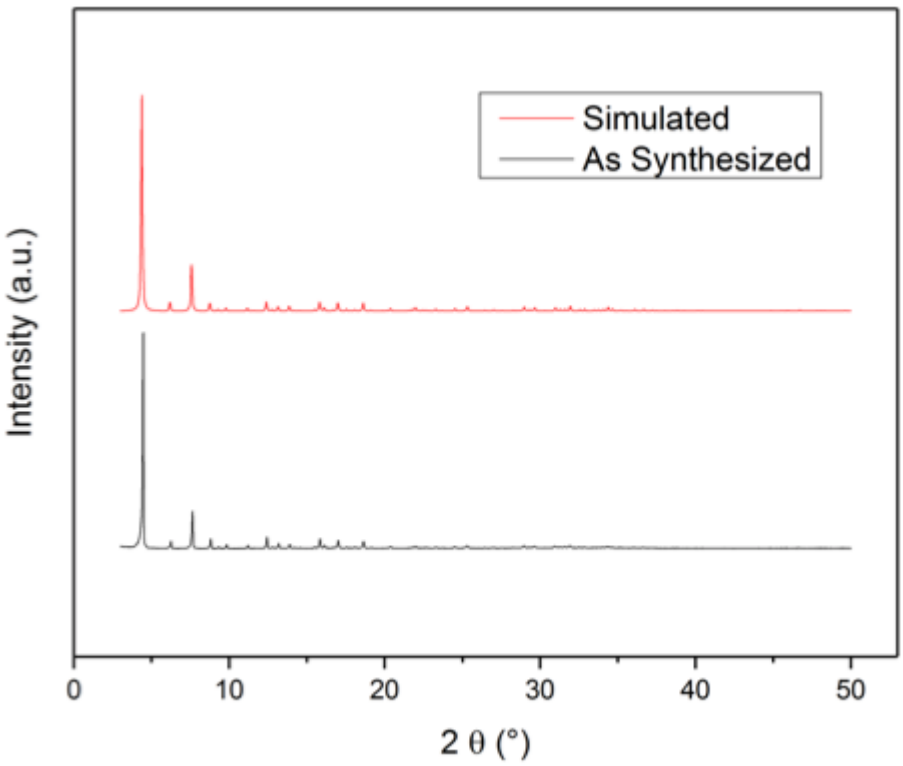

Figure S62. PXRD of as-synthesized ZIF-71.

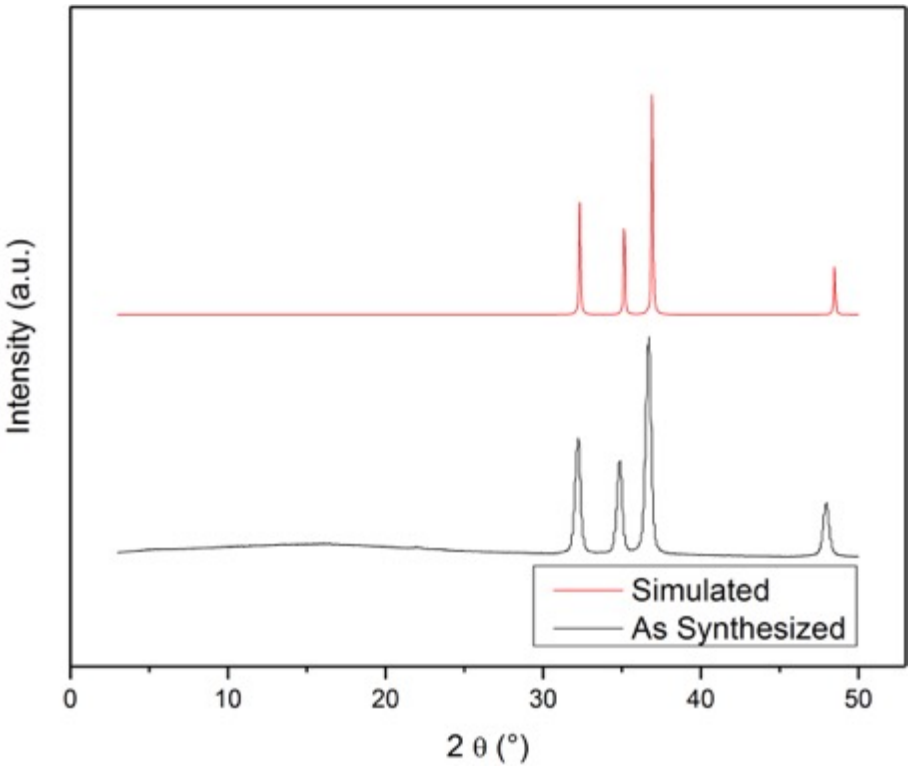

Figure S63. PXRD of as-purchased ZnO.

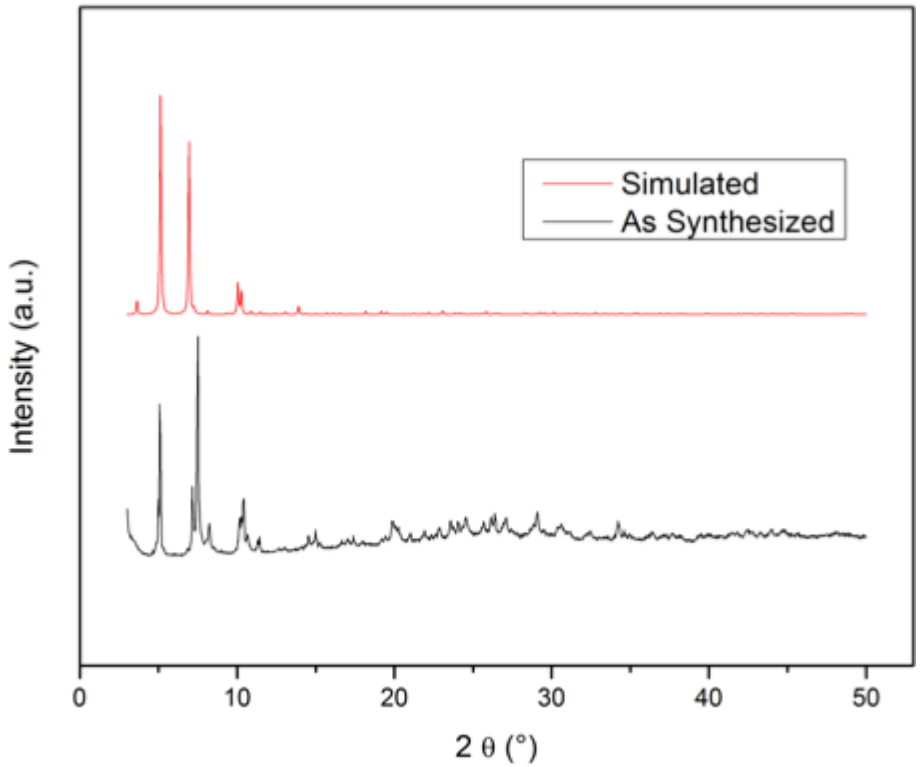

Figure S64. PXRD of as-synthesized PCN-700.

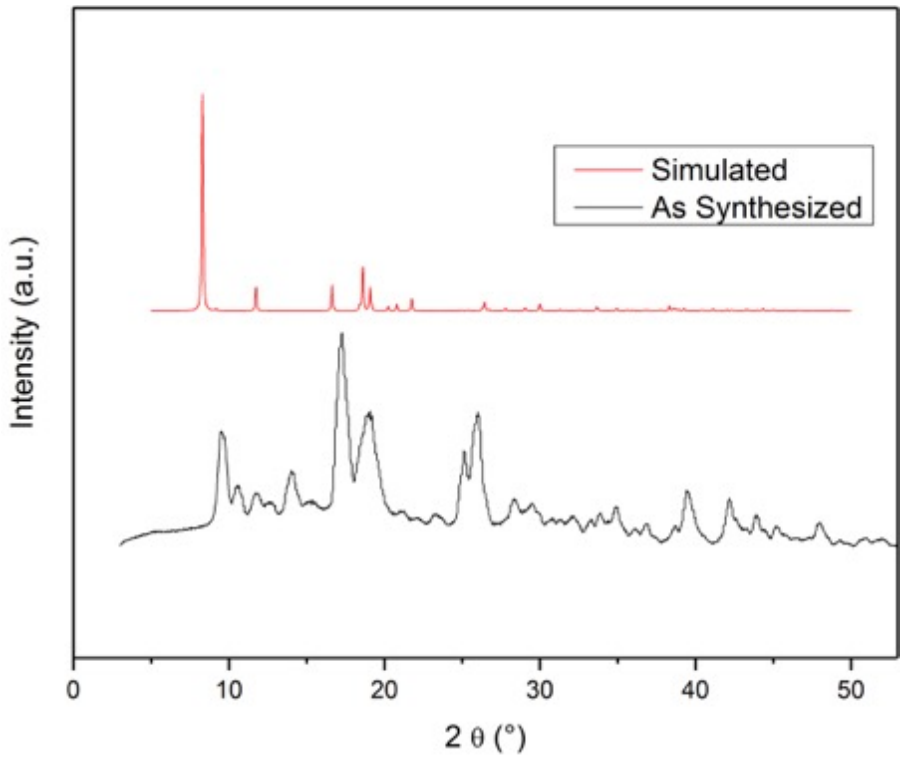

Figure S65. PXRD of as-synthesized DMOF-1.

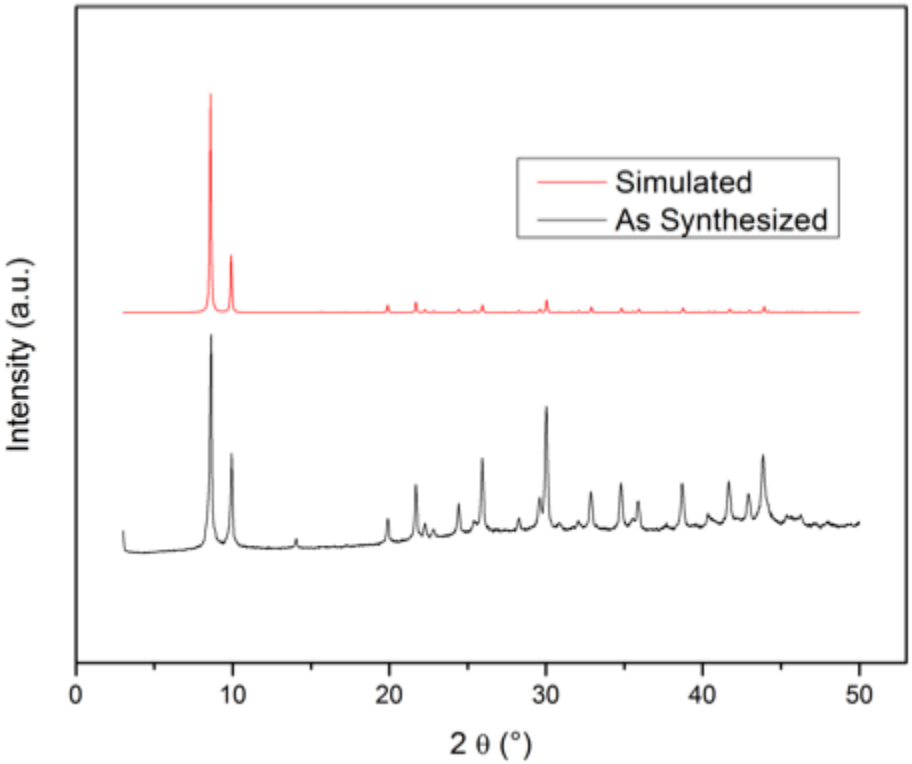

Figure S66. PXRD of as-synthesized MOF-801.

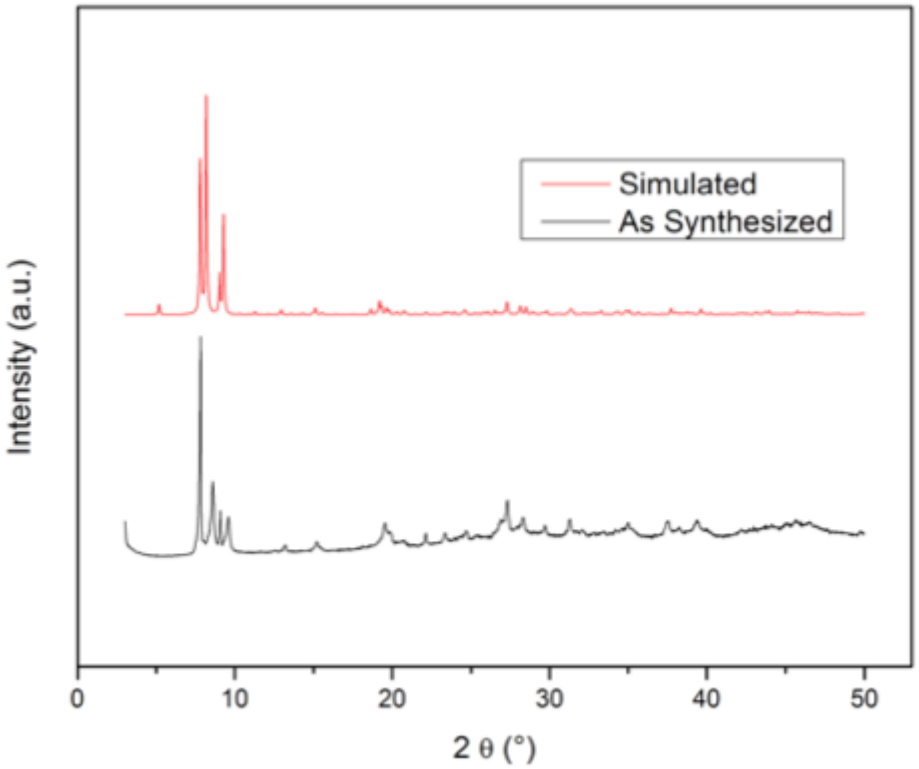

Figure S67. PXRD of as-synthesized MOF-802.

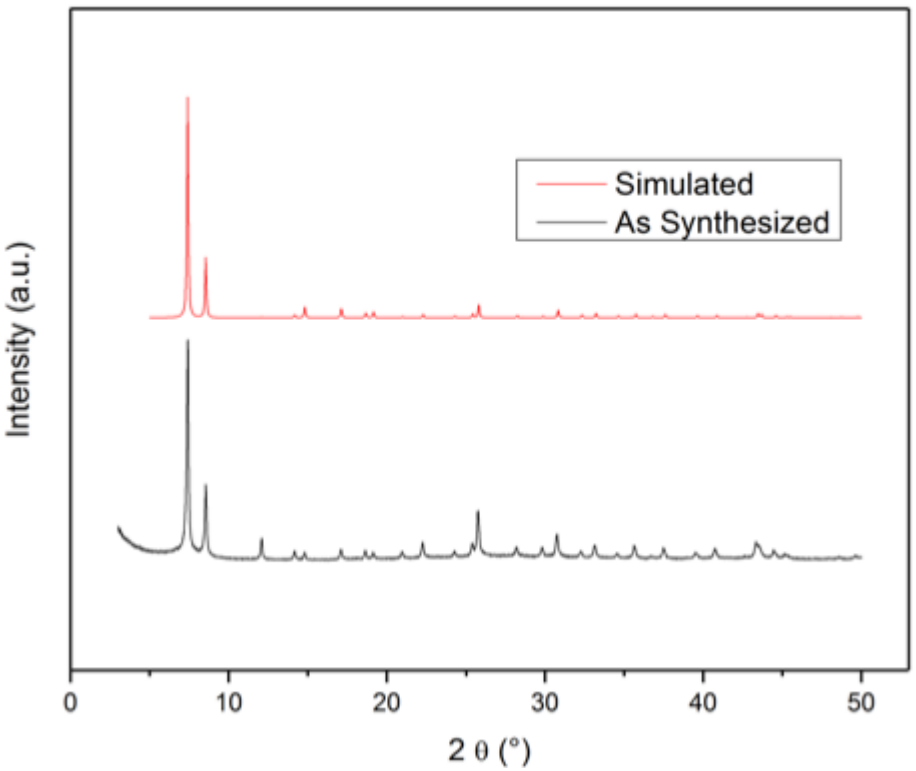

Figure S68. PXRD of as-synthesized UiO-66-NH_2 [AcOH].

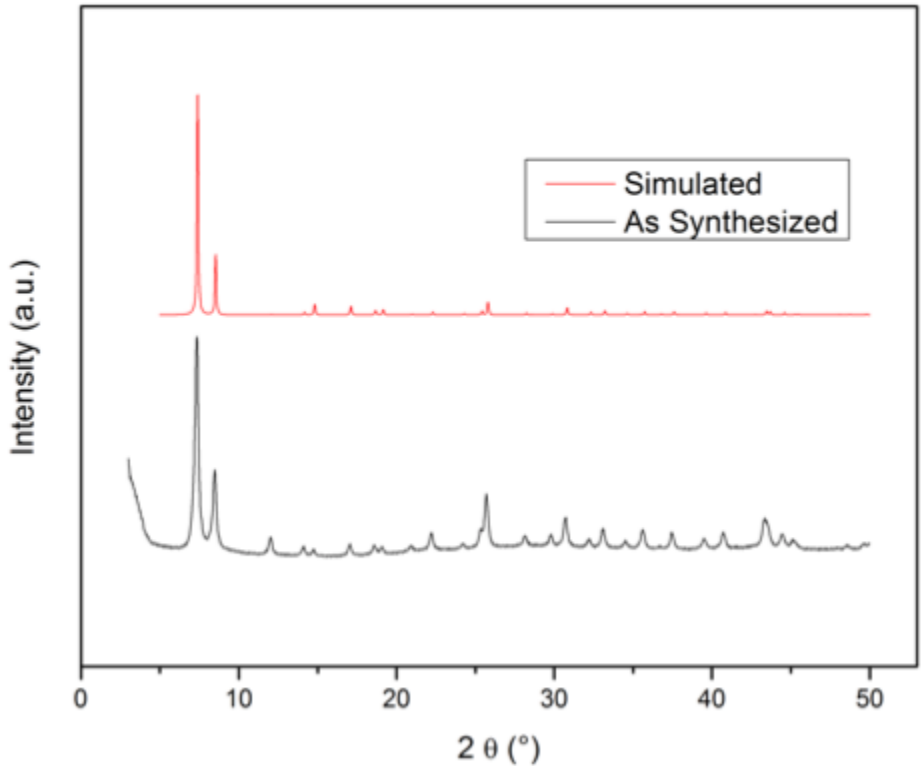

Figure S69. PXRD of as-synthesized UiO-66-NH_2 [DMF/HCl].

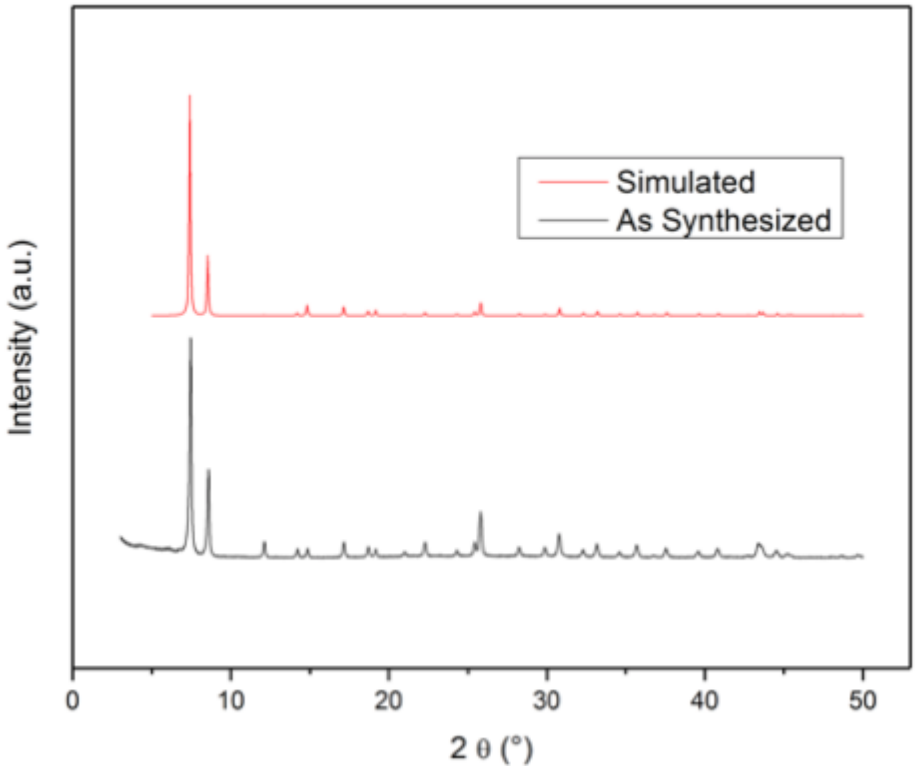

Figure S70. PXRD of as-synthesized Strem UiO-66-NH_2.

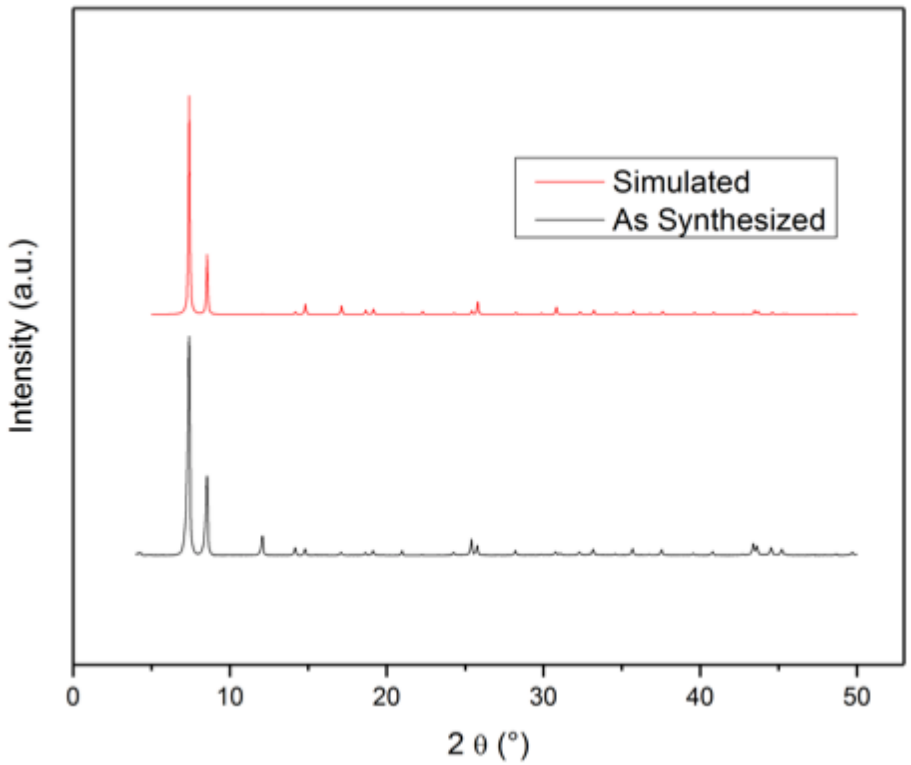

Figure S71. PXRD of as-synthesized UiO-66-SO_3H [DMF/HCOOH].

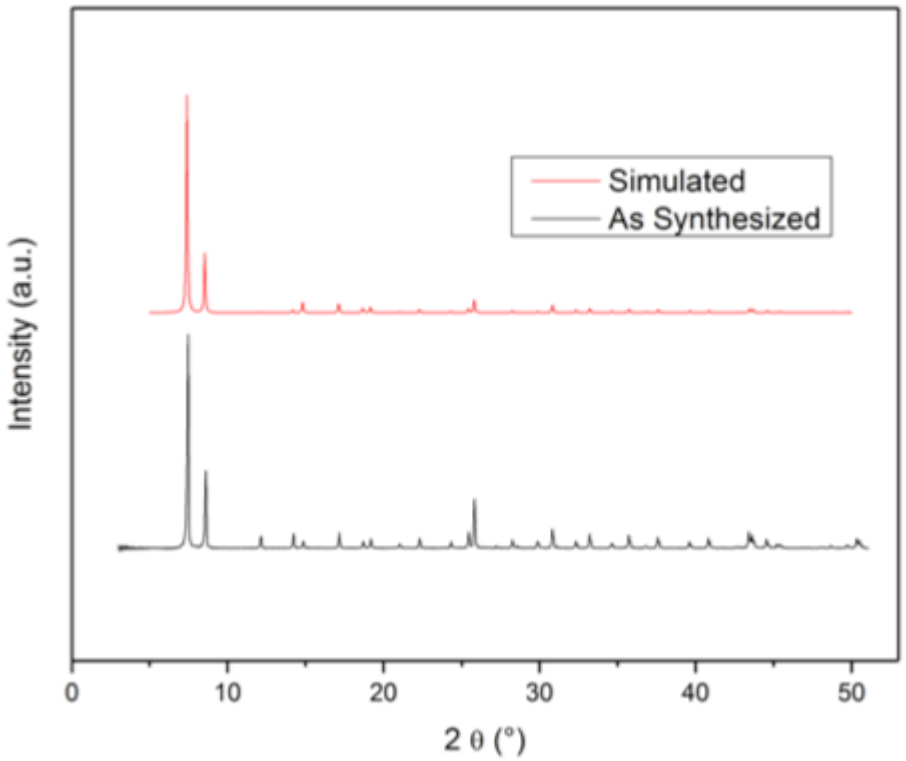

Figure S72. PXRD of as-synthesized UiO-66-COOH [DMF/BzOH].

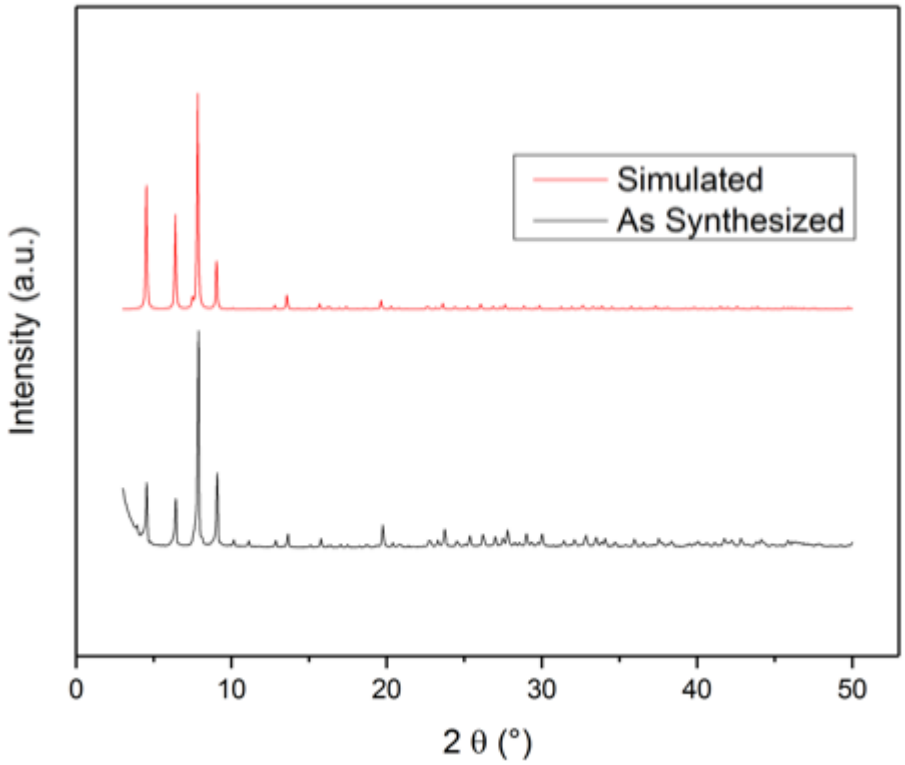

Figure S73. PXRD of as-synthesized DUT-67(Zr).

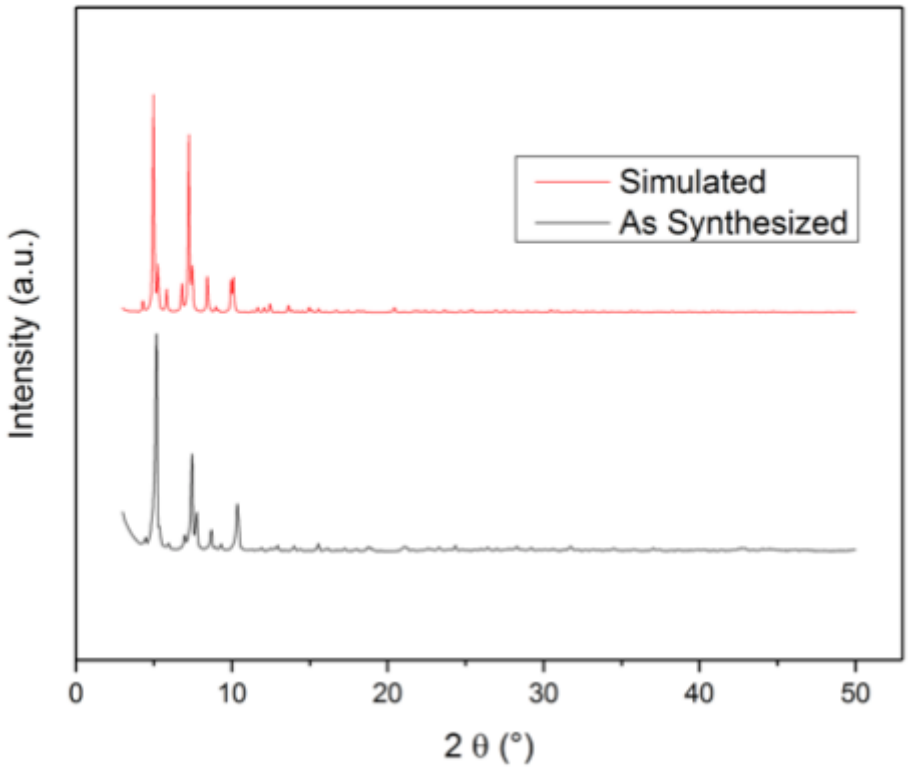

Figure S74. PXRD of as-synthesized NU-1000.

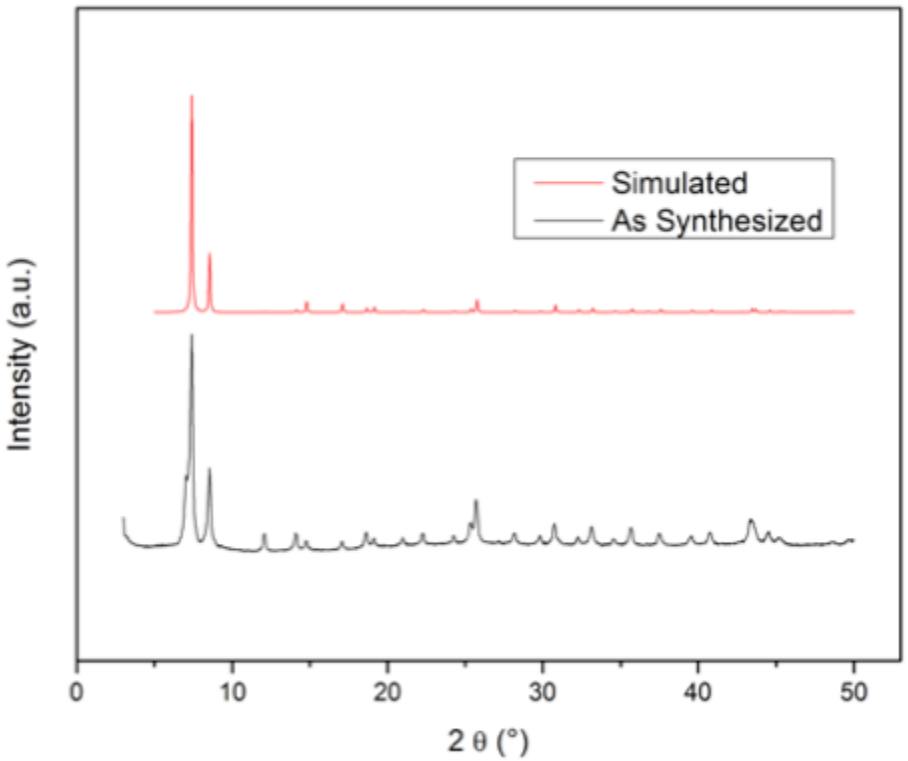

Figure S75. PXRD of as-synthesized polyUiO-66.

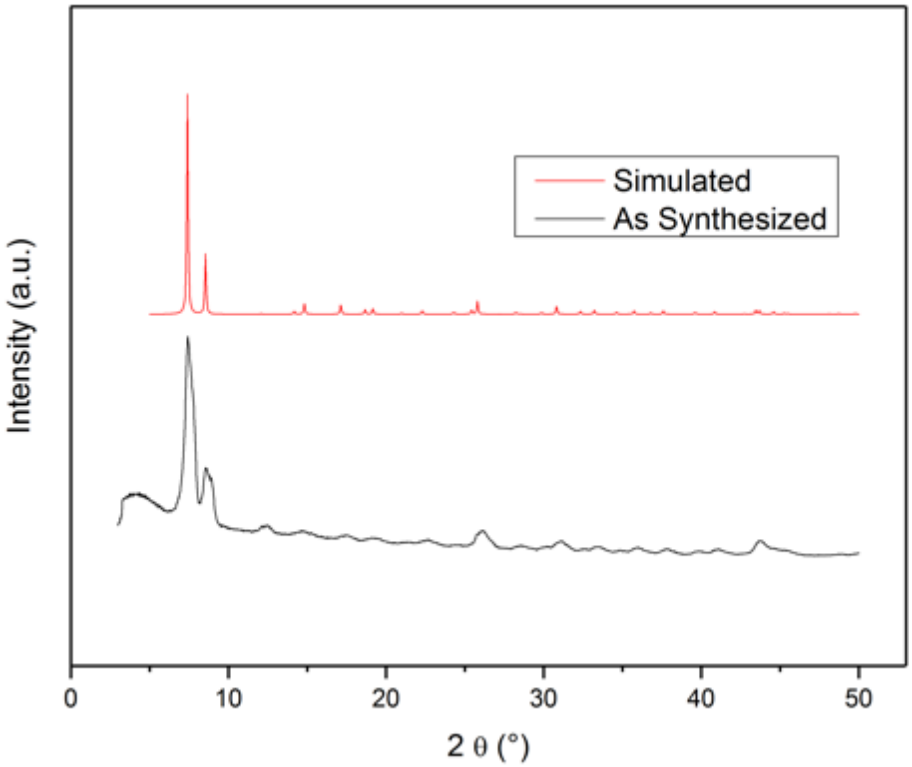

Figure S76. PXRD of as-synthesized UiO-66-NH_2-LD.

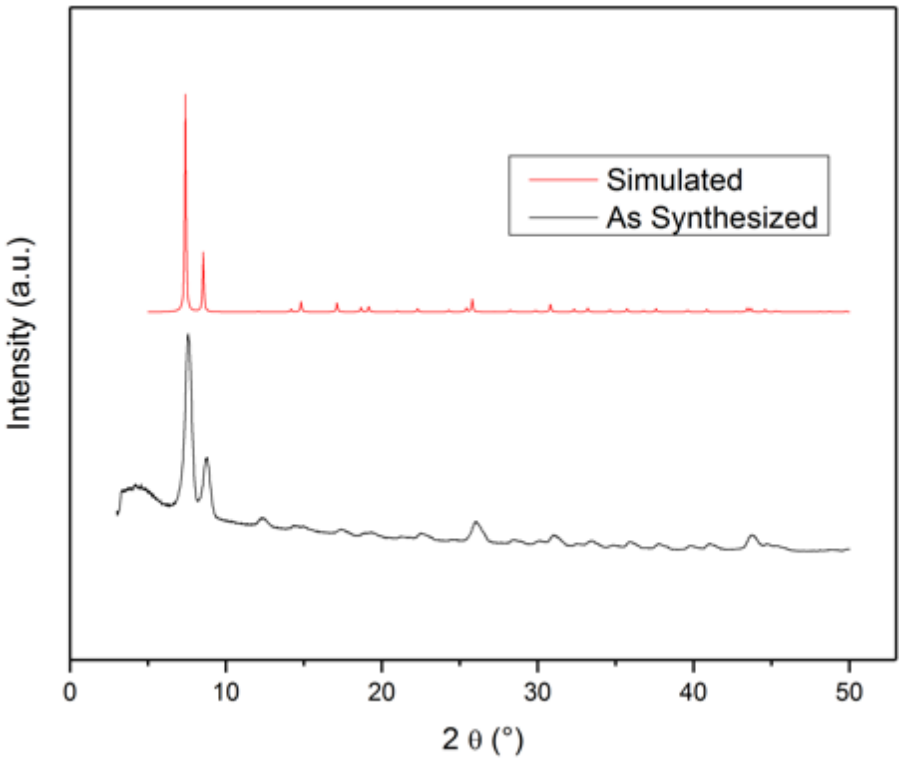

Figure S77. PXRD of as-synthesized UiO-66-NH_2-MD.

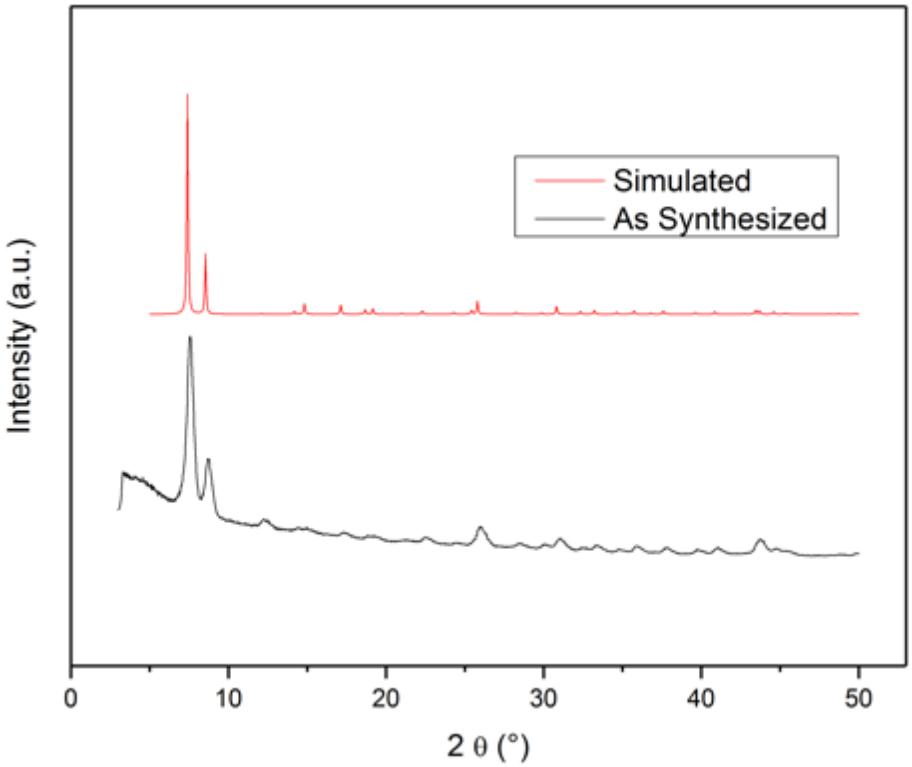

Figure S78. PXRD of as-synthesized UiO-66-NH_2-HD.

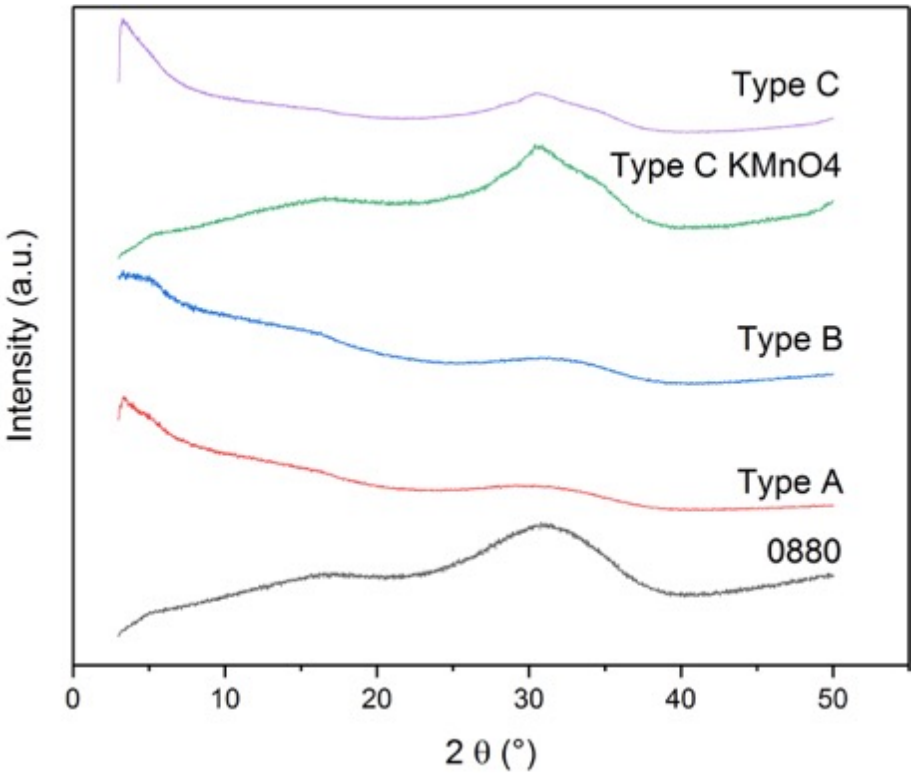

Figure S79. PXRD of as-purchased $Zr(OH)_2$ materials: 0880, Type A, Type B, Type C-$KMnO_4$, and Type C.

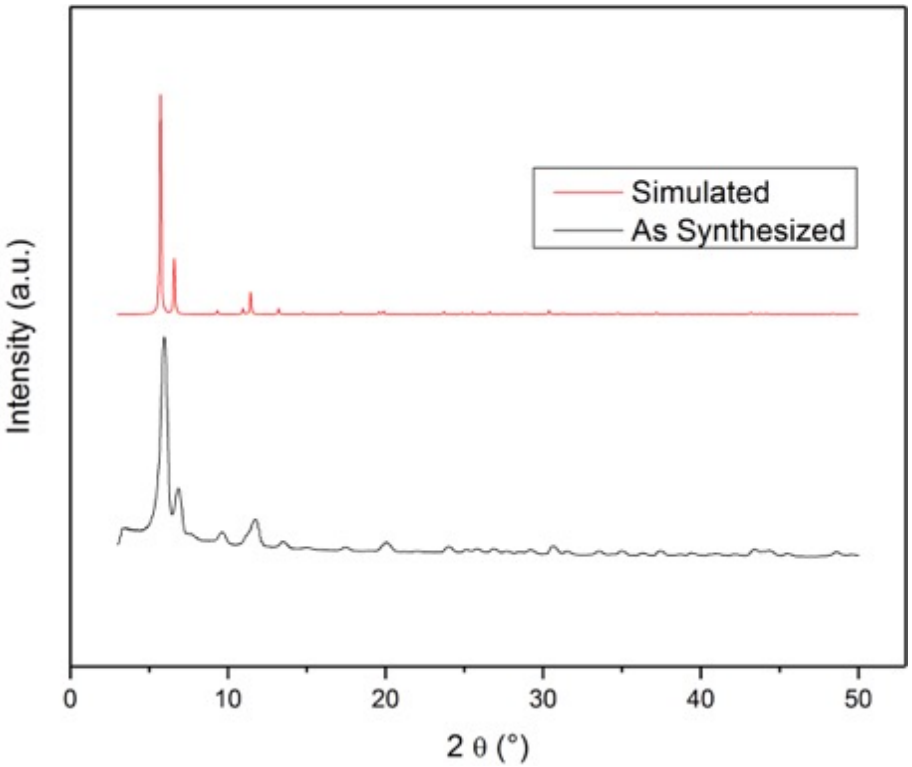

Figure S80. PXRD of as-synthesized UiO-67.

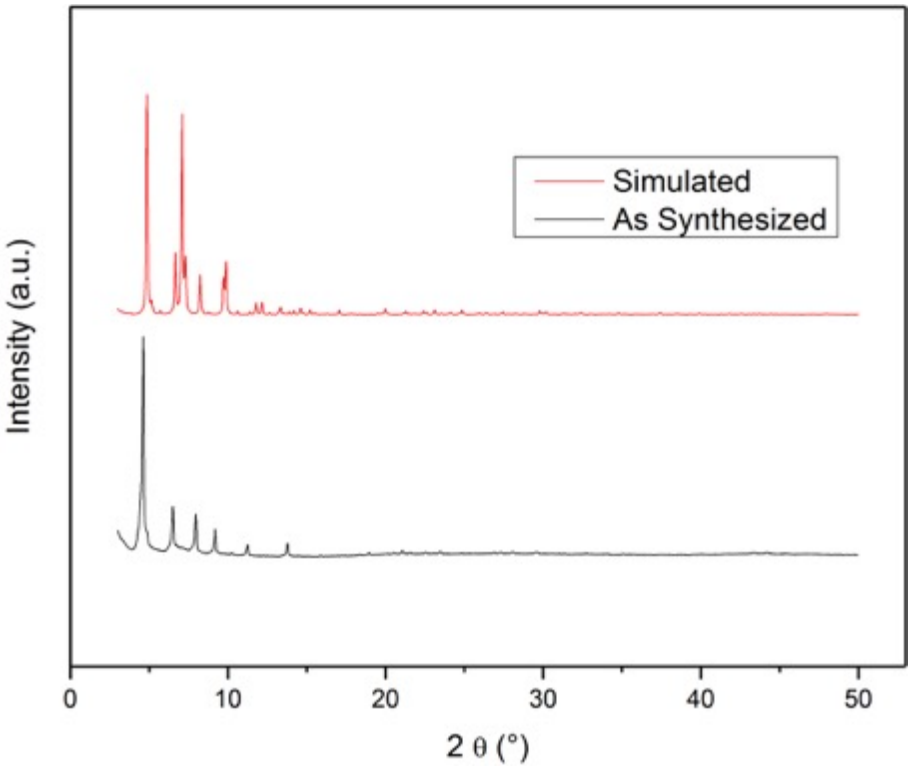

Figure S81. PXRD of as-synthesized PCN-222.

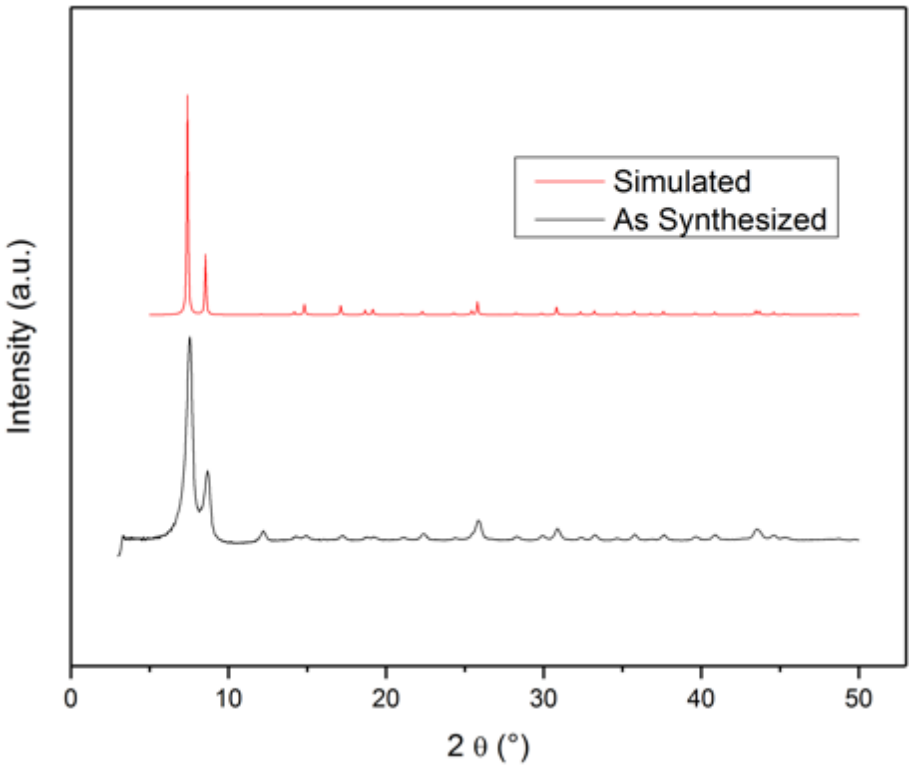

Figure S82. PXRD of as-synthesized UiO-66-NH_2 [Acetone/HCl].

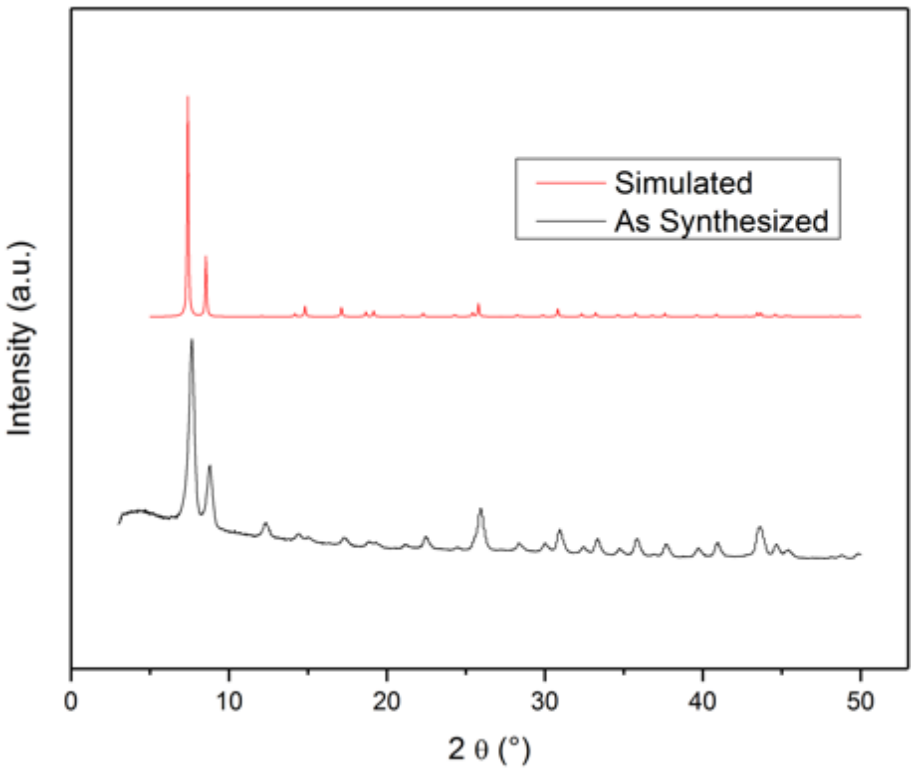

Figure S83. PXRD of as-synthesized UiO-66-NH_2 [DMF/HCOOH].

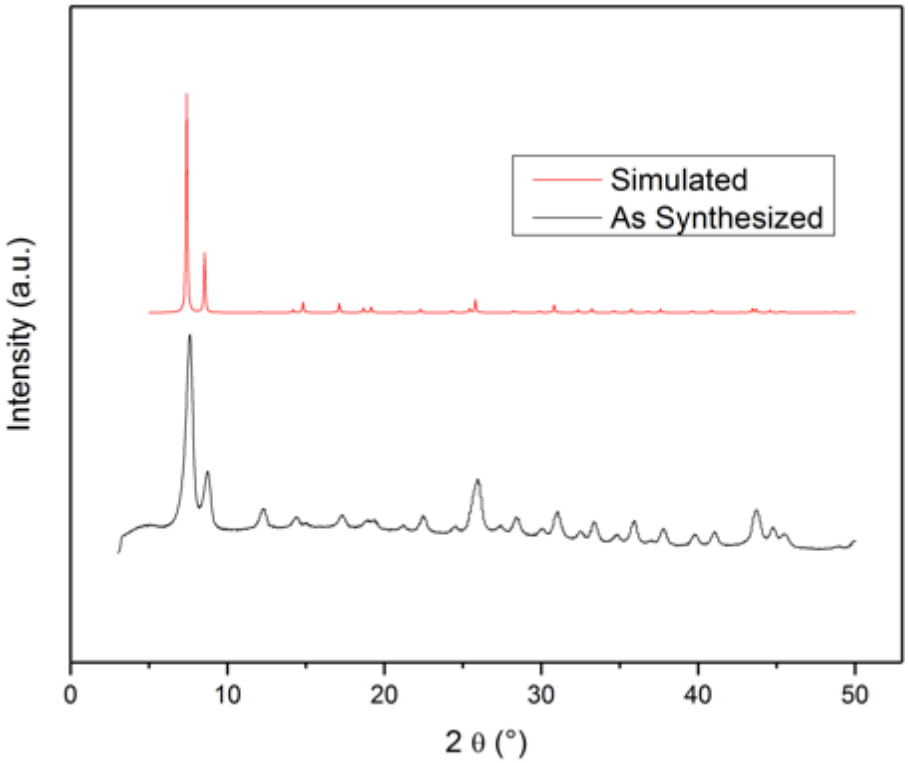

Figure S84. PXRD of as-synthesized UiO-66-$(COOH)_2$ [DMF/HCOOH].

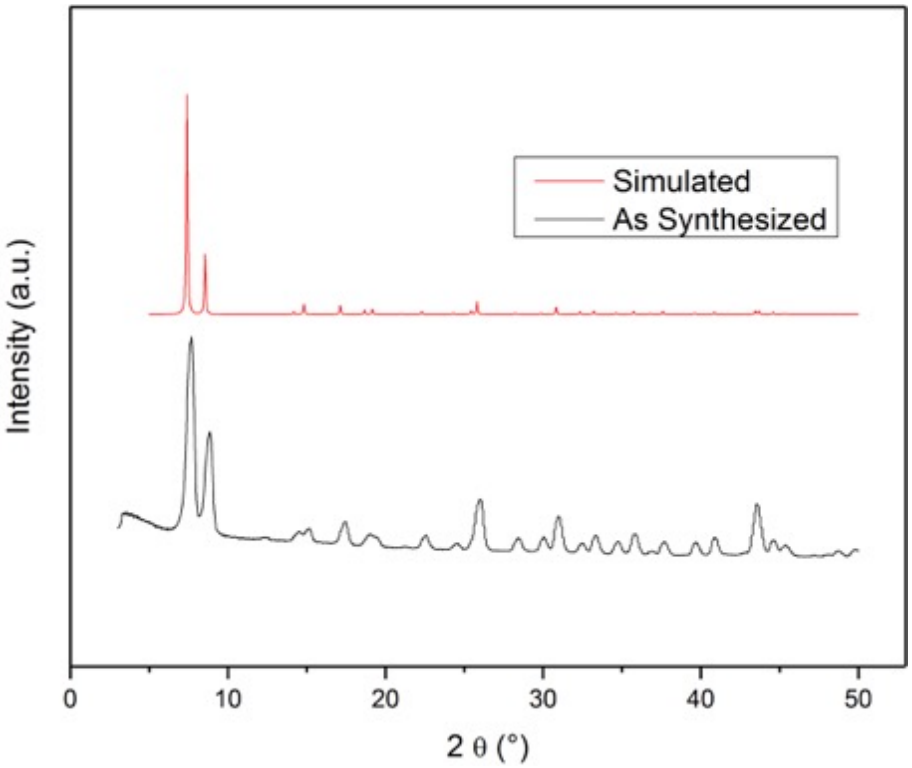

Figure S85. PXRD of as-synthesized UiO-66-$(OH)_2$ [DMF/HCOOH].

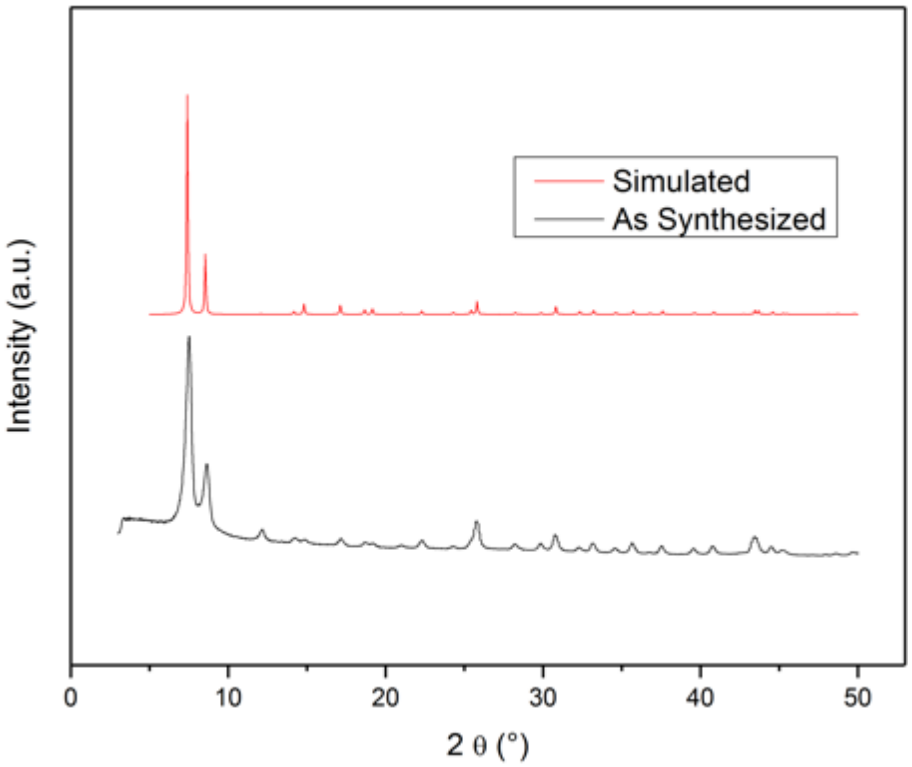

Figure S86. PXRD of as-synthesized UiO-66-OH [DMF/HCOOH].

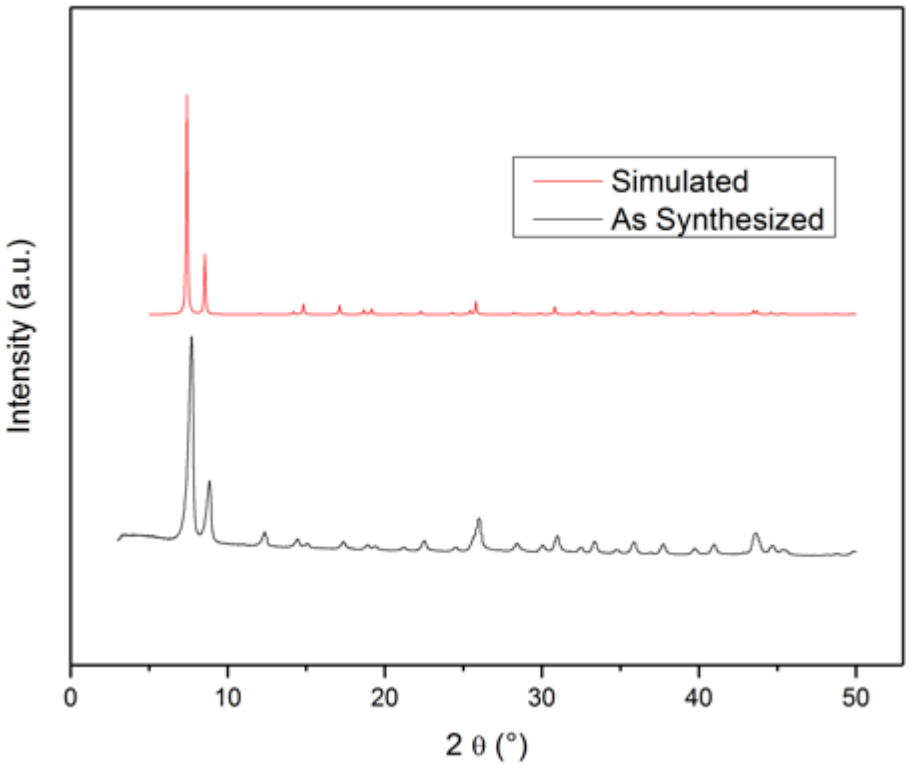

Figure S87. PXRD of as-synthesized UiO-66-NO_2 [DMF/HCOOH].

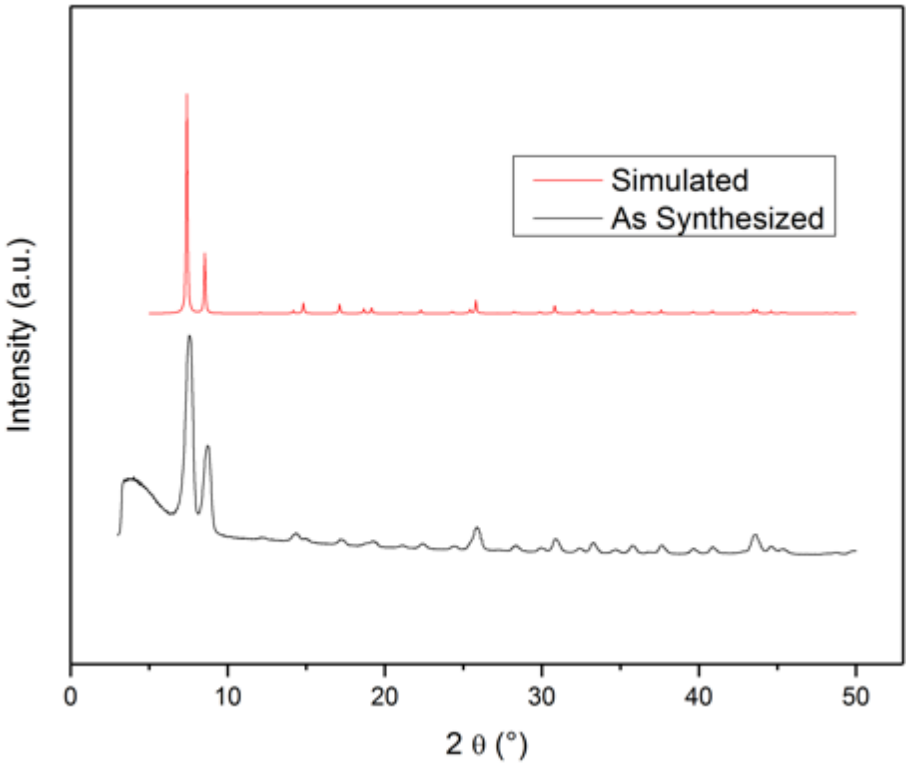

Figure S88. PXRD of as-synthesized UiO-66-OCF_3 [DMF/HCOOH].

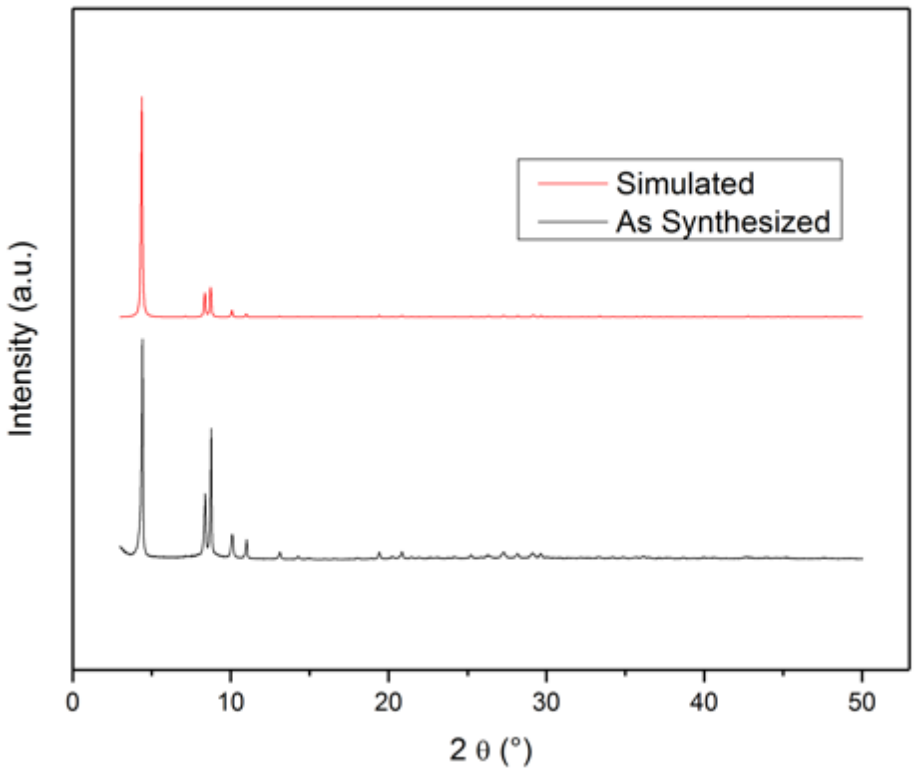

Figure S89. PXRD of as-synthesized MOF-808.

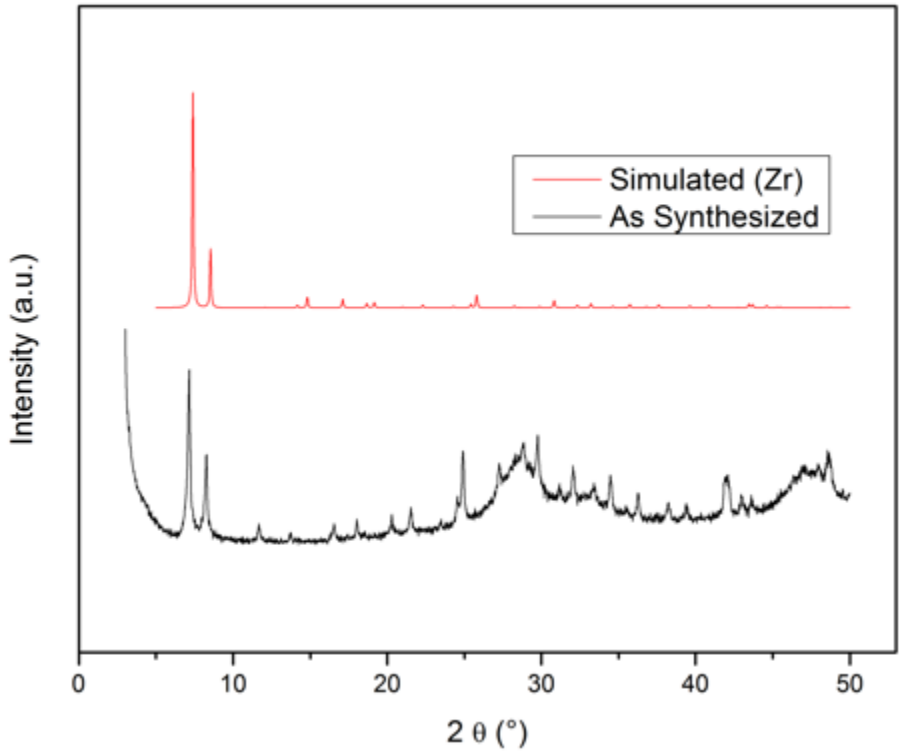

Figure S90. PXRD of as-synthesized UiO-66(Ce).

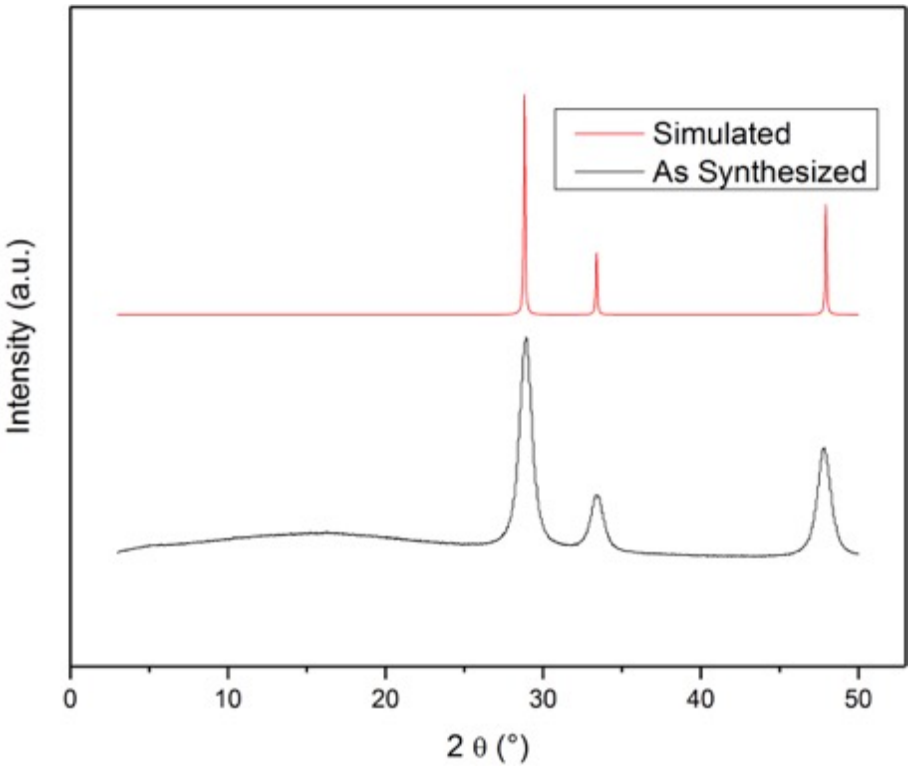

Figure S91. PXRD of as-purchased CeO_2.

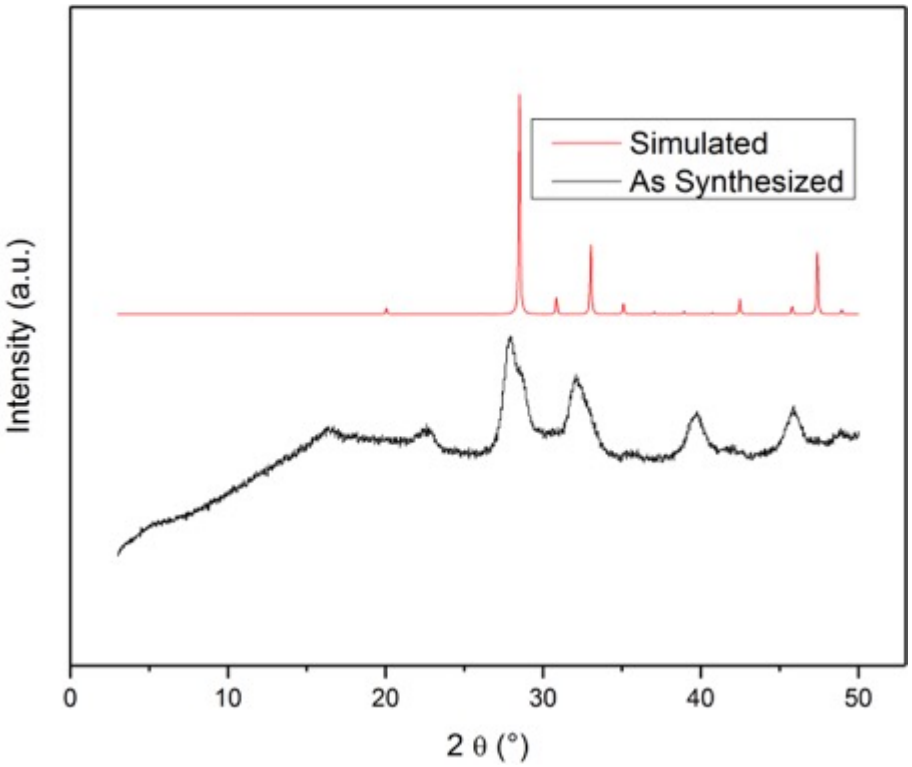

Figure S92. PXRD of as-purchased Eu_2O_3.

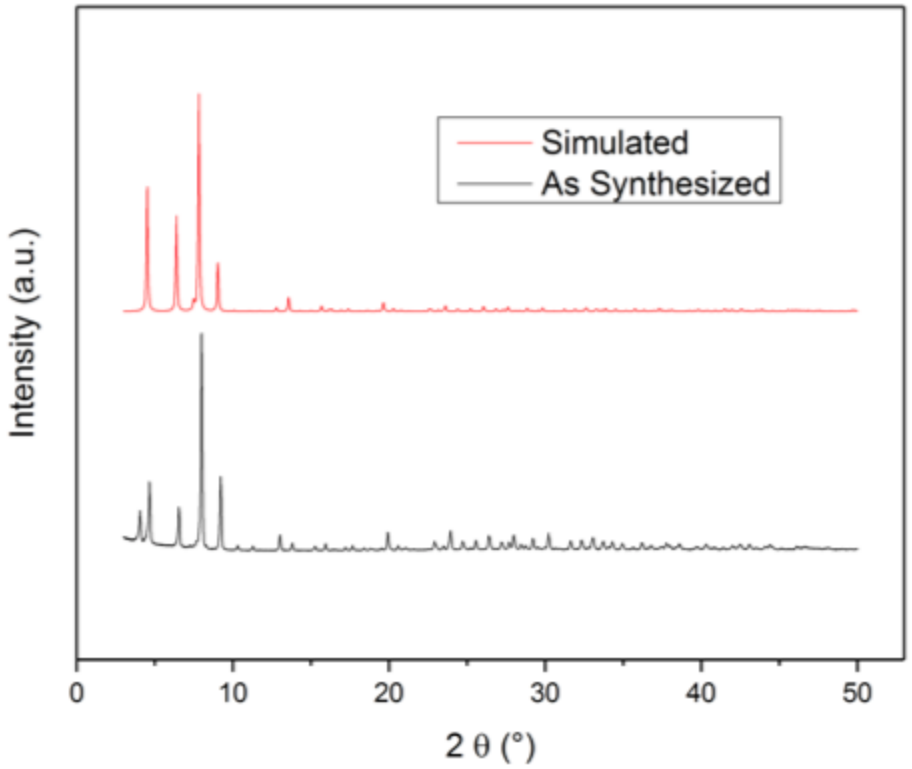

Figure S93. PXRD of as-synthesized DUT-67(Hf).

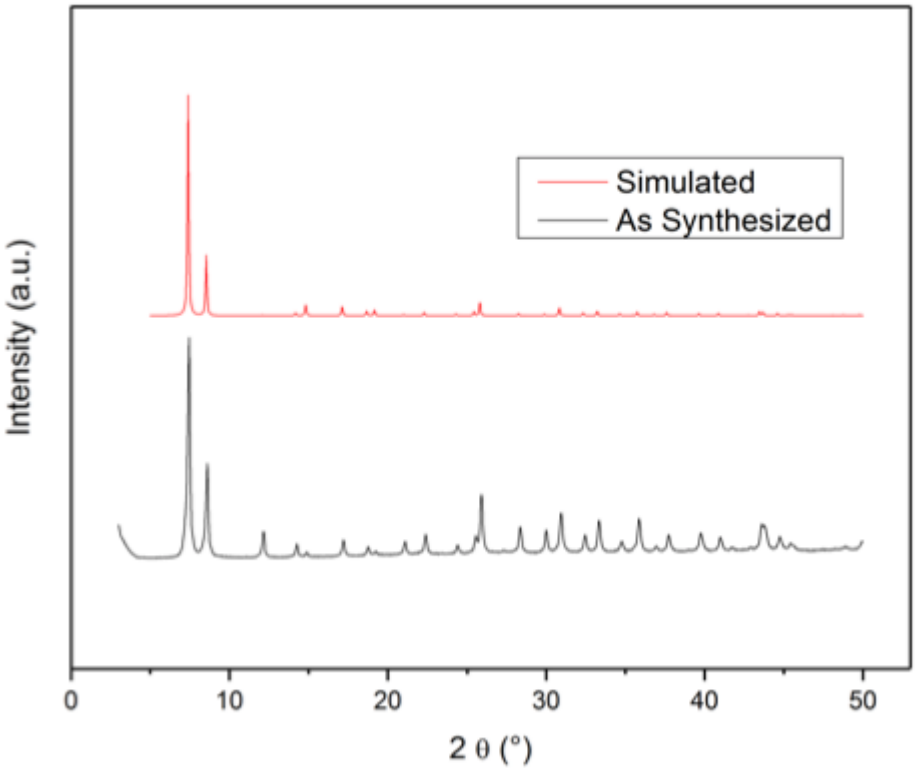

Figure S94. PXRD of as-synthesized UiO-66(Hf).

References

1. G. Lu, C. Cui, W. Zhang, Y. Liu and F. Huo, *Chem-Asian J.*, 2013, **8**, 69-72.
2. K. M. Zwolinski, P. Nowak and M. J. Chmielewski, *Chem. Commun.*, 2015, **51**, 10030-10033.
3. K. B. Daniel, J. L. Major Jourden, K. E. Negoescu and S. M. Cohen, *J. Biol. Inorg. Chem.*, 2011, **16**, 313-323.
4. C. Perez, J. Li, F. Parlati, M. Rouffet, Y. Ma, A. L. Mackinnon, T.-F. Chou, R. J. Deshaies and S. M. Cohen, *J. Med. Chem.*, 2017, **60**, 1343-1361.
5. Z. Ji-Hu, D. Y. C. Thomas and R. O. Kevin, *J. Biomol. Screen.*, 1999, **4**, 67-73.
6. M. J. Katz, J. E. Mondloch, R. K. Totten, J. K. Park, S. T. Nguyen, O. K. Farha and J. T. Hupp, *Angew. Chem.*, 2014, **126**, 507-511.
7. M. J. Katz, S.-Y. Moon, J. E. Mondloch, M. H. Beyzavi, C. J. Stephenson, J. T. Hupp and O. K. Farha, *Chem. Sci.*, 2015, **6**, 2286-2291.
8. S.-Y. Moon, G. W. Wagner, J. E. Mondloch, G. W. Peterson, J. B. DeCoste, J. T. Hupp and O. K. Farha, *Inorg. Chem.*, 2015, **54**, 10829-10833.
9. J. E. Mondloch, M. J. Katz, W. C. Isley, P. Ghosh, P. L. Liao, W. Bury, G. Wagner, M. G. Hall, J. B. DeCoste, G. W. Peterson, R. Q. Snurr, C. J. Cramer, J. T. Hupp and O. K. Farha, *Nat. Mater.*, 2015, **14**, 512-516.
10. Y. Liu, S.-Y. Moon, J. T. Hupp and O. K. Farha, *ACS Nano*, 2015, **9**, 12358-12364.
11. P. M. Budd, B. S. Ghanem, S. Makhseed, N. B. McKeown, K. J. Msayib and C. E. Tattershall, *Chem. Commun.*, 2004, DOI: 10.1039/B311764B, 230-231.
12. A. Fateeva, P. A. Chater, C. P. Ireland, A. A. Tahir, Y. Z. Khimyak, P. V. Wiper, J. R. Darwent and M. J. Rosseinsky, *Angew. Chem. Int. Ed. Engl.*, 2012, **51**, 7440-7444.
13. H. Reinsch, M. A. van der Veen, B. Gil, B. Marszalek, T. Verbiest, D. de Vos and N. Stock, *Chem. Mater.*, 2012, **25**, 17-26.
14. M. Sindoro, A. Y. Jee and S. Granick, *Chem. Commun.*, 2013, **49**, 9576-9578.
15. T. Ahnfeldt, D. Gunzelmann, T. Loiseau, D. Hirsemann, J. Senker, G. Férey and N. Stock, *Inorg. Chem.*, 2009, **48**, 3057-3064.
16. M. Sohail, Y.-N. Yun, E. Lee, S. K. Kim, K. Cho, J.-N. Kim, T. W. Kim, J.-H. Moon and H. Kim, *Cryst. Growth Des.*, 2017, **17**, 1208-1213.
17. S. Yuan, J. S. Qin, H. Q. Xu, J. Su, D. Rossi, Y. Chen, L. Zhang, C. Lollar, Q. Wang, H. L. Jiang, D. H. Son, H. Xu, Z. Huang, X. Zou and H. C. Zhou, *ACS Cent. Sci.*, 2018, **4**, 105-111.
18. G. Férey, C. Mellot-Draznieks, C. Serre, F. Millange, J. Dutour, S. Surblé and I. Margiolaki, *Science*, 2005, **309**, 2040.
19. C. Serre, F. Millange, C. Thouvenot, M. Noguès, G. Marsolier, D. Louër and G. Férey, *J. Am. Chem. Soc.*, 2002, **124**, 13519-13526.
20. J. Gordon, H. Kazemian and S. Rohani, *Micropor. Mesopor. Mater.*, 2012, **162**, 36-43.
21. P. Horcajada, F. Salles, S. Wuttke, T. Devic, D. Heurtaux, G. Maurin, A. Vimont, M. Daturi, O. David, E. Magnier, N. Stock, Y. Filinchuk, D. Popov, C. Riekel, G. Férey and C. Serre, *J. Am. Chem. Soc.*, 2011, **133**, 17839-17847.
22. F. Zhang, J. Shi, Y. Jin, Y. Fu, Y. Zhong and W. Zhu, *Chem. Eng. J.*, 2015, **259**, 183-190.

23. S. R. Venna, J. B. Jasinski and M. A. Carreon, *J. Am. Chem. Soc.*, 2010, **132**, 18030-18033.
24. P. Ayyappan, O. R. Evans and W. Lin, *Inorg. Chem.*, 2001, **40**, 4627-4632.
25. S. R. Caskey and A. J. Matzger, *Inorg. Chem.*, 2008, **47**, 7942-7944.
26. C. G. Carson, K. Hardcastle, J. Schwartz, X. Liu, C. Hoffmann, R. A. Gerhardt and R. Tannenbaum, *Eur. J. Inorg. Chem.*, 2009, **2009**, 2338-2343.
27. S. Han, Y. Huang, T. Watanabe, Y. Dai, K. S. Walton, S. Nair, D. S. Sholl and J. C. Meredith, *ACS Comb. Sci.*, 2012, **14**, 263-267.
28. H. Jasuja and K. S. Walton, *Dalton T.*, 2013, **42**, 15421-15426.
29. M. Gustafsson and X. Zou, *J. Porous Mater.*, 2013, **20**, 55-63.
30. H. H. Fei, J. F. Cahill, K. A. Prather and S. M. Cohen, *Inorg. Chem.*, 2013, **52**, 4011-4016.
31. S. Yuan, W. Lu, Y.-P. Chen, Q. Zhang, T.-F. Liu, D. Feng, X. Wang, J. Qin and H.-C. Zhou, *J. Am. Chem. Soc.*, 2015, **137**, 3177-3180.
32. H. Furukawa, F. Gándara, Y.-B. Zhang, J. Jiang, W. L. Queen, M. R. Hudson and O. M. Yaghi, *J. Am. Chem. Soc.*, 2014, **136**, 4369-4381.
33. M. J. Katz, Z. J. Brown, Y. J. Colon, P. W. Siu, K. A. Scheidt, R. Q. Snurr, J. T. Hupp and O. K. Farha, *Chem. Commun.*, 2013, **49**, 9449-9451.
34. S. Biswas and P. Van Der Voort, *Eur. J. Inorg. Chem.*, 2013, **2013**, 2154-2160.
35. V. Bon, I. Senkovska, I. A. Baburin and S. Kaskel, *Crystal Growth & Design*, 2013, **13**, 1231-1237.
36. S. Ayala, Z. Zhang and S. M. Cohen, *Chem. Commun.*, 2017, **53**, 3058-3061.
37. G. W. Peterson, M. R. Destefano, S. J. Garibay, A. Ploskonka, M. McEntee, M. Hall, C. J. Karwacki, J. T. Hupp and O. K. Farha, *Chem-Eur J.*, 2017, **23**, 15913-15916.
38. A. M. Ploskonka, S. E. Marzen and J. B. DeCoste, *Industrial & Engineering Chemistry Research*, 2017, **56**, 1478-1484.
39. D. Feng, Z. Y. Gu, J. R. Li, H. L. Jiang, Z. Wei and H. C. Zhou, *Angew. Chem. Int. Ed. Engl.*, 2012, **51**, 10307-10310.
40. M. Lammert, M. T. Wharmby, S. Smolders, B. Bueken, A. Lieb, K. A. Lomachenko, D. D. Vos and N. Stock, *Chem. Commun.*, 2015, **51**, 12578-12581.